Load G-level as a Truck-Ground KPI

by

Cayce Kerr

A thesis submitted in partial fulfillment of the requirements for the degree of

Master of Science

in

Mining Engineering

Department of Civil and Environmental Engineering
University of Alberta

© Cayce Kerr, 2017

Abstract

A mine's haul road network has a large influence upon the success of a mine, and aside from occasional visual inspections, a significant number of mines put little emphasis on monitoring the condition of haul surfaces. The opportunity exists for a haul road benchmarking system, which can be achieved utilizing truck suspension cylinder data that is readily available to a mining operation. Understanding the interaction between road profiles and haul trucks can provide valuable information on the stress imposed on the truck by large road defects, and be utilized as a condition monitoring tool for maintenance. Applying novel analyses to g-level forces generated by suspension cylinders can assist mine planners diagnose the cause of potential truck damaging road conditions, to prioritize where to dispatch road maintenance support equipment.

Acknowledgment

I could have never written this thesis without the continued love and support from my wife and my dog, and I appreciate their patience during tough times. I would like to thank my parents, sisters, and friends for their words of encouragement, and my professor for guiding me through this thesis and university.

Contents

List of Figures

List of Tables

1 Introduction

1.1 Background

An earthmoving mining operation is volatile and harsh, unlike any other industry in the world, specifically on the tools used to mine. With mines developing deeper and extracting lower grades than ever before, the need to trim costs and increase production is a must for any mine manager. It has been estimated that haulage accounts for 30% to 55% of total mining costs, with maintenance and repair expenditures, including tires, representing 50% to 60% of the haulage costs (Knights & Boebner, 2001).

A mine haul network can have a large impact on haulage costs, both operational and in maintenance, which is driven by the rolling resistance of the road material. The life of haul truck components are heavily influenced by the road conditions on which the truck operates, which includes but is not limited to truck tires, suspension cylinders, frame, axles, and engine. Mechanical issues with any of these components will cause the haul truck to be removed from operation, costing a mine significant lost production. To better understand the effect of a road profile on a haul truck, analyzing suspension cylinder data can aid in determining the road reaction forces translated through the tires and struts, and the generating stress on the truck frame.

Conversely, suspension data also provides a method to monitor haul road conditions, which can be advantageous to operations by targeting troublesome haul areas. Utilizing haul truck data provides an inexpensive and simple road management system, allowing a lower mining cost per tonne through improved production and availability.

1.2 Research Objective

The goal of this thesis is to provide (a) a model that defines rolling resistance as a function of suspension cylinder g-level loading, and (b) utilizing this data to determine the tire workload capacity and truck frame impact. The concept of rolling resistance is well understood in the mining industry, where it provides a simple variable as a function of truck component life and operating costs under specific haul conditions. The tire model will reference the tire industry standard TKPH (tonnes kilometer per hour) rating system; however the analysis will use real-time TKPH calculated from the loading measured at the haul truck suspension cylinders. Using the suspension cylinder load data to calculate strut g-level, a frame analysis will be completed considering rack, pitch, and bias g-level events. Detailed distributions of such data and comparisons to road conditions is targeted to future work in predicting the number of events to structural fatigue/failure as a function of rolling resistance. During this work, novel methods to investigate g-level are demonstrated to suggest a haul road monitoring system, with a recommendation for future work to create a database as a road condition classification metric.

2 Literature Review

2.1 Truck Basics

Before we can conduct an analysis on a rigid frame, rear dump haul truck and specific components, we must first understand the haul truck itself. Figure 2-1 shows a typical rear dump mine haul truck, which the design of varies slightly between different manufacturer models and machine class size, from 100 to 400 ton payload class.

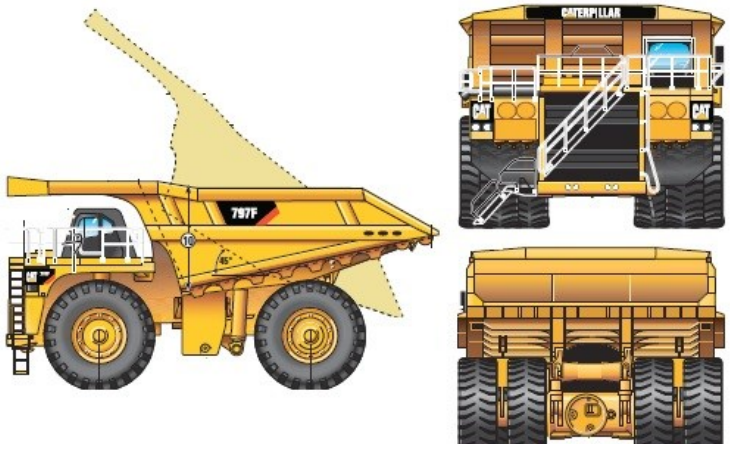

Figure 2-1 – Mining Haul Truck - Caterpillar 797F (Caterpillar Inc., 2013)

Haul trucks have two axles, each supporting two pin connected suspension cylinders (strut) which link directly to the frame of the truck. The struts on the front axle are responsible for dampening the force from only a single tire, whereas the rear struts are accountable for two 'dual' tires, each with a smaller stroke and diameter than the front axle suspension counterparts. A simplified outline of the truck axle, suspension, and tire configuration can be seen in Figure 2-2.

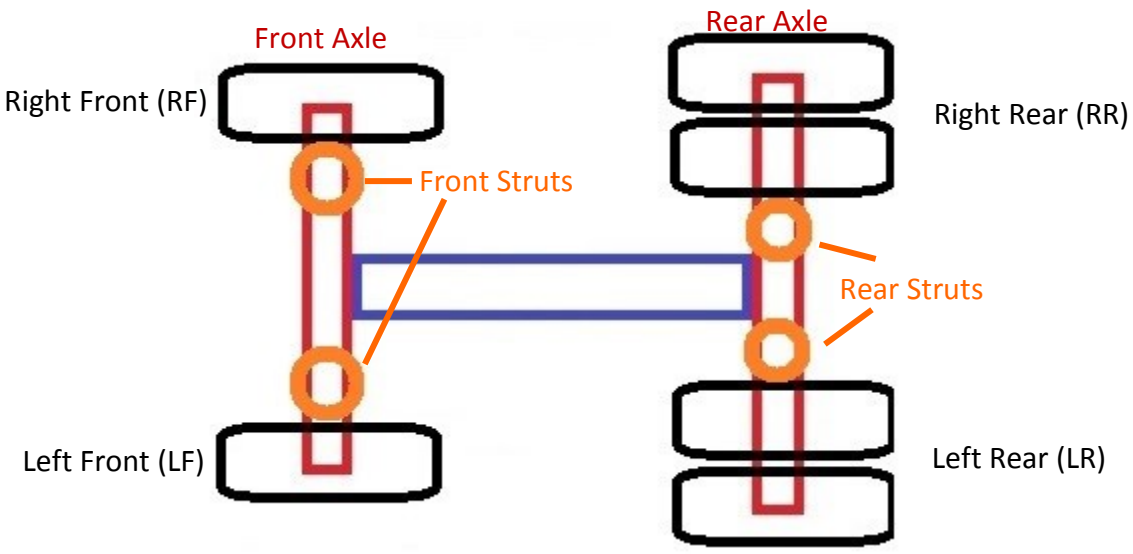

Figure 2-2 – Simplified Haul Truck Axle, Suspension, and Tire Configuration (Not to scale)

Suspension on a haul truck has several purposes, the first being to protect the vehicle itself, as well as passengers and cargo by absorbing energy caused by rough road surfaces. In the case of a mine truck, the struts specifically protect the frame from the truck's payload, which can be 30% to 40% additional weight over than the empty tare weight of the truck. Without the dampening of the struts, the frame of the vehicle would come under frequent high stress and fatigue events, causing premature frame failure. The second purpose of struts is to keep the tires in constant contact with the road, to ensure the vehicle is able to maneuver. Lastly, the struts aid in transferring the weight in a vehicle, such as when driving around a corner, (Harris, 2005), to the ground reaction.

To design specifications of the original equipment manufacturer (OEM), when a haul truck is loaded, each of the 6 tires should support an equal portion of the gross vehicle weight (GVW), with one third (33.3%) of the weight on the front axle and two thirds (66.7%) on the rear axle, such that each tire carries one sixth (16.7%) of the GVW evenly. This can only be achieved if the

truck is loaded evenly, front to rear, as well as left to right. When the truck is empty, the GVW is distributed closer to a 50:50 ratio from front to rear axle. Table 2-1 has a full breakdown of the weight distributions of a loaded and empty haul truck, showing both axle and tire loading ratios.

Table 2-1 - GVW Distribution Percent in a Haul Truck

%	Front Axle	Rear Axle	Front Tires	Rear Tires
Empty	46-50	50-54	23-25	12.5-13.5
Loaded	33.3	66.7	16.7	16.7

2.2 Off-The-Road Tire Basics

There are two different kinds of off-the-road (OTR) tire used in the mining industry for haul trucks, as well as other mobile equipment such as graders, loaders, scrapers, and wheel dozers; termed Radial or Bias Ply tires. While radial tires cost 10% to 20% higher, they prove as a more durable product, achieving a 30% to 40% longer tire life (Otraco, 1993) along with many other advantages compared to bias tires, illustrated in Table 2-2. The difference between the designs of the two types of tires can be seen in Figure 2-3.

Table 2-2 – Radial & Bias Ply Tire Advantages (Caterpillar Inc., 2012)

Bias & Radial Tire Advantages		
	Bias	Radial
Tread Life		X
Heat Resistance		X
Cut Resistance - Tread		X
Cut Resistance - Side Wall	X	X
Traction		X
Flotation		X
Stability	X	
Fuel Economy		X
Repairability		X

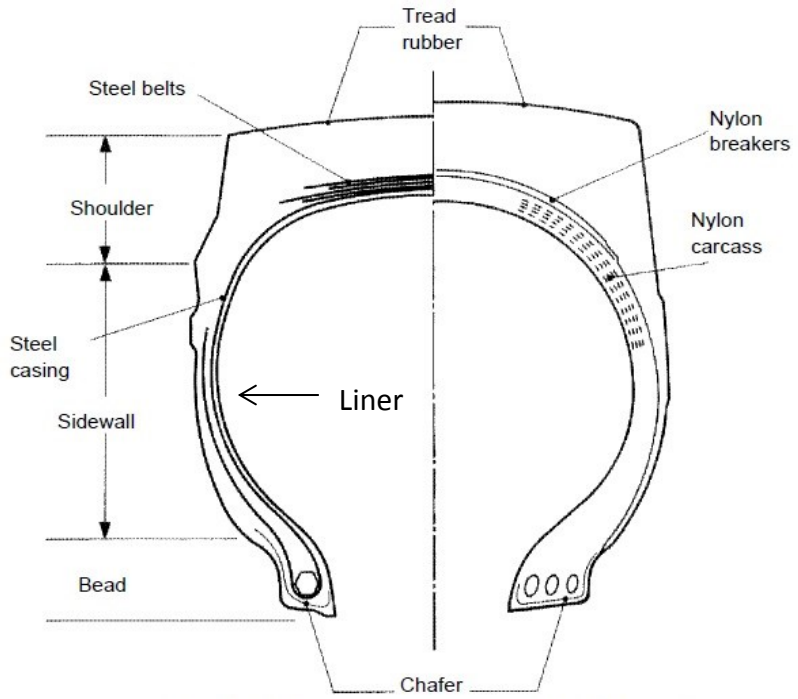

Figure 2-3 - Radial & Bias Ply Tire Comparison (after Otraco, 1993)

For this thesis, radial tires were the focus as they are more predominant in North American surface mines and heavy earthmoving operations. The scope of off-the-road (OTR) tires specifically for haul trucks will focus on the 100 to 400 ton (97 to 363 tonne) payload class. In Table 2-3, tire sizes corresponding to payload class are shown, with the main haul truck manufacturer models represented in those classes. Looking at the tire size classification scheme, XX.YYRZZ, the XX represents tire width in inches, YY represents height to width ratio or aspect ratio (as a percent), and finally RZZ denotes rim diameter in inches. In addition, the tire industry has designations which determine the type of equipment on which OTR tires should be mounted, as well as the recommended tread depth of the tire itself. These tire standards are shown in Figure 2-4.

Capacity (mt)	Truck Manufacturer				GVW (mt)	Empty GVW (mt)	Tire Size
	Cat	Komatsu	Liebherr	Hitachi			
91	777	HD785		EH1700	165	68	27.00R49
136	785	HD1500			250	114	33.00R51
180	789	730E		EH3500	320	140	37.00R57
220	793	830E	T264	EH4000	390	170	40.00R57
290	794AC	930E		EH5000	500	210	53.80R63
313	795				570	257	56.80R63
327		960E			576	249	56.80R63
360			T282/T284		600	237	56.80R63
363	797	980E			623	260	59.80R63

Table 2-3 - Haul Truck Payload Classes and Tire Size
***Trucks capacity and GVW have been rounded minimally to fit in a respected class**
****Several trucks are able to accommodate different tire sizes, with the standard size shown (Caterpillar Inc., 2017; Liebherr, 2017; Komatsu America Corp., 2017; Hitachi Construction Machine Co., 2017)**

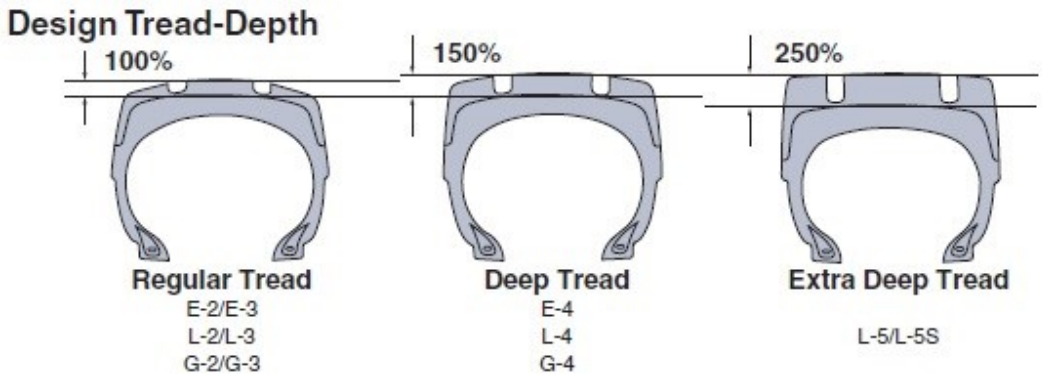

Figure 2-4 - Tire Industry Tread Depth Standards (Bridgestone Corporation, 2011)
E = Earthmover G = Grader L = Loader & Dozer

59.80R63 Tread Code TC E4

Figure 2-5 - Full Tire Description Example – TC = Tire Compound

To complete a classification designation for an OTR tire, an OEM code specific to the tire manufacturer describes the tread type and rubber compound of the tire, as shown in Figure 2-5. OTR tires are generally made from 80% natural rubber, with the balance being synthetic. In comparison, light truck and passenger vehicle tires are composed closer to a 50:50 ratio of natural and synthetic rubber (McGarry, 2007). While the general make up of an OTR tire is synthetic and natural rubber, OEMs add several other "ingredients" and cure the tire proportionate to diverse environments and uses. Generally, OTR tires are designed to either protect from cuts or from heat generation, as shown in Table 2-4.

Table 2-4 - OEM Tire Compound Codes
(Bridgestone Corporation, 2011; Goodyear, 2003; Michelin, 2010)

OEM Tire Compound Codes						
Manufacturer	Cut Resistant		Standard		Heat Resistant	
Goodyear	6		4		2	
Bridgestone	2A		1A		3A	
Michelin	A4	A	B4	B	C4	C

The representation of the codes on the scale in Table 2-4 are simply an estimation of the author and do not reflect how the compounds would actually match up against one another. As previously mentioned, the primary functions of a haul truck tire in conjunction with the design of a haul truck is to support the truck and its payload, aid in absorbing shock from haul road reaction, provide traction and braking forces to the ground and to change and maintain direction of travel.

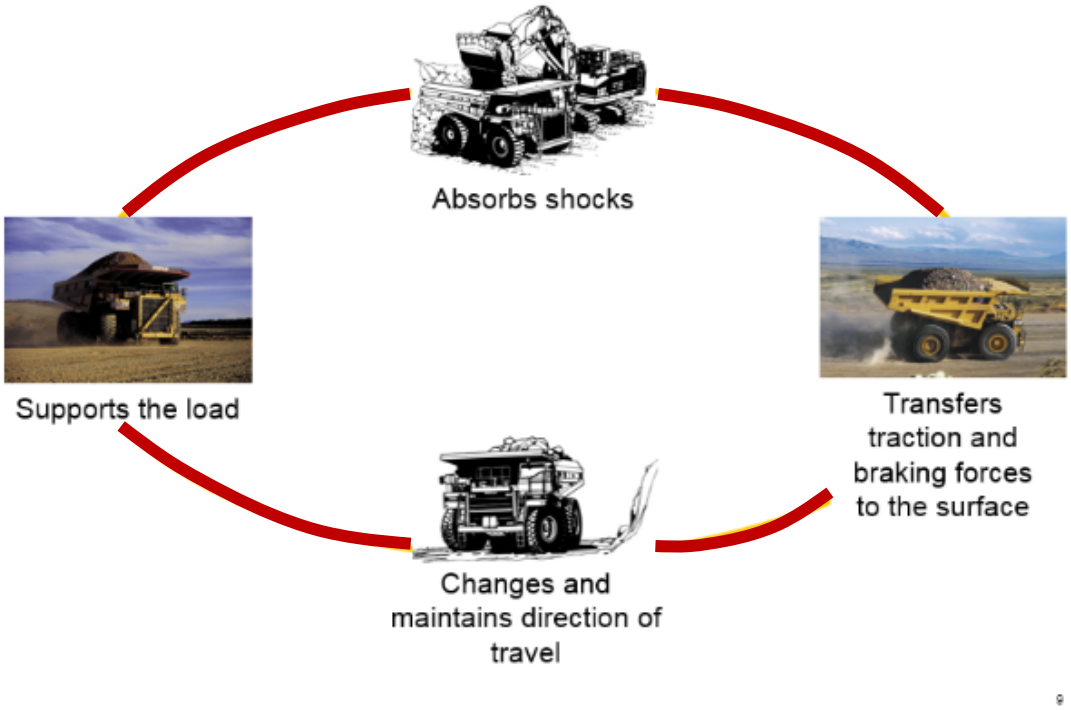

Figure 2-6 – Functions of a Haul Truck Tire (Caterpillar Inc., 2008)

With the largest size OTR tires, designated 59.80R63, costing around $70,000-$100,000 CDN per tire, it is imperative that mining companies include a tire maintenance and management program in their operation. While tires of this size are generally designed to last 8,000+ hours, we rarely see them make it to full life; with a good tire management program usually only able to achieve an average tire life between 5,000 and 6,000 hours; which is usually classified as success in the Canadian mining industry. Many tires fail before this; so what is causing these very expensive, high demand, & short supply assets to not perform to expectation? There are many factors that have the potential to cause a tire to fail prematurely, shown in Figure 2-7. The 3 most common types of failures we see in the industry are cuts, impacts, and separations, which will be examined in section 2.4.

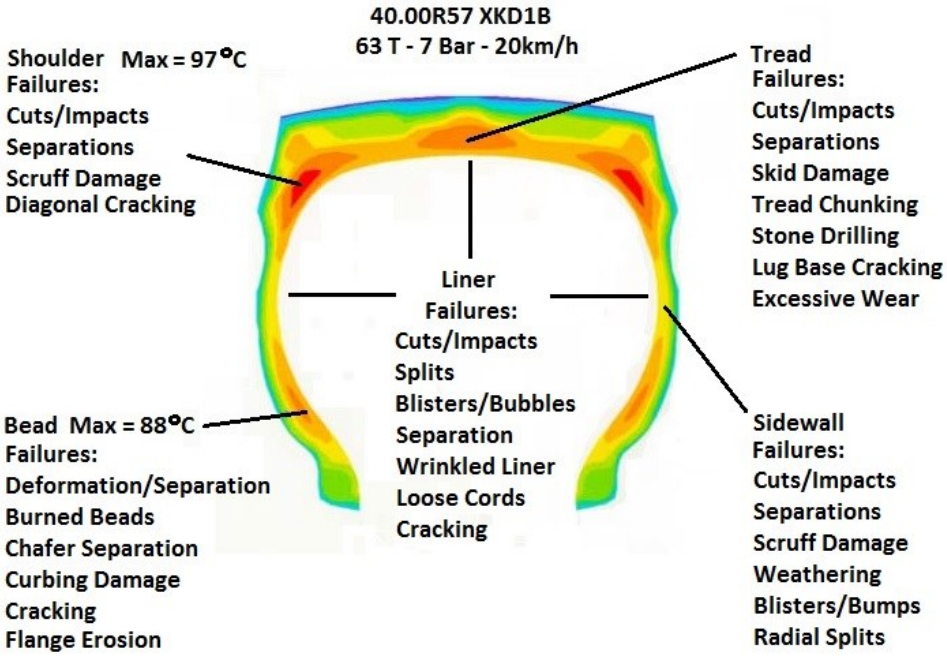

Figure 2-7 - Tire Failure Methods (Zhou J., 2007; Tire Maintenance Council, 1994) & Heat Build-up Diagram (after Joseph, 2012)

2.3 TKPH

The tonne-kilometer per hour rating system devised by tire manufacturers is a maximum workload capacity of a tire. The system is targeted to help operations regulate the heat generation in tires to avoid early failure due to heat separation. When operating under the manufacturer recommended tkph value, the tire's temperature "should" stabilize after ~160km of operation (SAE International, 1995), typically at a temperature between 80 and 100˚C, depending on the operating environment. To calculate an operation tkph value, the SAE standard given in equation 1 (SAE International, 1995), is virtually the same as the tire OEM standard.

$$TKPH = \frac{(T_L D_L N_L + T_E D_E N_E)}{H} \quad 1$$

Where:

T_L, T_E = Highest Tire Load (tonnes) – Loaded or Empty Haul Truck

D_L, D_E = Haul Distance (Km) – Loaded or Empty Haul Truck

N_L, N_E = Number of Trips – Loaded or Empty Haul Truck

H = Total Time Period of Study (Hours)

The average speed of a haul truck may also be used in place of distance, number of total cycles, and time. From equation 1, the highest tire load, comparing the front and rear tire positions, is used to govern the "workload" of the truck. As shown in Table 2-1, the front tires of a haul truck typically experience the average highest loads, as they accept a higher percentage of the GVW when the truck is empty and an equal percentage when the truck is loaded. Tire OEMs have also added several correction factors to make this value more site specific, K_1 and K_2, for haul distance and site temperature respectively. These factors are multipliers to the equation 1 calculation, where the method to calculate such coefficients can be found in the OEM data book. (Michelin, 2010) (SAE International, 1995) (Goodyear, 2003) (Magna Tyres Group, 2014).

Calculating a tire tkph value may be accomplished using an alternative method, similar to that used by tire manufacturers and tailored to haul truck models. Tire manufacturers' first determine the weight distributed on tires when the truck is empty and loaded, accounting for a haul truck 10/10/20 overload rule. This OEM generic rule states that a haul truck may be overloaded by more than 10%, for no more than 10% of its loads, while no load should exceed 20% of its rated payload (Colquhoun, et al., 2012). Once the tire loading distribution has been determined, the average weight on the tires is determined for empty and loaded conditions, for front and rear tires respectively, all of which are then averaged.

To estimate the tkph value of a tire, the manufacturers' multiply the average tire weight value with a specific tire workload capability factor (in km per hour), which is determined by the type of compound used in manufacturing the tire; measured as the maximum distance a tire can travel in one hour. For most ultra-class tire sizes the workload factor is 28 to 30 kph. Equations 2, 3, & 4 show the tire manufacturer tkph determination.

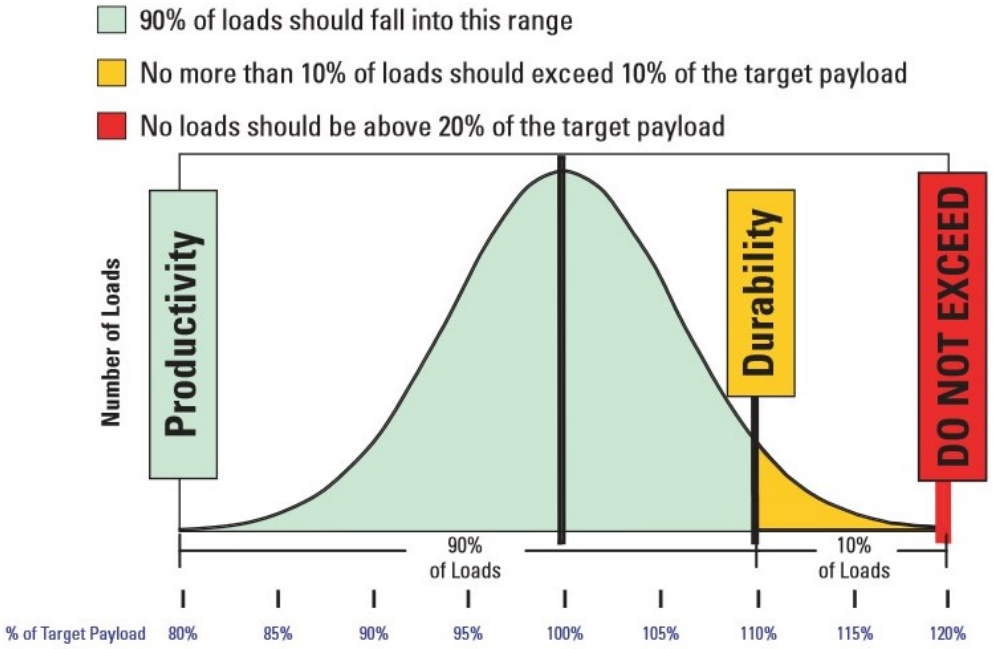

Figure 2-8 – Caterpillar Haul Trucks 10/10/20 Policy (Colquhoun, et al., 2012)

$$Tire\ AVG\ Carrying\ Weight = \frac{[Tire\ CW\ Empty + Tire\ CW\ Loaded]}{2} \quad \mathbf{2}$$

$$OEM\ TKPH = AVG[Front\ Tire\ CW, Rear\ Tire\ CW] \times WF \quad \mathbf{3}$$

$$OEM\ TKPH = AVG\left[\frac{[{}^{1}/_{4}T + {}^{1}/_{6}(T+1.2P]}{2}, \frac{[{}^{1}/_{8}T + {}^{1}/_{6}(T+1.2P]}{2}\right] \times \mathbf{WF} \quad \mathbf{4}$$

CW = Carrying Weight (tonnes)
WF = OEM Tire Workload Factor (Max. Km/Hour)
T = Haul Truck Tare Weight (tonnes)
P = Haul Truck Rated Payload (tonnes)

2.4 Heat Separation

A major concern is the number of tires that continue to fail prematurely due to heat separation, even when the calculated site tkph is below the tire manufacturer tkph rating; described in equation 1. As mentioned in the previous section, cuts, impacts, and separations are the most common causes of early tire failures. While the solution to minimizing cuts and impacts can be as simple as improving road maintenance, and hauler loading practices to reduce spillage onto the roads; preventing heat separation is a more complex issue to resolve.

Heat separation involves the separation of the tire rubber from its steel belt package (Werner & Barrowman, 2001), which can occur at temperatures as low as 104˚C (MacMahon; Rhino Tyres; Tyre Innovations Ltd., 2009), also the curing temperature of the tire when manufactured. To prevent heat build-up in a tire, either the road surface quality must be improved to decrease tire temperature hysteresis, the truck speed must be decreased, or the payload of the truck, and therefore on the tire, must be decreased.

This can prove to be problematic for mine sites, as consequently by decreasing productivity, it usually involves adding more trucks, slowing production, or increasing support equipment and road maintenance cost. Depending on the operation and the haul road surface material, 10% to 30% of heat separations account for early tire failure.

Temperature hysteresis is the internal friction inside of a tire between the rubber molecules and bonding of the steel belt package; caused by dynamic flexing of the tire due to road undulations and truck motion. Rolling resistance, described in section 2.5, is a direct cause of temperature hysteresis, where a proportion of the kinematic energy generated by a haul truck engine is lost as heat, due to the constant cycle deformation of tires (Netscher, Aminossadati, & Hooman, 2008). The rubber composition of a tire prevents heat dissipation, as rubber is an excellent insulator. If the rate of heat generation at the flexing steel belt package exceeds the rate of heat dissipation, the tire will continue to increase in temperature until it succumbs to

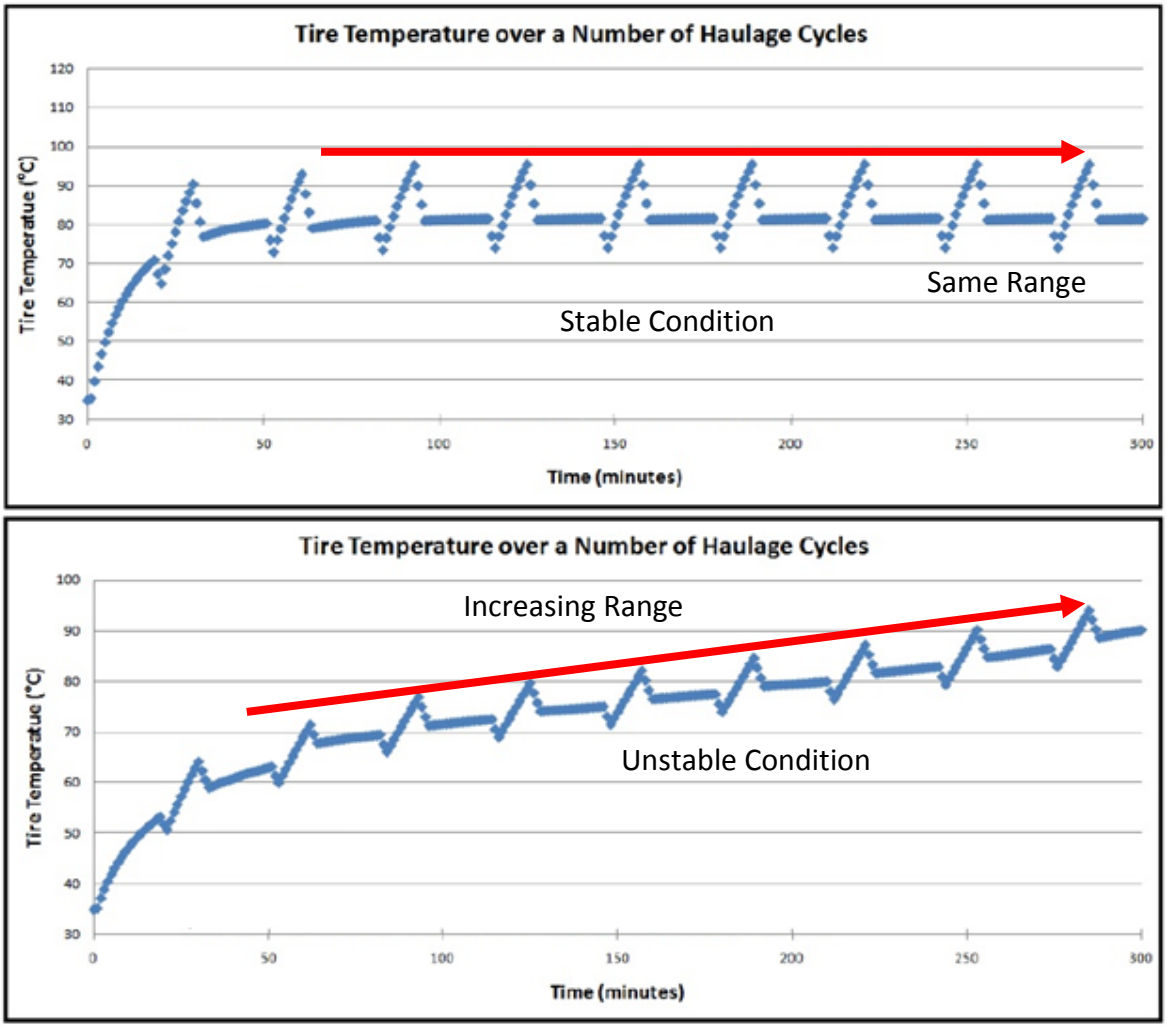

Figure 2-9 – Tire Heat Generation Example – Stable and Unstable Conditions (after Parreira, 2013)

pyrolysis, or decomposition of the rubber at the belt package contacts. This is shown in Figure 2-9 , demonstrating a tire in stable condition, in which the heat dissipation is equal to or lesser than the heat generation, as well as an example of steady temperature increase due to insufficient heat loss, (Parreira, 2013).

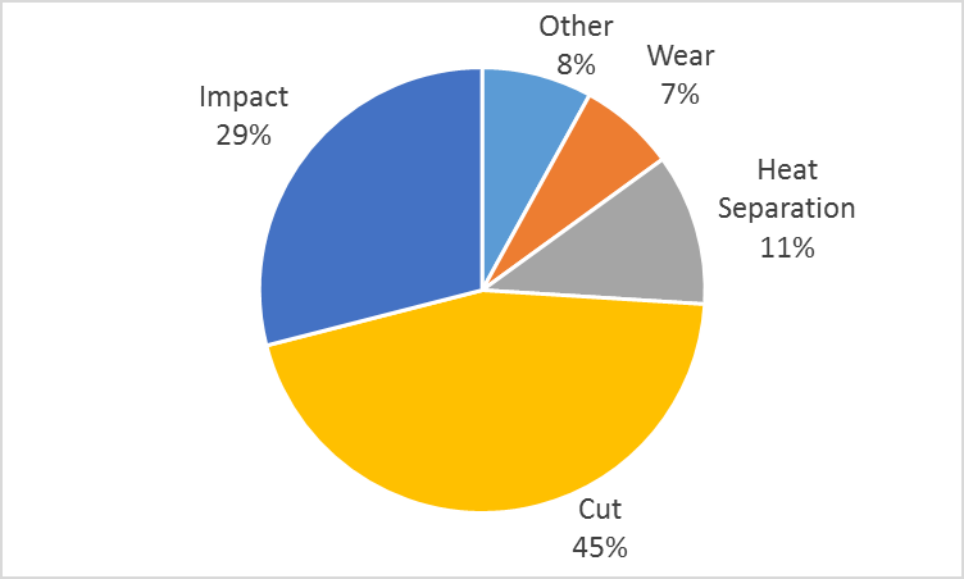

Figure 2-10 Tire Failures Case Study 1 - Metal Mine (Caterpillar Inc., 2008)

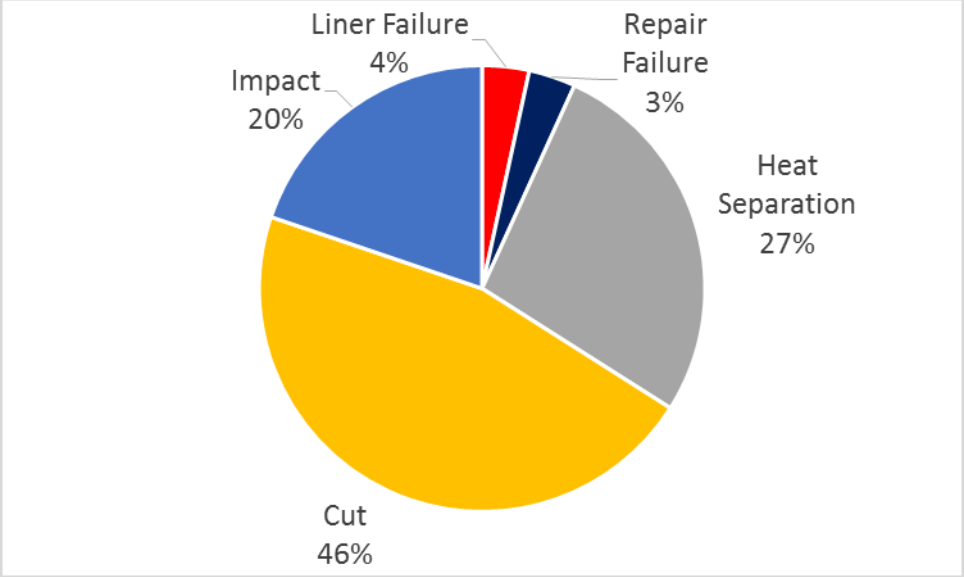

Figure 2-11 – Early Tire Failures Case Study 2 – Soft Rock Mine (Rasche, 2001)

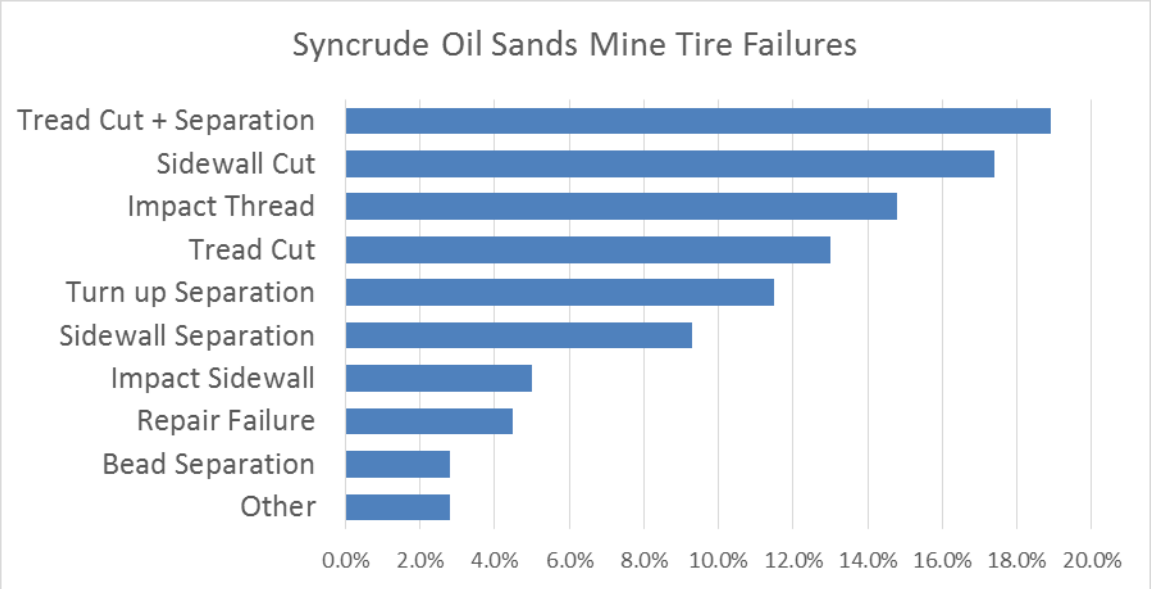

Figure 2-12 - Early Tire Failure Case Study 3 – Syncrude Oil Sands Mine (Lipsett & Anzabi, 2011)

Table 2-5 – Tire Failure vs Rotation Frequency Case Study – Kemess Copper/Gold Mine (Zhou, Hall, Huntingford, & Fowler, 2008)

Failure	Rotation Frequency 0	Rotation Frequency 1	Rotation Frequency 2	Rotation Frequency 3
Cut Separation	8.0%	10.7%	8.8%	18.2%
Cut Sidewall	12.0%	15.3%	10.5%	18.2%
Cut Tread	12.0%	16.0%	3.5%	0.0%
Heat Separation	20.0%	0.8%	1.8%	0.0%
Impact Break	16.0%	13.7%	8.8%	9.1%
Repair Failure	0.0%	0.8%	0.0%	0.0%
Turn up Separation	4.0%	2.3%	0.0%	0.0%
Worn out	28.0%	40.5%	63.2%	54.5%
Ply Ending Separation	0.0%	0.0%	1.8%	0.0%
Chipper Separation	0.0%	0.0%	1.8%	0.0%

Typically a higher percentage of early failures by heat separation is experienced in soft rock mines compared to hard rock mines, due to a high percentage of tires being punctured and damaged by rut entrained sharp rocks in the roads, and rough ruts at hard rock mines. That is not to say that hard rock mines experience a smaller number of tires failing due to heat separation overall, but merely that they also experience a higher number of impacts and cuts that lower the percentage of failed heat separated tires at such mines. Any mine that experiences long hauls, high truck body fill factors, high rolling resistance, large uphill climbs, fast haul speeds or any combination of these factors, likely has troubles with overheated tires.

In Figure 2-10 we see data from a hard rock metal mine with a low percentage of heat separations, while the case study in Figure 2-11 has a large percentage of heat separation failures, from a soft rock mine . Figure 2-12 doesn't directly show heat separation as failures, but it is most likely a cause of some of the turn up and sidewall separations, and a large proportion of the tread separation failures noted. In Table 2-5 we see another case study from a metal mine, but this time we see a high percentage of tires failing due to heat separation, with this percentage dropping significantly with increasing frequency of tire rotations.

Knights & Boerner (Knights & Boerner, 2001) also performed a study correlating tire failures to haul routes in Chilean Copper/Molybdenum mines. In their 10 month study, 51 tires were pulled from service with 8 being retired due to wear, 32 failing due to impacts and cuts, and 11 failing due to separations. During the study, it was found that the haul route with the highest elevation change in the mine experienced 5 separations in a 5 month period, suggesting that heat played a vital role in failure. This is quite a high number of separation failures, especially for a single haul route.

2.5 Rolling Resistance

Rolling resistance has several different characterizations depending on the application and industry of discussion, but generally can be explained by two definitions in which one is in relation to the tire itself, while the other is defined in terms of the ground or underfooting of the tire. The first definition is more representative of the automobile industry, in which rolling resistance is defined as the mechanical loss of a tire, or in simpler terms, the energy consumed by a tire as it travels its haul route (Michelin, 2011). The second definition is more representative of mining and agriculture industries, in which rolling resistance is classified as the tractive effort required to overcome the retarding effect of the ground beneath the tire (Tannant & Regensburg, 2001).

Both definitions are correct, but relative to this thesis and the mining industry, both applications are relative to a haul truck tire in its duty cycle. In this manner, rolling resistance can be viewed as both a force and energy, demonstrated in Figure 2-13.

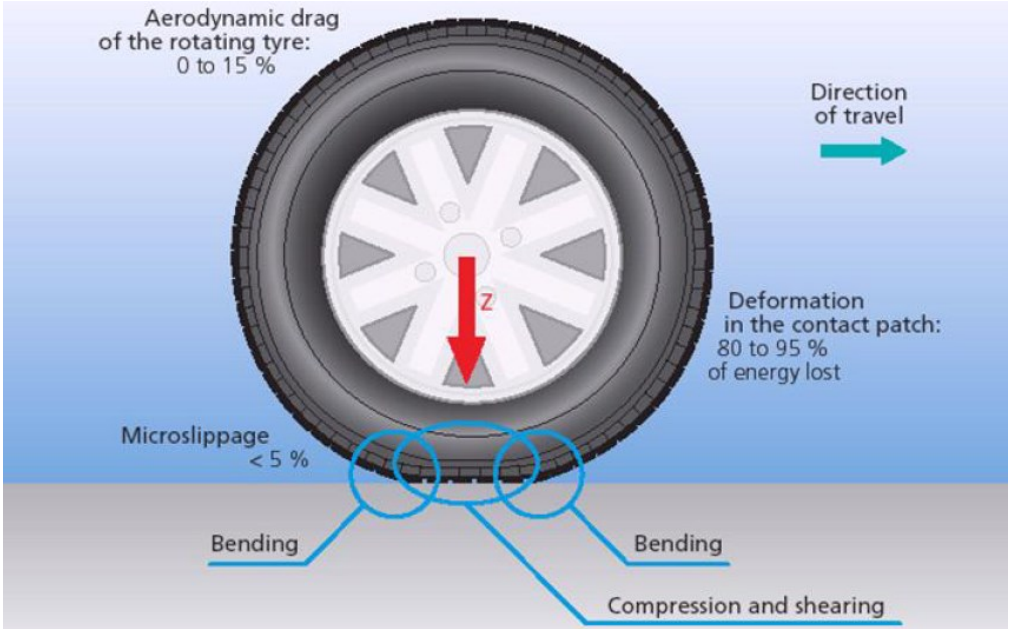

Figure 2-13 – Rolling Resistance of a Tire & Energy Lost (Michelin, 2011)

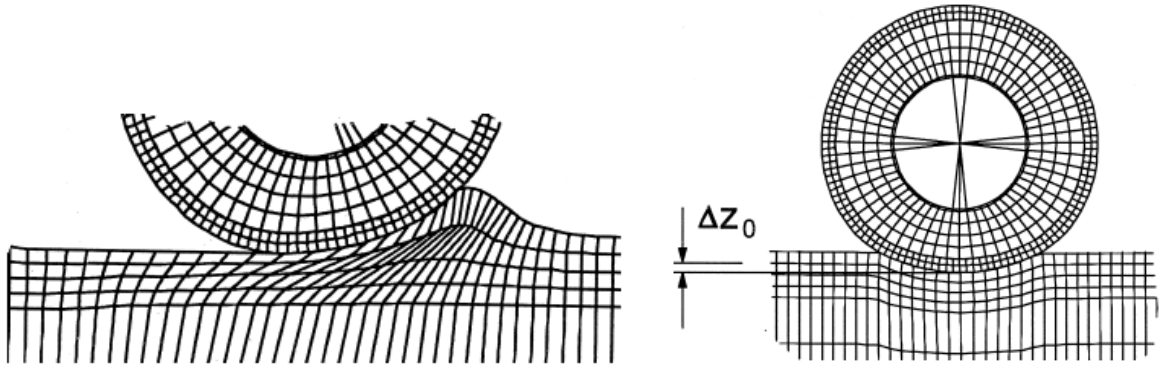

Figure 2-14 – Rolling Resistance of the Ground & Tire (Stumpf & Hohl, 2000)

Figure 2-14 demonstrates both definitions of rolling resisting by showcasing deflection of the ground as well as flexing of the tire. While rolling resistance is typically thought of in terms of tires and the ground, there are many other factors that can have an effect on the rolling resistance variable, shown below.

Vehicle

- Size & weight
- Static & dynamic weight distribution
- Number of tires
- Suspension system
- Vehicle speed
- Wheel rotational speed / slip
- Vehicle acceleration

Road Surface

- Material
- Slope
- Cross slope / crowning
- Roughness
- Temperature & precipitation
- Moisture content
- Ground bearing pressure

Tire

- Construction material
- Radial/Bias ply
- Chemical composition
- Elastomeric / hardness properties
- Tread depth & pattern
- Age & condition
- Tire pressure
- Tire temperature
- Nominal contact area

When considering ground surfaces, rolling resistance is also seen as a material property, allowing the classification of underfoot conditions for any tracked or wheeled machine, which in turn will dictate the performance and efficiency of the respective vehicle. Figure 2-15 is an example of a published classification of rolling resistance by Caterpillar (2012), which translates a general material type to an estimated rolling resistance.

UNDERFOOTING	ROLLING RESISTANCE, PERCENT*			
	Tires		Track	Track
	Bias	Radial	**	+Tires
A very hard, smooth roadway, concrete, cold asphalt or dirt surface, no penetration or flexing . .	1.5%*	1.2%	0%	1.0%
A hard, smooth, stabilized surfaced roadway without penetration under load, watered, maintained	2.0%	1.7%	0%	1.2%
A firm, smooth, rolling roadway with dirt or light surfacing, flexing slightly under load or undulating, maintained fairly regularly, watered	3.0%	2.5%	0%	1.8%
A dirt roadway, rutted or flexing under load, little maintenance, no water, 25 mm (1") tire penetration or flexing	4.0%	4.0%	0%	2.4%
A dirt roadway, rutted or flexing under load, little maintenance, no water, 50 mm (2") tire penetration or flexing	5.0%	5.0%	0%	3.0%
Rutted dirt roadway, soft under travel, no maintenance, no stabilization, 100 mm (4") tire penetration or flexing	8.0%	8.0%	0%	4.8%
Loose sand or gravel	10.0%	10.0%	2%	7.0%
Rutted dirt roadway, soft under travel, no maintenance, no stabilization, 200 mm (8") tire penetration and flexing	14.0%	14.0%	5%	10.0%
Very soft, muddy, rutted roadway, 300 mm (12") tire penetration, no flexing	20.0%	20.0%	8%	15.0%

Figure 2-15 – Caterpillar Rolling Resistance Classification Chart (by commission of Caterpillar Inc., 2012)

2.6 Haul Truck Suspension Cylinder

The most common suspension system installed on mining haul trucks can be described as an oleo pneumatic sliding pillar design, which consists of nitrogen gas over hydraulic oil, where the gas provides the spring effect. The oil offers dampening via two orifices, which control the flow of oil between the piston and cylinder to absorb the force applied on the piston (van de Loo, 2003). The pressure of the nitrogen gas and level of oil is important, as the system is designed to function at specific parameters provided by the OEM. A common cause of poor suspension cylinder performance is the gas pressure or oil level specifications are overlooked and not checked frequently during suspension cylinder maintenance. This can potentially lead to damage of the strut, tires, truck frame, and increased vibration on the operator causing fatigue and possible long term whole body vibration health repercussions.

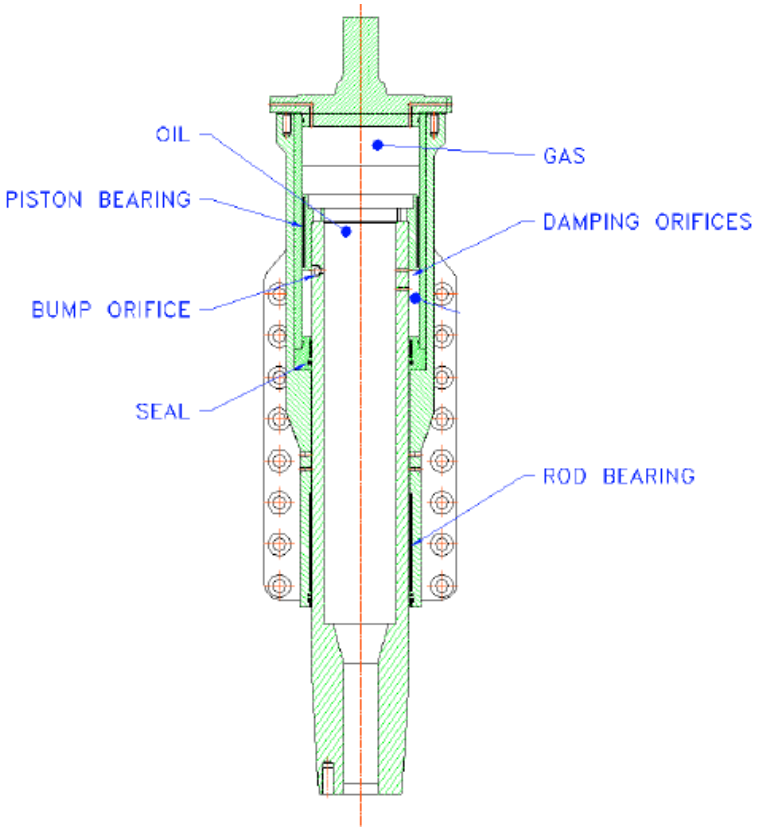

Figure 2-16 – Oleo pneumatic Sliding Pillar Suspension Cylinder (van de Loo, 2003)

2.7 Road Management Systems

Technology advances have permitted the majority of mines to record and transmit real time information from their haul fleet through various OEM or third party systems. This includes information on the health and performance of a haul truck, and typically includes GPS for dispatching purposes. Several examples of these systems include Komatsu Komtrax, Cummins Cense engine condition monitoring, MTU Friedrichshafen Engine Monitoring Unit (EMU), or Caterpillar's Vital Information Monitoring System (VIMS). The Caterpillar Road Analysis Control (RAC) system provides mines the ability to monitor road conditions by alerting operations of truck frame events as they occur, as well as having the capability to document them on a mine map through GPS (Caterpillar Inc., 2017). The RAC system has limitations, as it takes a high level approach for road monitoring, which is discussed in further detail in sections 3.7 and 5.1.

Thompson & Visser have been integral in researching into what they have termed "maintenance management systems", utilizing haul truck data to profile haul road conditions. This included outfitting a haul truck with an accelerometer to track the vertical acceleration in g-level units (Thompson R. J., Visser, Heyns, & Hugo, 2006). Utilizing the accelerometer readings, Thompson and Visser track g-level change (dg) events, explained in section 4.1, over a certain threshold value as their metric to profile ground conditions, whereas this thesis utilizes all suspension cylinder g-level change data to monitor road conditions, including small events.

Research has also been conducted on monitoring haul truck component health using suspension cylinder pressure data, as Lipsett & Hajizadeh demonstrated a wavelet-based analytical technique for detecting strut faults (Hajizadeh & Lipsett, 2015). Joseph also discusses documenting rack frame events from strut data to estimate haul truck frame life (Joseph, 2003).

3 Haul Truck Data Analysis

3.1 Oil Sand Data Set

Haul truck data was recorded from a Caterpillar 797 operating in an Oil Sand Mine, North of Fort McMurray, Alberta, Canada. The information was data logged by Caterpillar's onboard health & performance monitoring system, Vital Information Management System (VIMS). The first task was to plot the GPS coordinates from the data to determine the haul route of the truck, and distinguish between the different sections of the haul, such as pit area, secondary haul, main haul road, and dump area. Utilizing Google Earth, the GPS coordinates were overlain a satellite image from the same time frame, shown in Figure 3-1 to aid in determining the different sections of road.

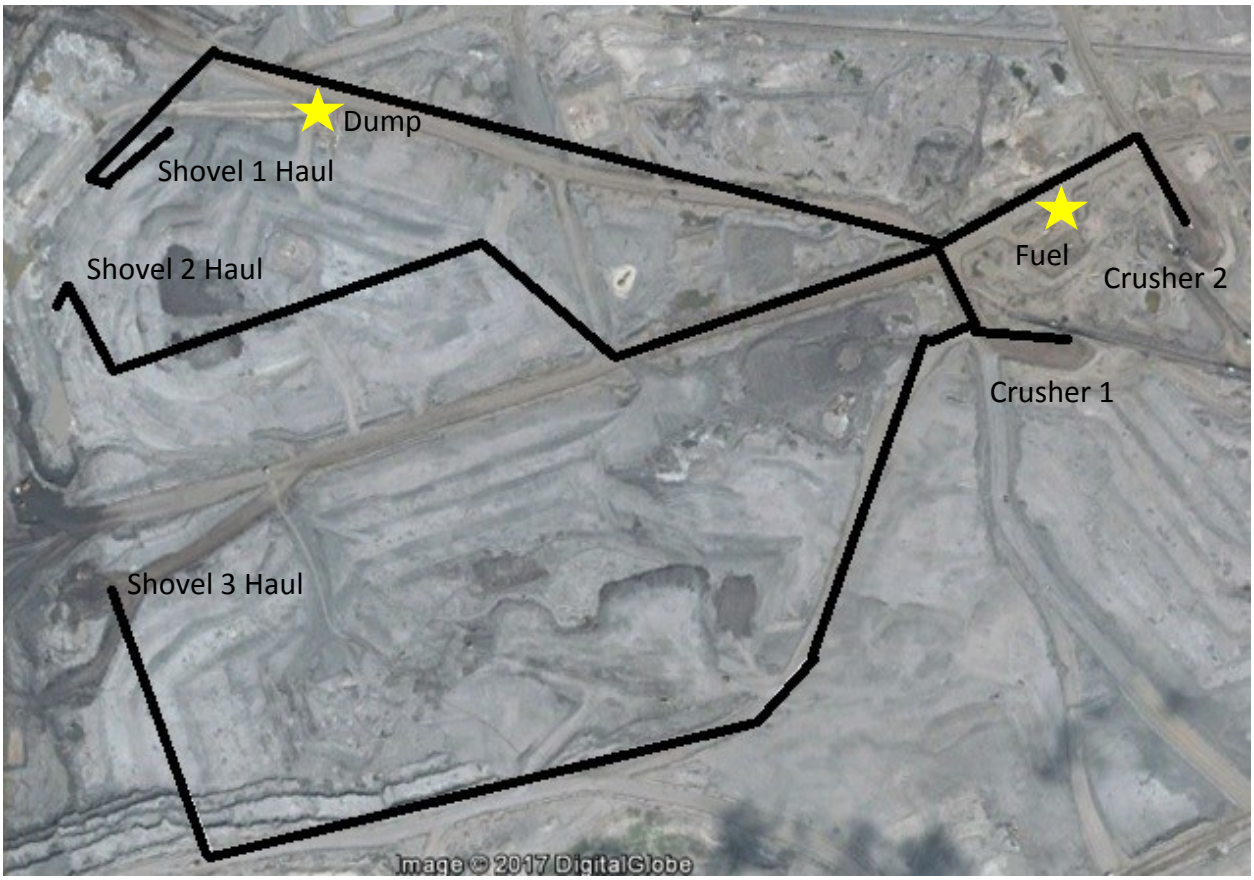

Figure 3-1 – Oil sands Haul Route Map

It was determined that the haul truck visited a total of 3 shovels, 2 crushers, and 1 dump which formed 5 different haul routes over 16 payloads delivered, demonstrated in Table 3-1.

Table 3-1– Haul Routes in Oil sands Truck Data

Haul Routes
Shovel 1 to Crusher 1
Shovel 1 to Crusher 2
Shovel 2 to Crusher 2
Shovel 3 to Crusher 2
Shovel 3 to Dump

From the haul routes, it was determined that 5 different haul sections were present; “crusher, dump, secondary haul (HR2), main haul road (HR), pit”.

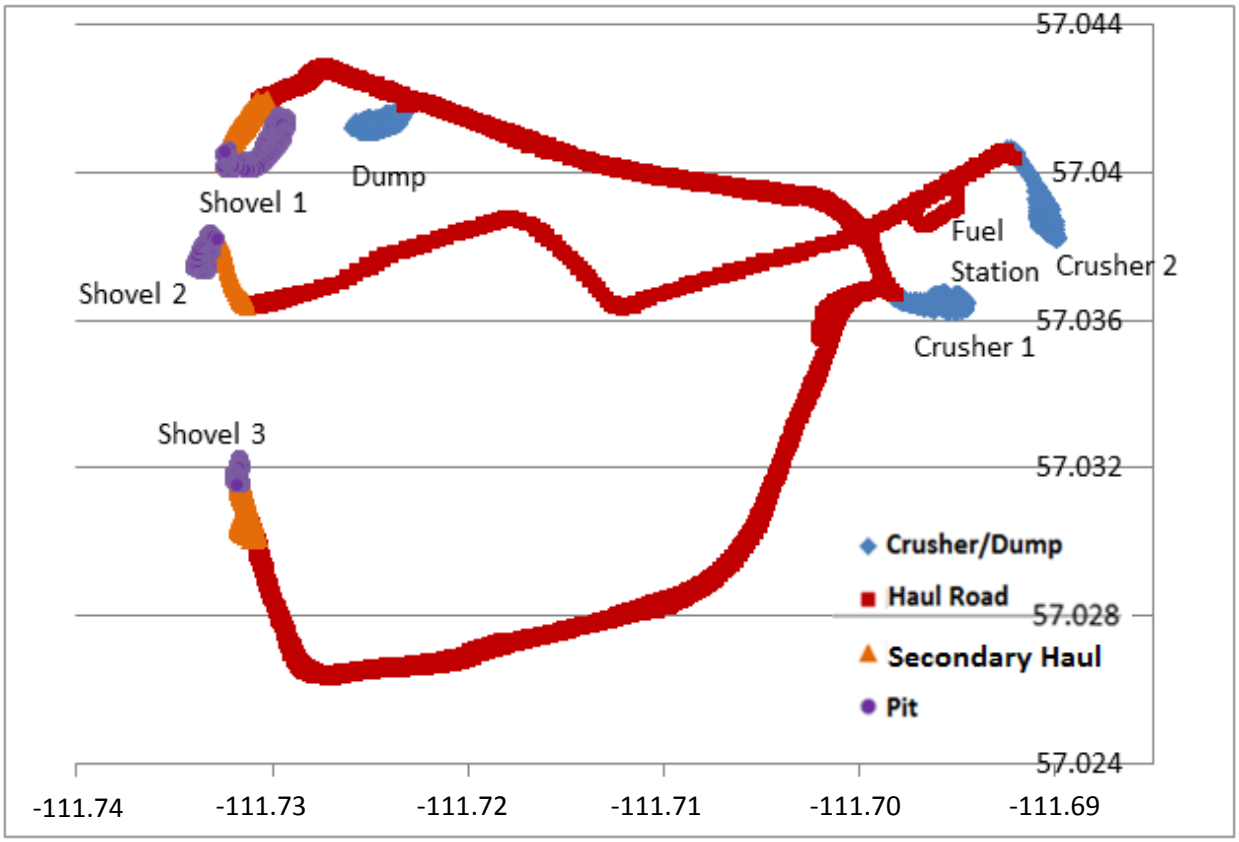

Figure 3-2 – Haul Section Map for Oil Sand Truck Data

The different sections of the haul routes are more clearly shown in Figure 3-2, defined by GPS coordinates so that a level of consistency was maintained. Elevation was not present in the data, therefore the capability to distinguish haul ramps was not possible, although previous knowledge of the mine site was known. It was hence decided to include a portion of the haul as a "Secondary Haul", which was to be directly after the "Pit" area. Having knowledge of a typical oil sands mine, this portion that was selected as a "Secondary Haul" is generally a rougher section of road compared to the main hauls, which is why it was separated from the main haul road. Table 3-2 shows the full list of parameters that were recorded from the haul truck to make up the data set used in this analysis. The data was downloaded at a 1 Hertz frequency and tracked the haul unit for a total of 8 hours over a day shift period in October 2004. The only data emitted from the analysis was during truck loading, dumping, and delay events such as the haul truck refueling; all remaining data was included.

Table 3-2 – Oil Sand Data Set Downloaded Parameters

Date	Distance (m)	Suspension Cylinder LTF (kPa)
Time	Ground Speed (km/h)	Suspension Cylinder LTR (kPa)
Longitude	Payload (metric tonnes)	Suspension Cylinder RTF (kPa)
Latitude		Suspension Cylinder RTR (kPa)

From the parameters in Table 3-2, the variables in Table 3-3 were calculated for further analysis of the haul data.

Table 3-3 – Oil Sand Data Calculated Parameters

Suspension Cylinder Force (kN)	Truck Frame Rack	Suspension Cylinder G-level Change (Δg)
Suspension Cylinder Weight (metric tonne)	Truck Frame Pitch	Suspension Cylinder G-level Magnitude (mg)
Suspension Cylinder G-level	Truck Frame Bias	Suspension Cylinder Wave (mg/D, mg/T, mg/speed)
Tire TKPH		

3.2 Suspension Cylinder Data

As mentioned in section 3.1, strut suspension data from the haul truck onboard information system was downloaded in kilopascals (kPa). To determine the mass on each strut, the pressure data was converted to a force knowing the geometry of the suspension cylinder from the manufacturer, equation 5. The front suspension cylinder on a haul truck typically have a larger internal ram area than those at the rear, to allow for greater steering control of the haul truck (Joseph, 2003), with a Caterpillar 797 haul truck having areas of 0.126m^2 and 0.114 m^2 for the front and rear suspensions respectively.

$$\boldsymbol{Force} = \mathbf{mg} = \frac{\boldsymbol{Pressure}}{\boldsymbol{Area}} \qquad 5$$

Then dividing by gravity (g = 9.81m/s^2), we can transform the strut force into suspended mass, regardless of whether the truck is stationary or moving. If in motion, then the mass is the effective dynamic mass felt by the system. By transforming all strut data to mass, theoretically the payload on a strut can be calculated by determining the mass on the strut while the haul truck is in tare condition, and the mass on the strut after a payload has been added, then finding the difference of the two values (equation 9).

This is discussed at length Joseph's 2003 paper "Large Mobile Mining Equipment Operating on Soft Ground". The force loading on the strut, F_{Tare} and F_{Load}, can be calculated when the truck is in a state of rest (V = 0) or equilibrium, with equilibrium being defined as the haul truck moving (V > 0) on a relatively flat surface providing minimal vertical acceleration to the strut, or over a large data set with frequent similar loading events.

However, the dynamic motion described above permits an evaluation regardless of this requirement, as it is demonstrated later in section 3.4, Figure 3-13, that horizontal speed has a minimal effect on the calculation of the mass on the suspension cylinder. From such calculations, the payload of the haul truck can be determined using equation 6 (Joseph, 2003).

$$\sum_{1}^{4}(\boldsymbol{m_{Load}} - \boldsymbol{m_{Tare}}) = \frac{\boldsymbol{F_{Load} - F_{Tare}}}{\boldsymbol{g}} \qquad 6$$

This approach allows for the calculation of the haul truck payload based on the suspension cylinder pressure readings during its full duty cycle. This analysis was conducted for all cycles in the collected data set to determine a calculated payload based on the strut readings, which can be found in section 3.5. Furthermore to this analysis, we can determine the magnitude of events in g-level experienced by the suspension struts as they perform their duty cycle, utilizing Newton's second law (Joseph, 2003), equation 7.

$$\boldsymbol{G\ Level_{Strut}} = \frac{\boldsymbol{F_{Dynamic}}}{\boldsymbol{F_{Load}}} = \frac{\boldsymbol{(g+a)}}{\boldsymbol{g}} \qquad 7$$

Where $F_{Dynamic}$ can be defined as the truck in motion (v > 0) during its haul cycle. Given the difficulty to identify a static 1g state; if an average mass for the tare and loaded states is determined, and it is known that the dynamic nature of the motion is a distribution around 1g, the expectant 1g mass in each state can be calculated.

G-level can also be applied to determine the rack, pitch, and bias of a truck in motion. Rack, pitch, and bias are important KPI's of which only rack plays the major role in frame life

qualification of a mining machine, although all parameters partially indicate the quality of a haul road, as it is the road conditions that predominantly cause frame life reductions.

Rack can be defined as the twist motion imposed on a haul truck rigid frame due to uneven loading at the tire-ground contact, while pitch is the distribution of force loading between the front and rear axles. Caterpillar states that rack and pitch events experienced by a haul truck have the biggest effect on frame life (Caterpillar Inc., 2017), but when considering haul road quality, bias (roll) should also be considered, which is described by the load distribution from side to side of the truck. The uneven distribution in loading of a haul truck, caused by the misplacement of payload in the haul truck body, and the "rolling" ground conditions experienced by the haul truck contribute to rack, pitch, and bias events.

$$Rack = LF + RR - RF - LR \quad (8)$$

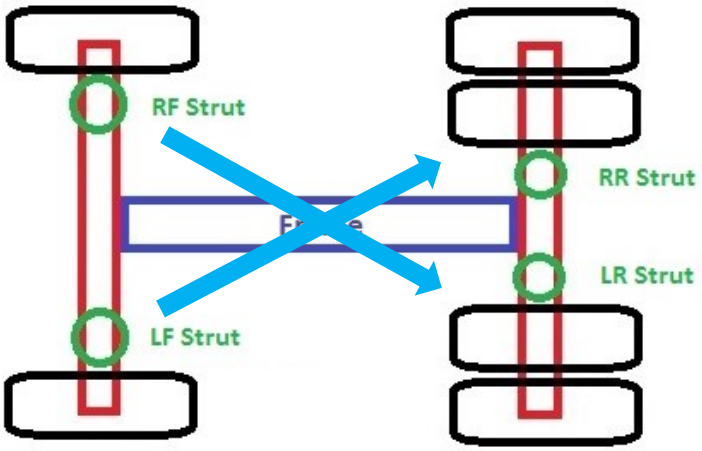

Figure 3-3 – Truck Frame Rack Event

$$Pitch = LF + RF - LR - RR \quad (9)$$

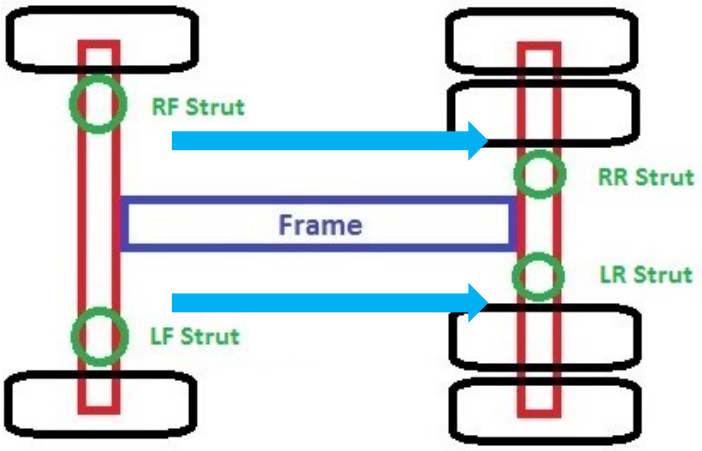

Figure 3-4 – Truck Frame Pitch Event

$$Bias = LF + LR - RF - RR \quad (10)$$

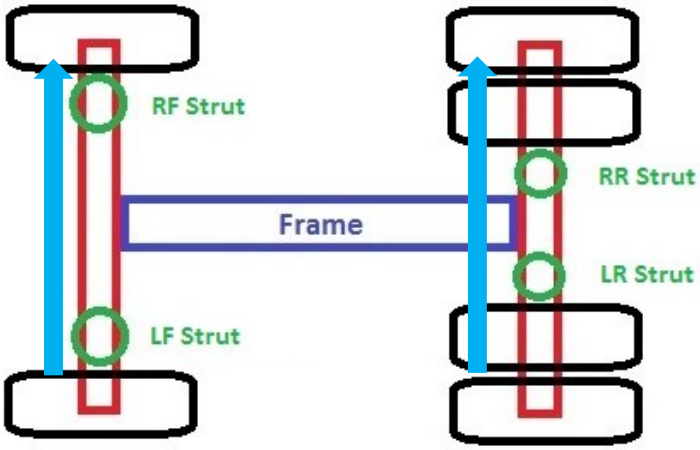

Figure 3-5 – Truck Frame Bias Event

Converting rack, pitch, and bias to g-level units is completed by utilizing the g-level results for each individual strut prior to the respective calculations from equations 13, 14, & 15 (Joseph, 2003), as illustrated in Figure 3-3, Figure 3-4, and Figure 3-5.

$$Rack = \frac{1}{g}(a_{LF} + a_{RR} - a_{RF} - a_{LR}) \quad (11)$$

$$\boldsymbol{Pitch} = \frac{\mathbf{1}}{\boldsymbol{g}}(\boldsymbol{a_{LF}} + \boldsymbol{a_{RF}} - \boldsymbol{a_{LR}} - \boldsymbol{a_{RR}}) \quad 12$$

$$\boldsymbol{Bias} = \frac{\mathbf{1}}{\boldsymbol{g}}(\boldsymbol{a_{LF}} + \boldsymbol{a_{LR}} - \boldsymbol{a_{RF}} - \boldsymbol{a_{RR}}) \quad 13$$

This method of calculating g-level for a machine as first identified by Joseph (2003), has been utilized for years and is understood and well accepted in the mining industry; as it delivers a means of relative magnitude for the events that occur during any haul truck duty cycle.

3.3 Assumptions in the Analysis

During the analysis, several assumptions were made, as the dynamic interaction of a haul truck and road surface can be complex in nature. One of the primary assumptions is that the haul truck data is accurate, or has a relatively small error associated, specifically the strut pressure data. Mining, in particular in the oil sands, presents very harsh operating conditions, and it is difficult to maintain a haul trucks components in good condition; it is possible the suspension cylinders were not in perfect health or charged to the correct OEM recommended pressure. It is demonstrated in this thesis that there is likely error associated with the strut pressure data, but it is assumed to be relative or consistent when under load. For the predominant analysis of g-level, this error is then removed or deemed minimal as the pressure data is divided into itself.

It was also assumed that a haul truck suspension cylinder is an isentropic system, with minimal change in temperature that can be dismissed for an operating haul unit. The isentropic strut system, equation 8, can be broken down to the suspension cylinder ride height and force loading, as the area of the strut does not change and is divided out.

$$P_1 V_1^{\gamma} = P_2 V_2^{\gamma} \quad (14)$$

$$\frac{F_1}{F_2} = \left(\frac{L_2}{L_1}\right)^{\gamma} \quad (15)$$

It is assumed that the force loading on the suspension cylinder is transmitted through the truck tire and applied to the ground, and vice versa. For this thesis, the interaction between the tire and the suspension cylinder will be considered a “black box”, focusing solely on the pressure readings from the suspension cylinder.

The frequency at which the data was recorded also brings about questions on the accuracy of the data. The Caterpillar VIMS system documents data at 1 hertz, but VIMS data is recorded at 10 hertz (Caterpillar Inc., 2017), specifically for RAC events; it is not understood how Caterpillar conglomerates the data from 10 Hz to 1 Hz. It could be argued that a faster acquisition frequency may present different results, as it may record more events that could have possibly been missed due to a recording rate that is too slow, which is explained by the Nyquist theorem (Joseph & Welz, 2011). Future work could investigate and compare the analysis presented in this thesis for several different recording rates, specifically 1 Hz, 2 Hz, 4 Hz, and 10 Hz.

The estimated rolling resistance of haul sections and road conditions was conducted in a quantitative manner, as there was no method present for mine operations to measure the rolling resistance during data collection. To truly understand the relationship with g-level KPI’s, a means to qualitatively measure the resistance of the surface material can be employed.

It should be stated that the mass calculated in equation 6 is the suspended mass on the cylinder versus total tare mass of the haul truck, and the force loading calculated in equation 9 is applied in addition to the total mass, including tires and rims.

3.4 Suspension Cylinder Tonnage and G-level

The tonnage and g-level were calculated for 16 cycles from the sample Oil sands mine haul truck data to better understand the loading on the truck and suspension cylinders during such a haul cycle. Figure 3-6 shows the full distribution of tonnage on the struts during these 16 haul cycles, with further detail shown in Figure 3-7 through Figure 3-10.

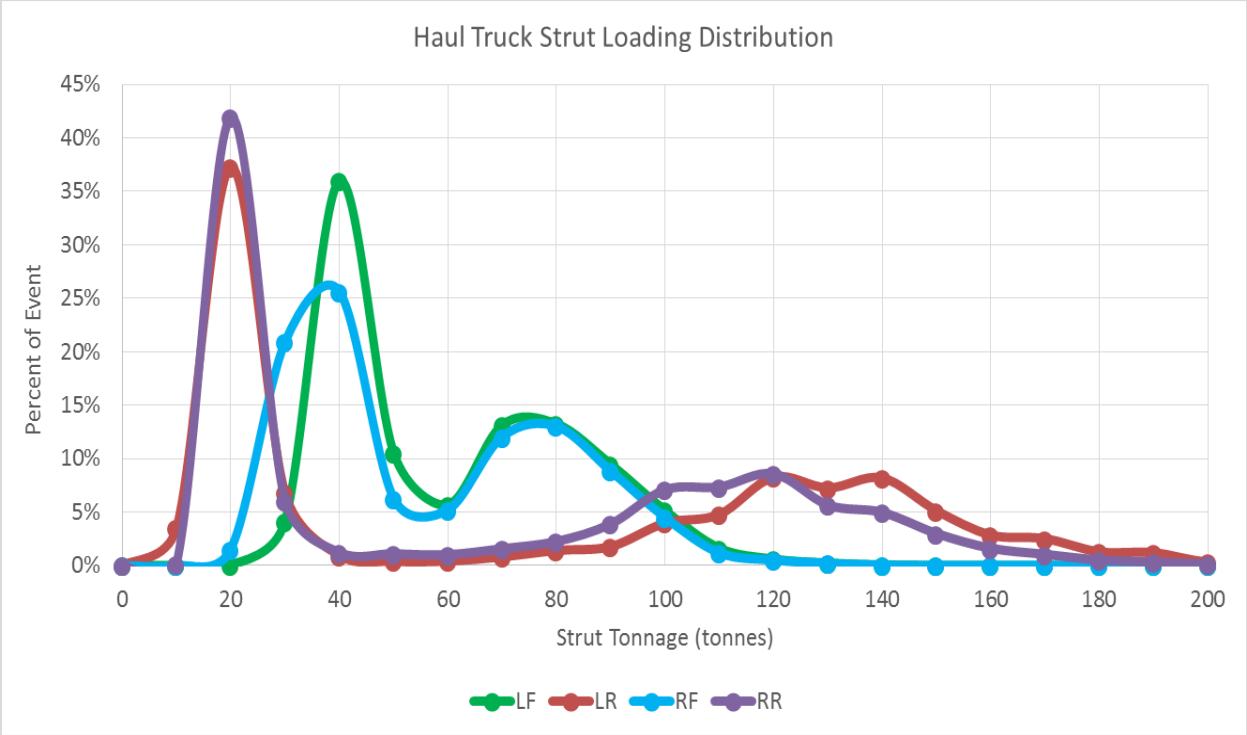

Figure 3-6 – Haul Truck Strut Tonnage Loading Distributions

Each strut demonstrates two different distributions associated with the data, which is expected for a truck loaded with a payload versus being unloaded. Once the data is split between loaded and unloaded cycles, we can clearly define normal distributions for each data set. This will allow the modeling of tonnage on a strut relative to the OEM recommended targeted payload for a specific model of haul truck, and comparable with other input variables such as recorded mine payload and estimated haul road conditions.

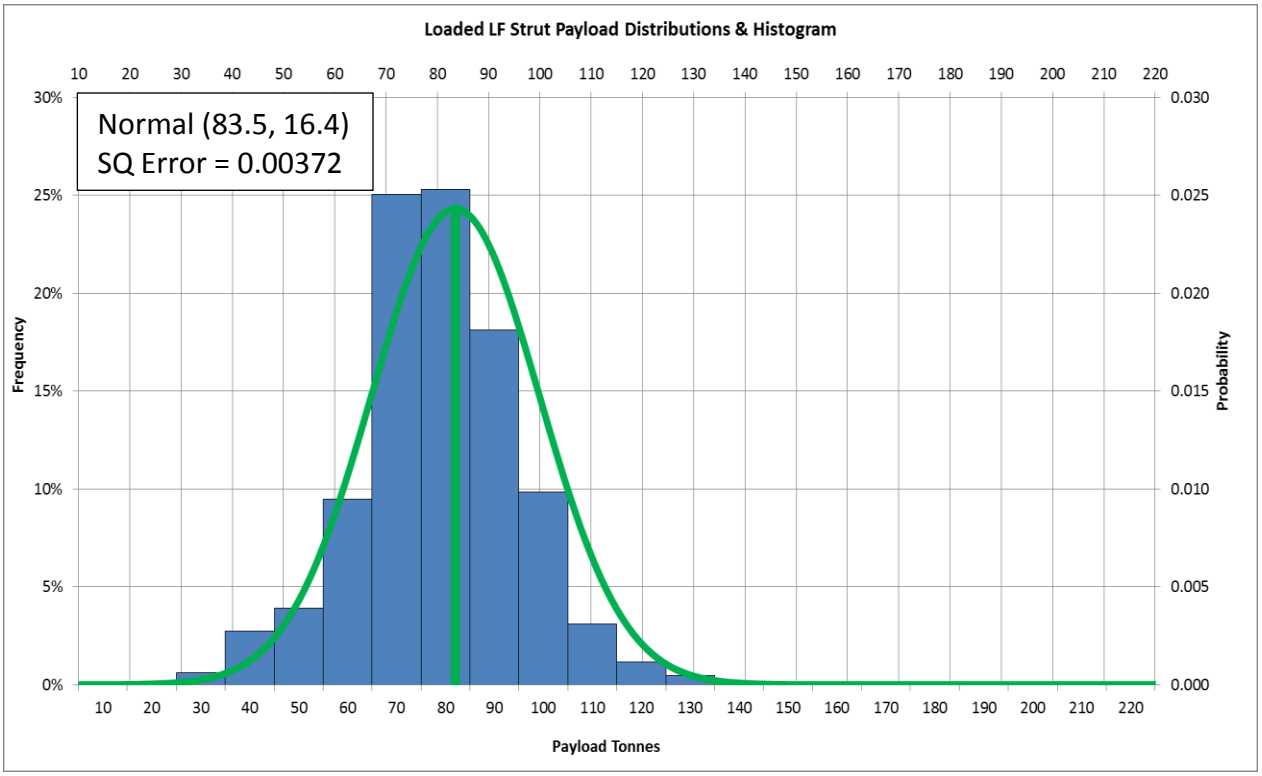

Figure 3-7 - Loaded Data from Haul Truck: Left Front Strut Tonnage Histogram Example

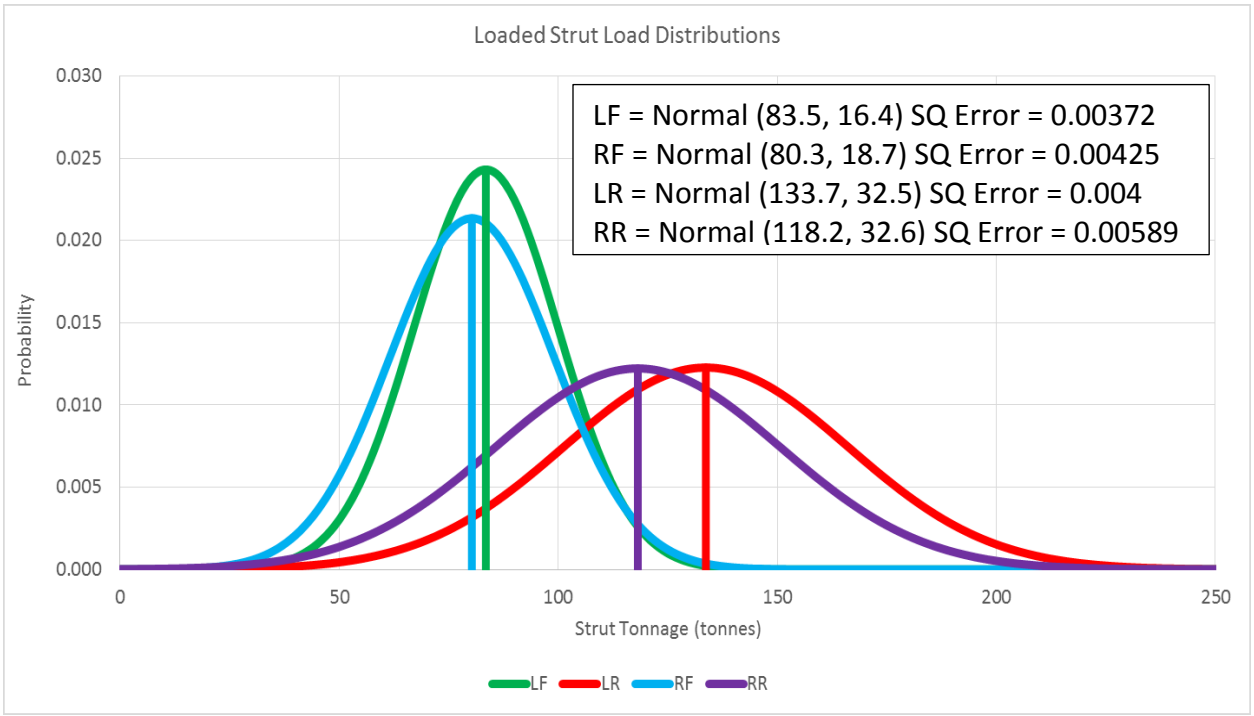

Figure 3-8 – Loaded Haul Truck Strut Tonnage Distributions

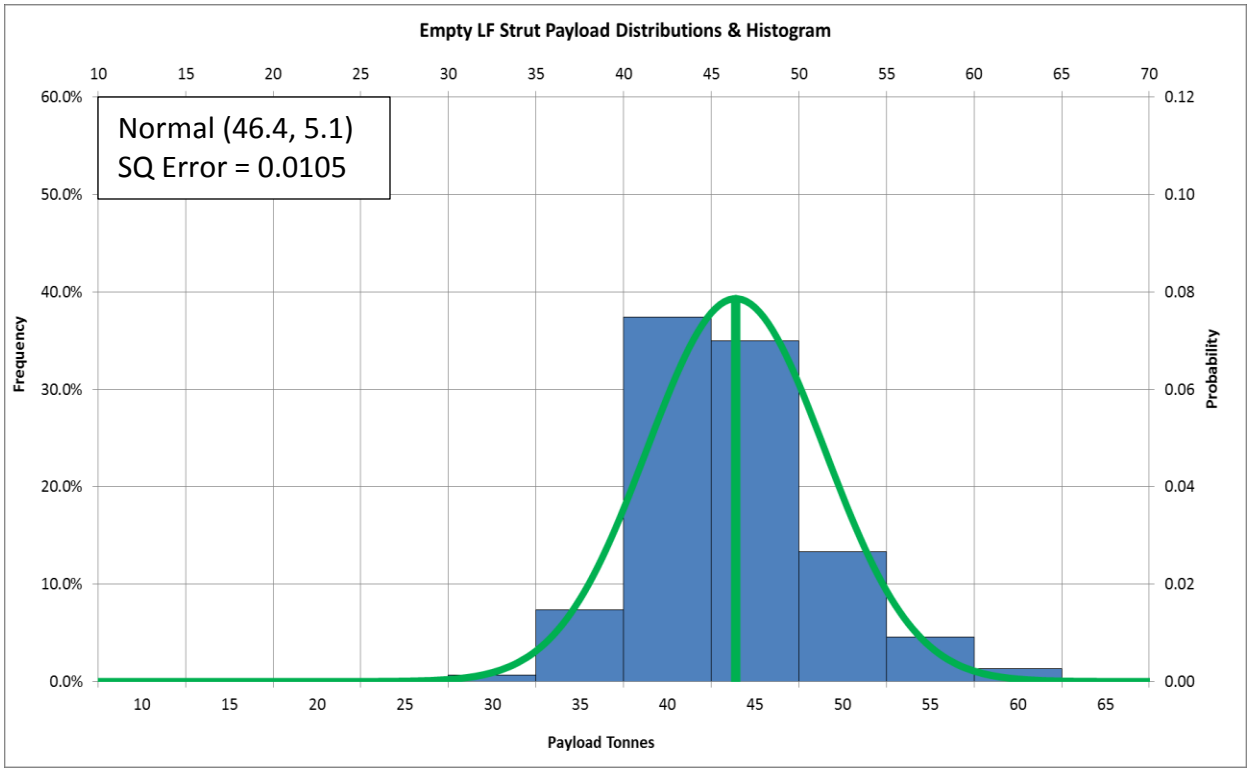

Figure 3-9 - Empty Data from Haul Truck: Left Front Strut Tonnage Histogram Example

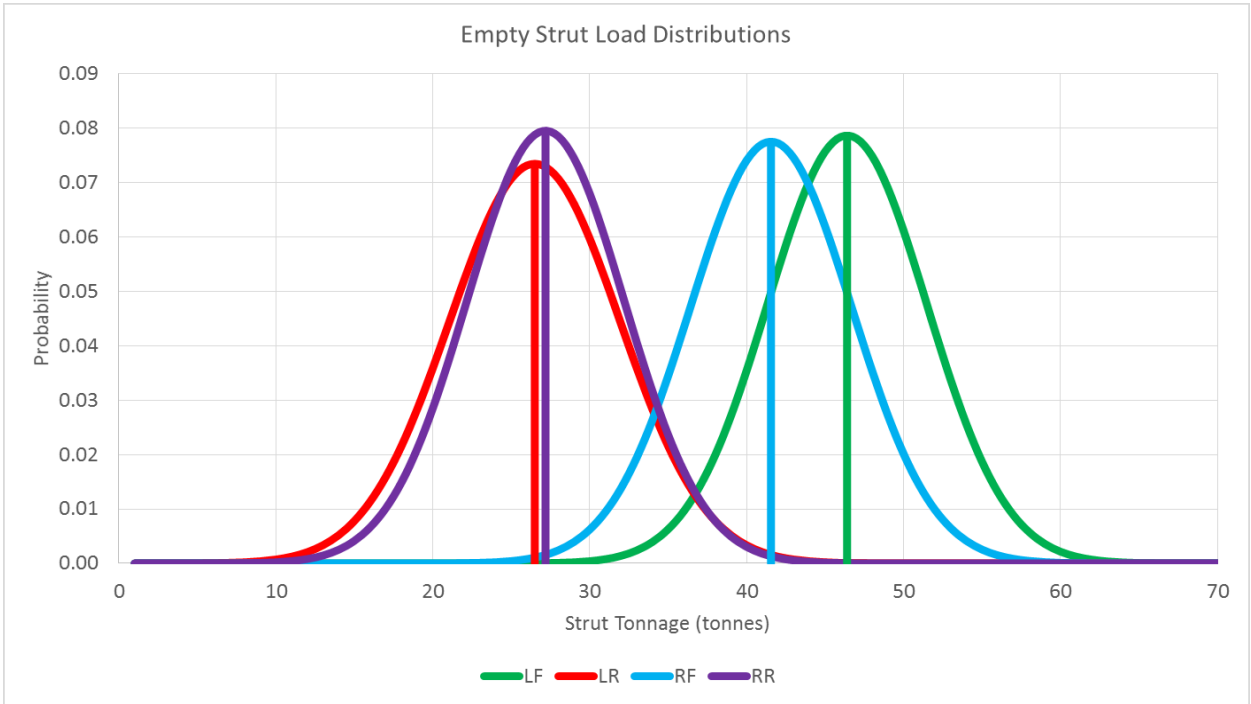

LF = Normal (46.4, 5.1) SQ Error = 0.0105
LR = Normal (26.5, 5.4) SQ Error = 0.0662
RF = Normal (41.5, 5.1) SQ Error = 0.0040
RR = Normal (27.2, 5.0) SQ Error = 0.0443

Figure 3-10 - Empty Haul Truck Strut Tonnage Distributions

In Figure 3-10, there is a discrepancy between the two front suspension cylinders, as the two rear cylinders demonstrate similar weight values, whereas a difference of 5 tonnes is seen between the front struts. This could possibly be due to improperly charged suspension cylinders causing an imbalance in loading, or the truck cab is located over the left front strut, adding extra mass. The likelihood does exist for error in the pressure data, which is further explained in section 3.9.

The strut tonnage distributions, Figure 3-8 through Figure 3-10, can also be broken out by haul section such that a relationship between haul road characteristics and strut tonnage may be derived. Figure 3-11 & Figure 3-12 demonstrate the strut tonnage normal distributions for the left front and left rear suspension cylinders, with the right side suspension cylinder distributions having similar parameters to their left side counterparts.

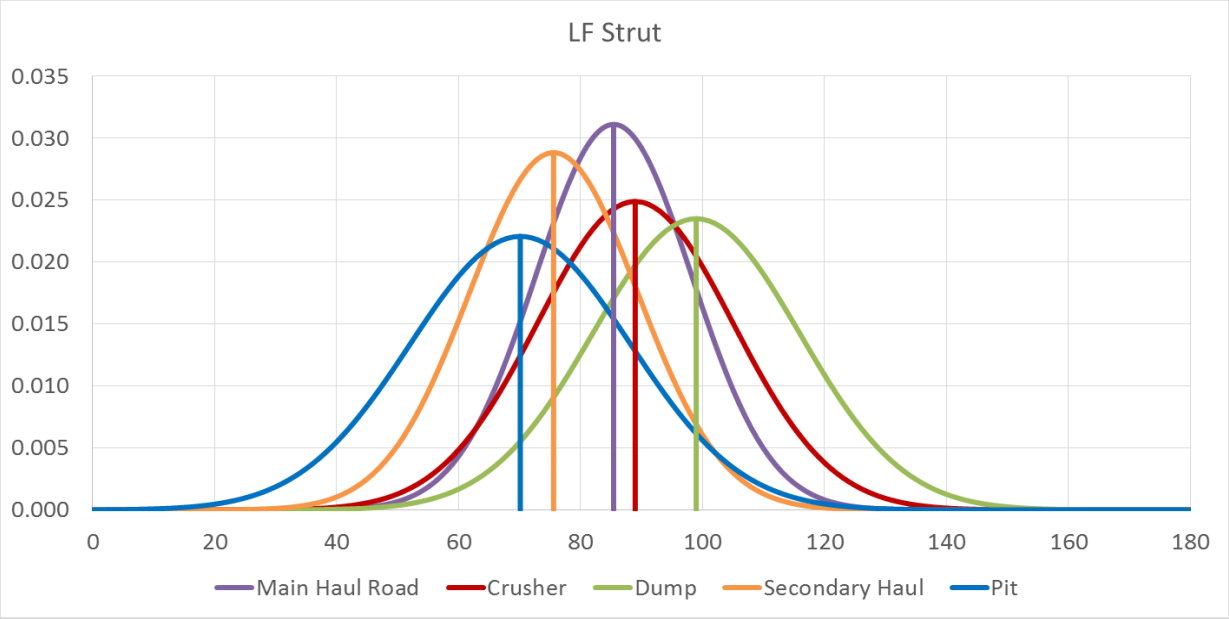

Main Haul Road = Normal (85.4, 12.8)	SQ Error = 0.00113
Crusher = Normal (89.0, 16.0)	SQ Error = 0.0204
Pit = Normal (70.1, 18.1)	SQ Error = 0.00472
Dump = Normal (99.0, 17.0)	SQ Error = 0.00347
Secondary Haul = Normal (75.6, 13.8)	SQ Error = 0.00673

Figure 3-11 – Loaded Haul Truck: Left Front Strut Tonnages per Haul Sections

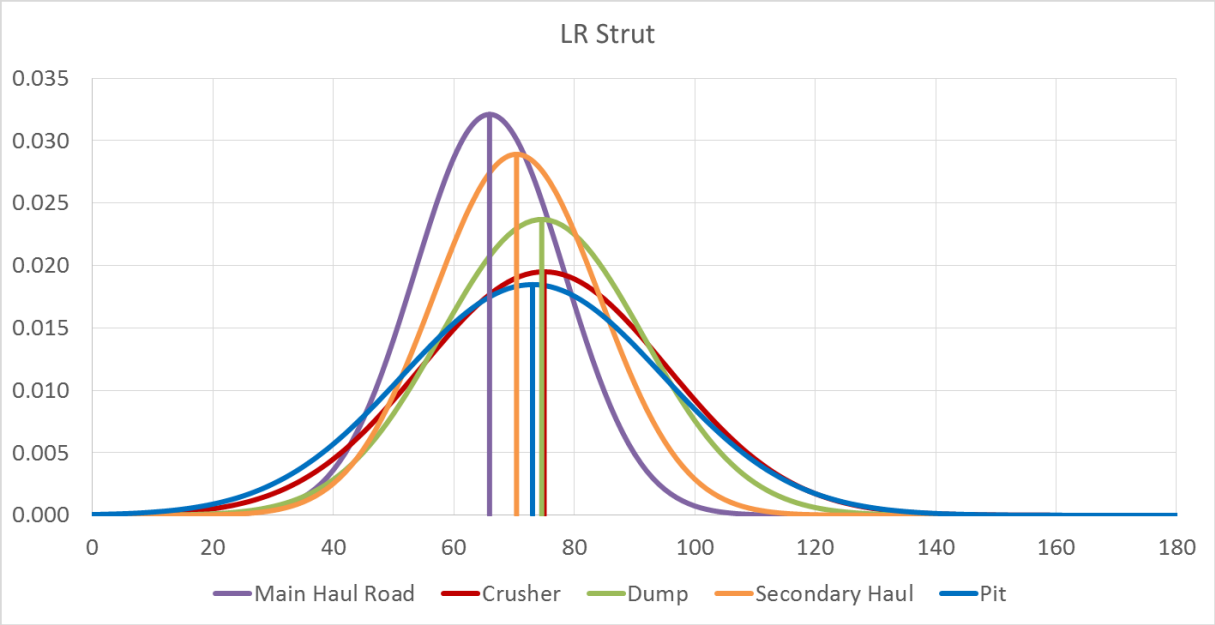

Main Haul Road = Normal (131.9, 24.9)	SQ Error = 0.00113
Crusher = Normal (150.0, 40.9)	SQ Error = 0.00646
Dump = Normal (149.2, 33.7)	SQ Error = 0.00347
Secondary Haul = Normal (140.8, 27.6)	SQ Error = 0.00663
Pit = Normal (146.2, 43.2)	SQ Error = 0.0128

Figure 3-12 – Loaded Haul Truck: Left Rear Strut Tonnages per Haul Sections

Modelling of the suspension cylinder distributions and determination of the square error was completed utilizing Rockwell's Arena Software Package. This package includes an Input Analyzer tool that has the capability to fit several different distributions and run a statistical analysis to determine the goodness of fit; this software was utilized throughout this thesis to aid in modelling.

One hypothesis considered in this work which might cause a difference in average strut tonnage by haul section was the impact of speed over a section. Typically a haul truck is able to travel faster on a main haul road compared to the pit or dump; as there are longer straight sections, better constructed road conditions, and less frequent traffic on main hauls compared to tighter or low speed imposed sections of road.

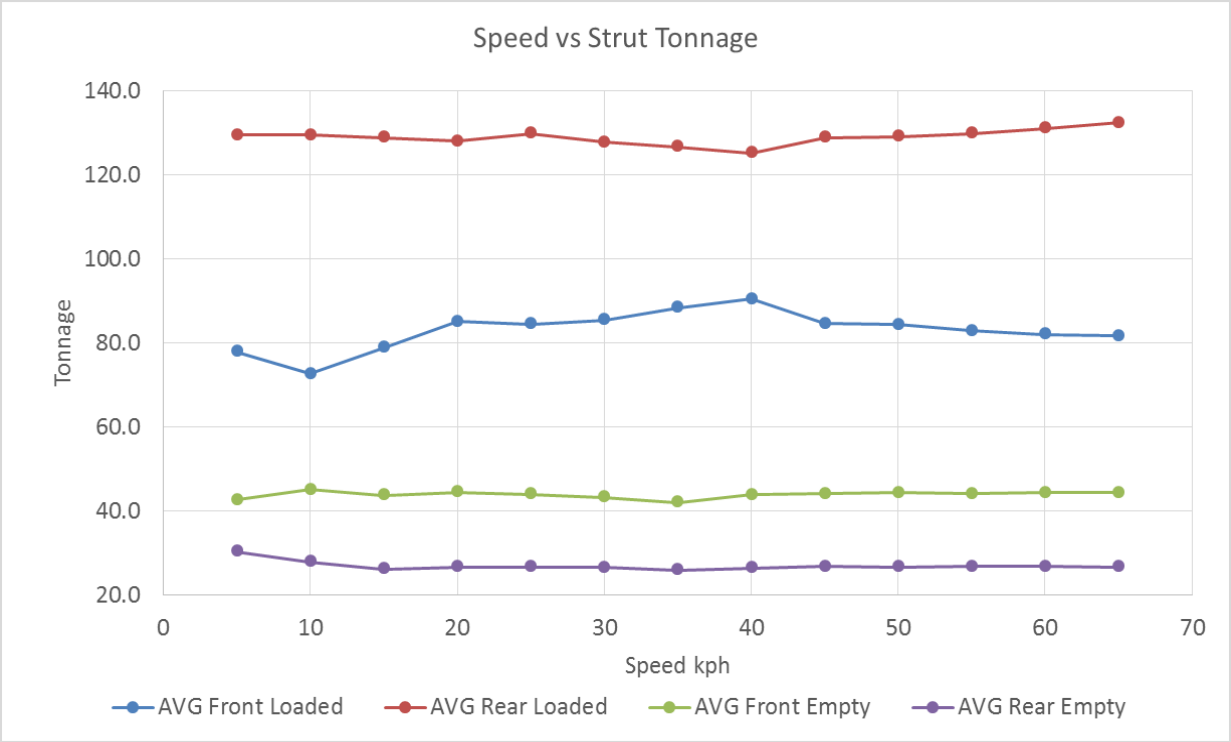

Figure 3-13 – Truck Speed vs Suspension Cylinder Tonnage

It would be expected that larger strut events and higher tonnages would be experienced by a suspension cylinder as speed increases, as anyone who has driven in a motor vehicle can relate to the repercussions of driving over a "pothole" at high speeds vs low speeds. However, the data in this thesis reveals the impact of speed having minimal effect on the loading on a strut, as demonstrated in Figure 3-13. Strut tonnage levels vary marginally by speed, but no clear correlation between increase in speed and increase in strut tonnage exists. It is possible that haul truck operators were capable to "slow down" prior to rough road conditions, to minimize the effect of speed on strut tonnage loading.

However, this leads to the hypothesis that the road conditions, per the rolling resistance and road roughness, must have greater accountability for the variance in strut load distribution presented in Figure 3-11 & Figure 3-12.

3.5 Calculation of Suspension Cylinder Equilibrium Weights

As demonstrated in section 3.2, F_{Tare} and F_{Load} were calculated for the strut data set, followed by corresponding m_{Tare}, m_{Load}; to determine the payloads for all 16 cycles where the results are shown in Figure 3-14.

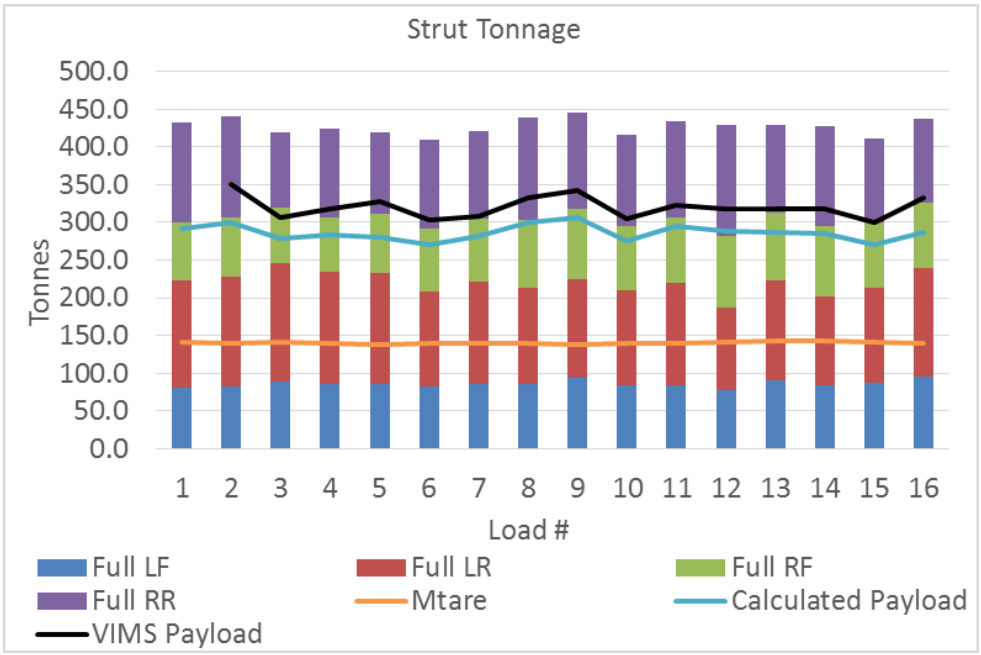

Figure 3-14 – Calculated Mass of Haul Truck Empty and Loaded for Oil Sands Data Set

The calculated m_{Tare} of 140.8 tonnes was reasonably consistent for all cycles, with the only variance determined as "carryback", which is payload or debris that remains stuck on a haul truck body, which is minimal during an October (fall) seasonal period. It should be noted that m_{Tare} should not be confused with the actual tare weight of the haul truck, as m_{Tare} does not include "unsuspended" components such as tires and rims.

For an operating Caterpillar 797B haul truck in the Canadian Oil sands, including debris and fuel, the tare weight is typically ~275 tonnes, suggesting a target payload of 349 tonnes. The average m_{Load} from the data was 427.2 tonnes, and subtracting the m_{Tare} of 140.8 tonnes provides a calculated payload of 286.3 tonnes, with a distribution range from 270 to 306 tonnes.

The calculated payloads are low compared to the Caterpillar 797 advertised 363 tonne (400 ton) payload or target payload of 350 tonnes based on a true empty operating weight, which raises the question, if the calculation method used here, is valid for calculating payload. The data set was recorded in fall (October), which in the Canadian Oil sands could mean onset poor weather with poor underfoot conditions, possibly resulting in operations having to "light load" haul trucks to ensure they do not become stuck, due to higher than expected rolling resistance. It is also conceivable that the material density of the material being hauled, oil sand or waste, was relatively lighter than expected causing the truck body to be filled not on a weight but on a volume basis prior to reaching the target payload. Recent work by Joseph (2017) shows loose density of oil sand in truck bodies maybe less than $1.5t/m^3$ (Joseph, Duncan, & Curley, 2017).

When compared to the Vital Information Management System (VIMS) payloads, the calculated payloads based on strut pressures indicated a 10.7% difference. While it cannot be verified that the VIMS payload is accurate, it is the experience of the author that VIMS payloads on Caterpillar haul trucks typically underestimate the haul truck payload by roughly -3% in oil sands operations. This difference is also in part due to the instant at which the VIMS system recognizes payload and locks the value, at a 2^{nd} gear transition re-weigh, which in an oil sands application would be generally within the pit area with extremely poor underfoot conditions, whereas in hard rock mines this would occur on better running surfaces.

3.6 Suspension Cylinder G-level

Utilizing the calculated m_{Tare} & m_{Load} from Figure 3-14, the g-level experienced by the suspension cylinders at any instant, can be calculated utilizing equation 7, for a haul truck as it performs its full duty cycle. As previously highlighted in section 3.1, the haul cycle was organized into 4 different haul sections, shown in Figure 3-15.

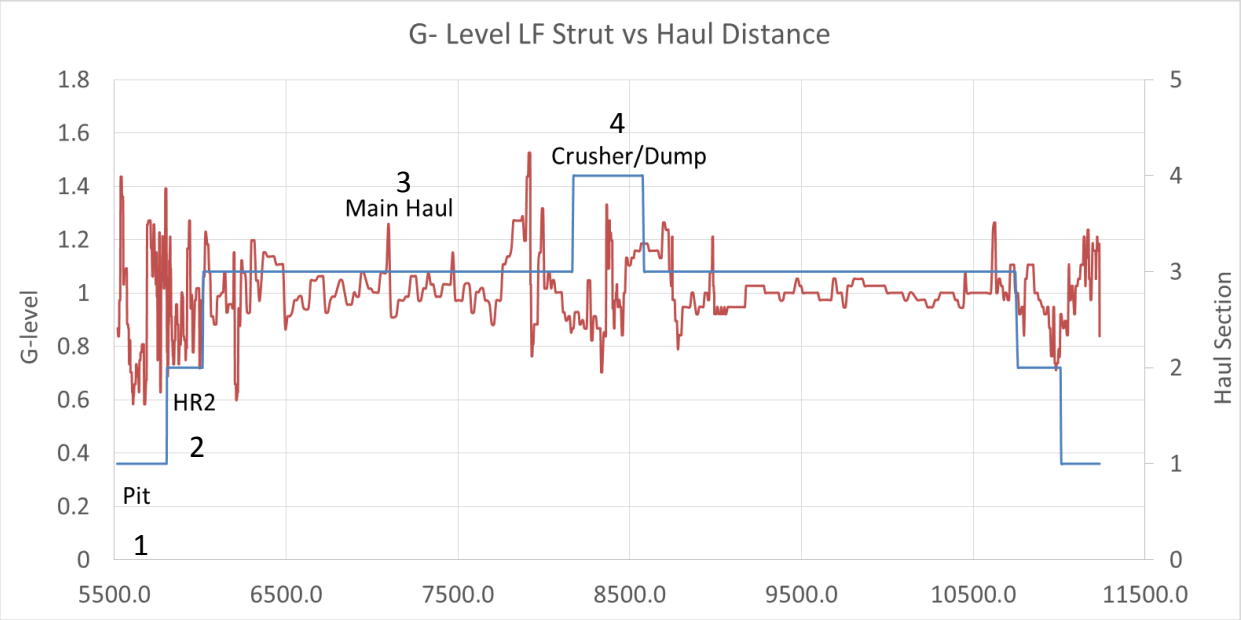

Figure 3-15 – Left Front Suspension Cylinder G-level Example

The suspension cylinder g-level response versus section of haul road is clearly identifiable by the frequency and magnitude of "change in g-level", Δg, shown in Figure 3-15. This would be expected, as for example the rolling resistance and road roughness in a shovel pit is almost guaranteed to be significantly higher than that of a main haul, especially in an oil sands application, due to the compositional material compacted stiffness of a main haul road versus a temporary haul or pit/dump section. An analysis was conducted on the average g-level by section, empty and loaded, to determine any correlation between rolling resistance and strut g-level.

One argument that arises when discussing suspension cylinder g-level for an empty haul truck is that large g-level events would not have the same effect on a strut or truck frame compared to when a haul truck is in a loaded condition. The g-level calculations may demonstrate similar values of g-level between an empty haul truck and loaded haul truck, but in reality the strut pressure will be significantly higher for a loaded haul truck. OEM's also design haul trucks for the unit to be loaded, therefore an empty truck would not register the same magnitude of stress on the frame or components as a loaded haul truck. The calculation of g-level for an empty haul truck is important however, when we are considering the haul road profile for a truck's empty haul route; as the possibility exists that the suspension cylinder may react differently to a road profile when empty compared to loaded, which will be investigated later. Therefore, events relating to haul truck structure will depend far more on loaded haul truck data interpretation, whereas analysis an overall considering the suspension cylinders reaction in regards to the haul profile will also include empty haul truck data, as shown in Figure 3-16.

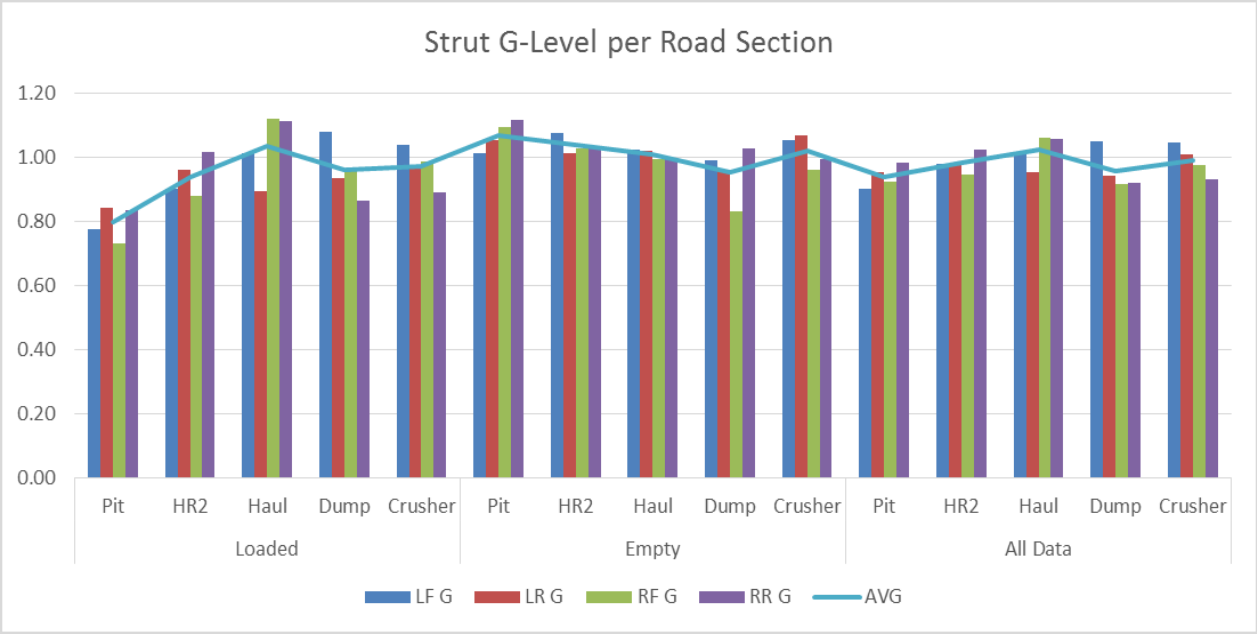

Figure 3-16 – Suspension Cylinder Average G-level per Haul Section

The rolling resistance for each section was qualitatively estimated, as opposed to quantitative methods, from mine site operations who collected the data and based on known oil sand running surface rolling resistance conditions, included in Table 3-4 (Anon., 2004). Rolling resistance was then plotted versus the average g-level by location section in Figure 3-17, with the results demonstrating that when hauling on soft underfoot conditions, g-levels for a suspension cylinder display lower values in areas of high rolling resistance. When empty, the opposite occurs with an increase in rolling resistance correlating to an increase in g-level.

Table 3-4 – Estimated Rolling Resistance for Oil Sands Data Set (supplied by oil sands site operations, (Anon., 2004))

Section	Loaded RR %	Empty RR %
Pit	10	8
Secondary Haul	6	5
Main Haul	4	3
Dump	8	6
Crusher	5	4

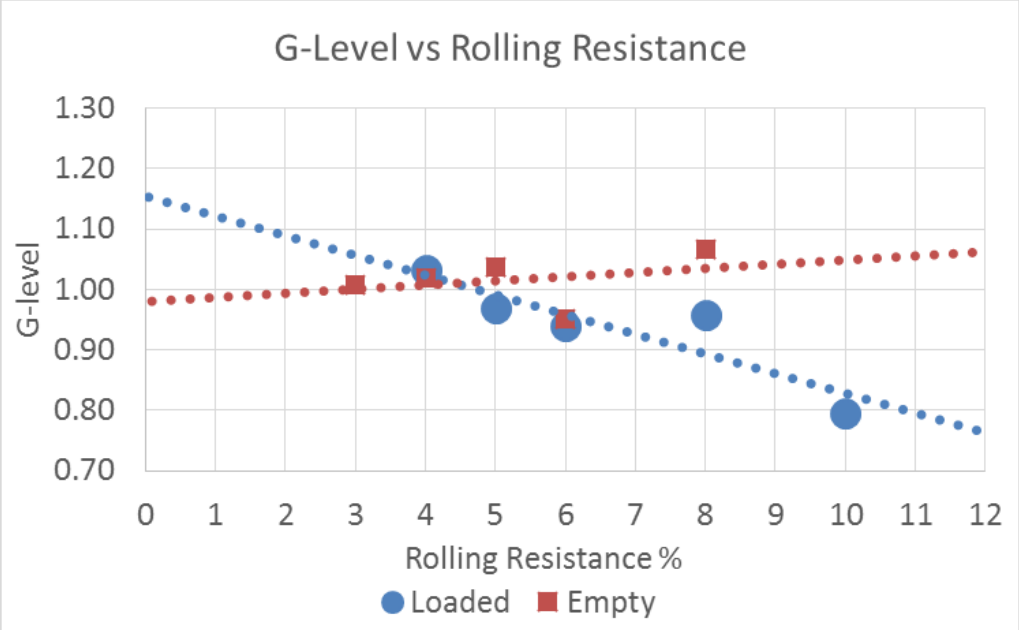

Figure 3-17 - Average G-level per Road Section versus Estimated Rolling Resistance

The overall interpretation of Figure 3-17 is that when a haul truck is loaded under soft ground conditions, high rolling resistance underfooting would exhibit more deformation than lower rolling resistance underfoot conditions, thereby dampening the force on the struts. When the haul truck is empty, the ground pressure imposed by the truck tire would be far less than when loaded, and overall the truck would experience a lower rolling resistance and decreased dampening effect from the ground. A strong relationship exists between rolling resistance and road roughness; thus in areas with high rolling resistance, an empty truck and its struts would be highly affected by rutting and rough roads, whereas a loaded truck may actually deform any rutting or “bumps” in the road, reducing the g-level response.

While the rolling resistance was estimated for the defined sections of the mine, most would agree for a typical oil sands mine, the pit and dump areas would prove to have higher rolling resistance compared to main hauls, therefore a trend can be established in reference to good or poor road conditions. Figure 3-17 demonstrates the trend between g-level & rolling resistance; the latter defined in Table 3-4, with the only outlier being the dump section of the haul cycle, most likely due to a good portion of the data set of that location being affected by a combination of the truck travelling in reverse and travelling with a raised body to effect the dumping action.

3.7 Rack, Pitch, & Bias

As defined in section 3.2 and calculated via equations 10 through 12, rack, pitch, and bias (RPB) are KPI's used to track the effect of a haul road on haul truck engines and components. Caterpillar is calculating rack and pitch data via a Road Analysis Control (RAC) system, and interpolating this data using a Fatigue Equivalent Load Analysis (FELA) tool, determines the severity of rack and pitch events, which attempts to benchmark road conditions (Caterpillar Inc., 2017). However, FELA is numbered in kPa pressure units, which provides little corresponding reference. To better understand rack, pitch, and bias, these events were plotted for the loaded haul truck using some oil sands data, shown in Figure 3-18, as g-level and statistics in Table 3-5.

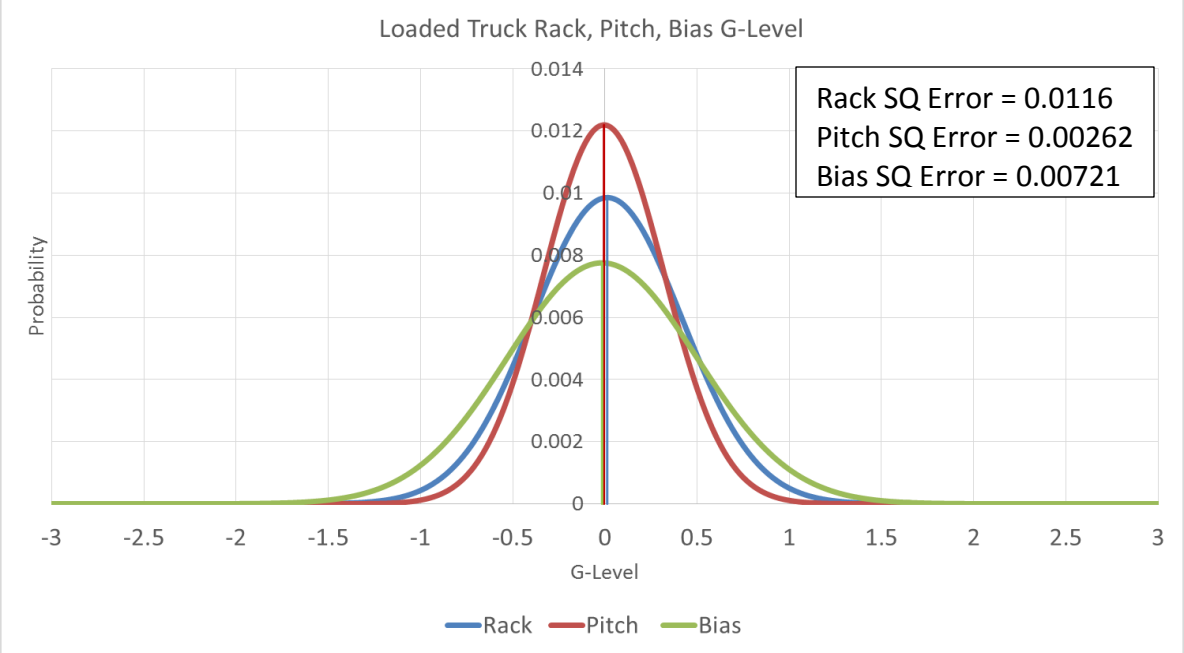

Figure 3-18 – Loaded Haul Truck Rack, Pitch, & Bias Events

Table 3-5 – Loaded Haul Rack, Pitch, & Bias Statistics

Statistics	Rack	Pitch	Bias
Average	0.01	0.00	-0.02
Std. Dev.	0.40	0.33	0.51
Maximum	2.59	1.63	2.21
Minimum	-1.71	-1.09	-2.11

From the data, RPB events generally follow a normal distribution, as demonstrated in Figure 3-19. This permits the estimation of the events under “normal” duty cycle conditions; but it must be understood how adverse road conditions contribute to rack, pitch, and bias experienced by a haul truck. In an effort to establish a relationship between road conditions and RPB events, distribution curves were plotted for each road segment in the haul data, Figure 3-20 through Figure 3-22.

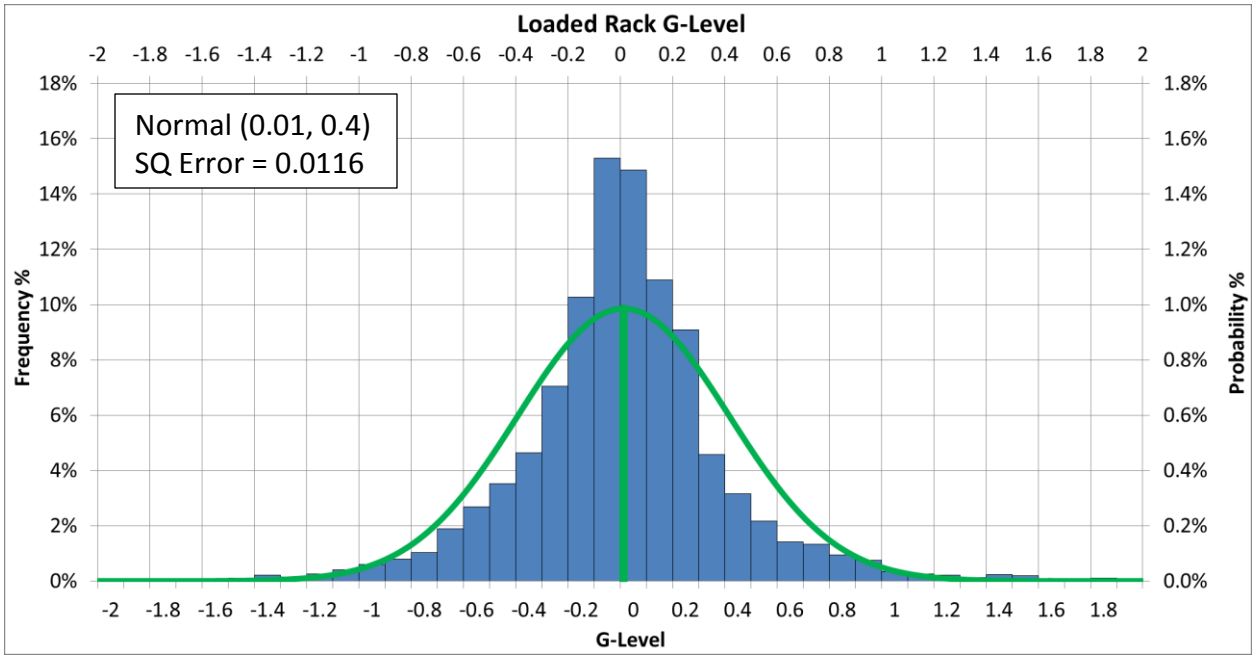

Figure 3-19 – Loaded Haul Rack Events Histogram Example

It was expected that sections with a higher rolling resistance and road roughness, such as the pit and dump areas, would exhibit a broader distribution with a larger standard deviation compared to a more established haul road. From the rack distributions in Figure 3-20, little variance exists between haul sections except for the range or standard deviation of the distributions, Table 3-6.

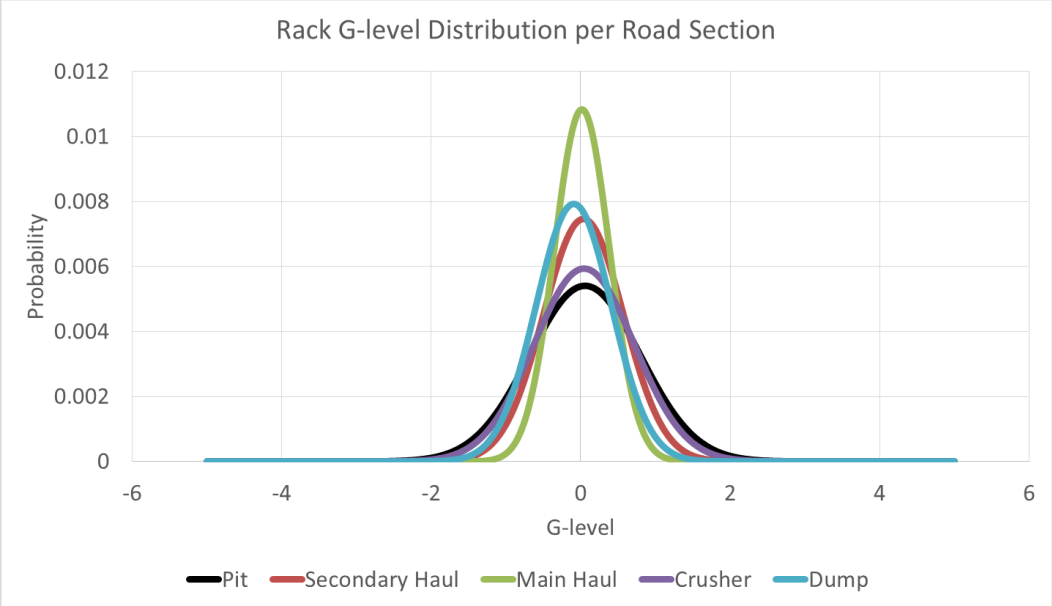

Main Haul Road SQ Error = 0.00602	Crusher SQ Error = 0.00461
Dump SQ Error = 0.00284	Pit SQ Error = 0.00604
Secondary Haul SQ Error = 0.00125	

Figure 3-20 – Loaded Haul: Rack G-level Distribution per Road Section

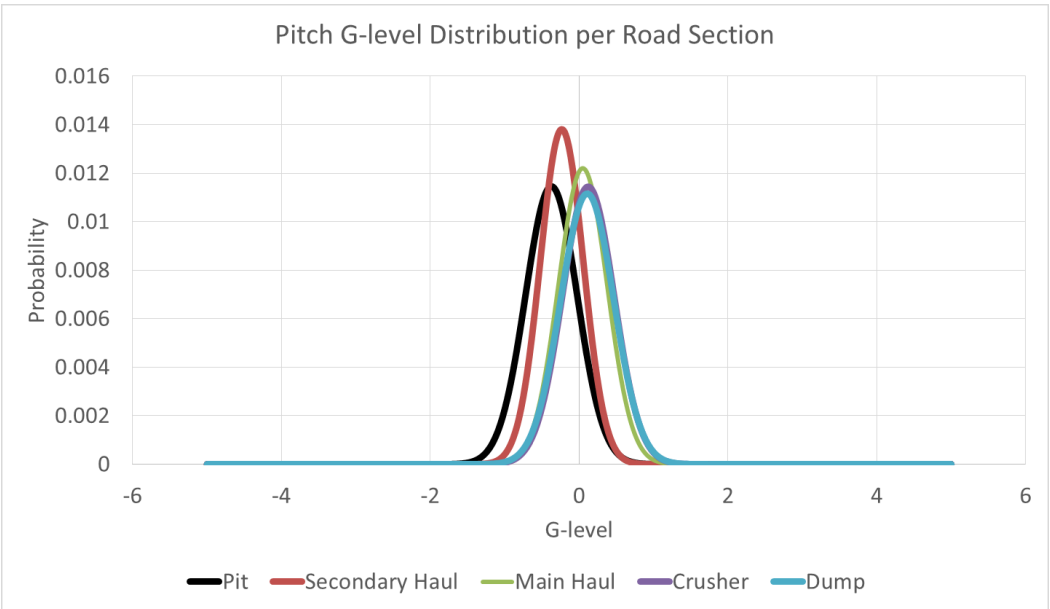

Main Haul Road SQ Error = 0.00383	Crusher SQ Error = 0.0171
Dump SQ Error = 0.00499	Pit SQ Error = 0.00873
Secondary Haul SQ Error = 0.0146	

Figure 3-21 – Loaded Haul: Pitch G-level Distribution per Road Section

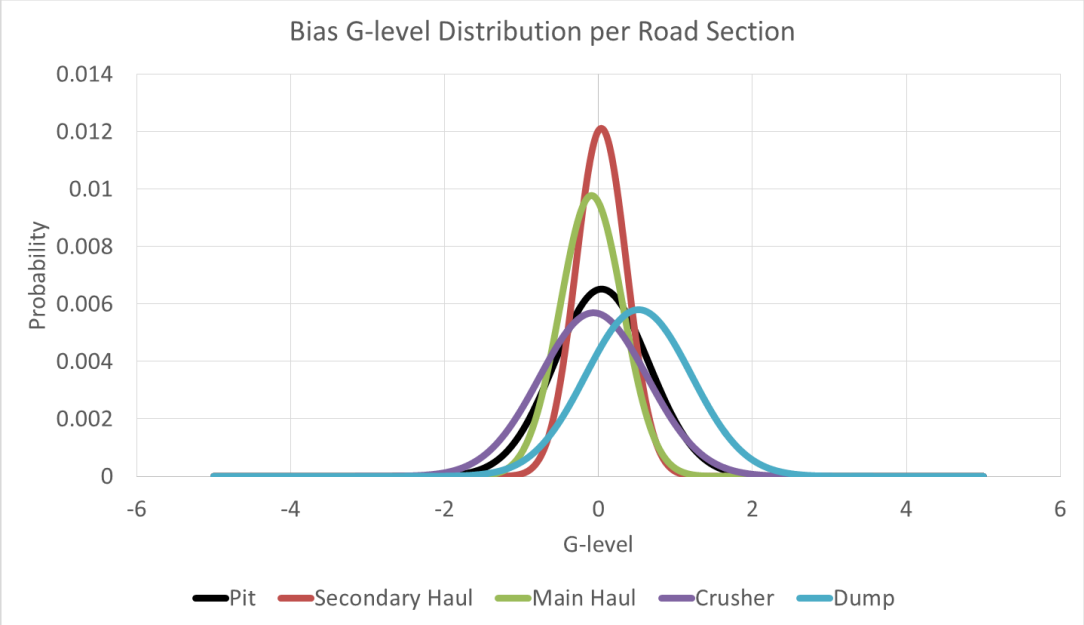

Main Haul Road SQ Error = 0.00667	Crusher SQ Error = 0.00917
Dump SQ Error = 0.00234	Pit SQ Error = 0.00614
Secondary Haul SQ Error = 0.00279	

Figure 3-22 – Loaded Haul: Bias G-level Distribution per Road Section

In Figure 3-21, it is interesting to see that for two different rough haul sections, Pit & Secondary Haul, the pitch distribution for the pit is predominantly negative and therefore rear load favoured, which would be considered normal; whereas the pitch distribution for the dump is forward favoured. The dump section also exhibits a positive (left) offset in the bias distribution curve. This is possibly explained by the fact that operators typically turn towards the opposite side of their cab (turn right) as they maneuver within the dump area, expressed in Figure 3-23, thus putting more stress on the left side of the machine.

Table 3-6 – Loaded Haul Rack, Pitch, & Bias Statistics per Road Section

Statistics		Pit	Secondary Haul	Main Haul	Crusher	Dump
Rack	Average	0.06	0.04	0.02	0.04	-0.09
	Std. Dev.	0.74	0.53	0.37	0.67	0.50
	Maximum	2.59	2.31	1.70	1.84	1.41
	Minimum	-1.71	-1.56	-1.11	-1.68	-1.67
Pitch	Average	-0.37	-0.23	0.05	0.12	0.11
	Std. Dev.	0.35	0.29	0.33	0.35	0.36
	Maximum	1.31	0.74	1.63	1.13	1.16
	Minimum	-1.09	-0.78	-0.94	-0.71	-0.74
Bias	Average	0.04	0.04	-0.09	-0.07	0.52
	Std. Dev.	0.61	0.33	0.41	0.70	0.69
	Maximum	1.31	0.92	1.90	1.90	2.21
	Minimum	-1.42	-0.84	-2.11	-1.99	-1.47

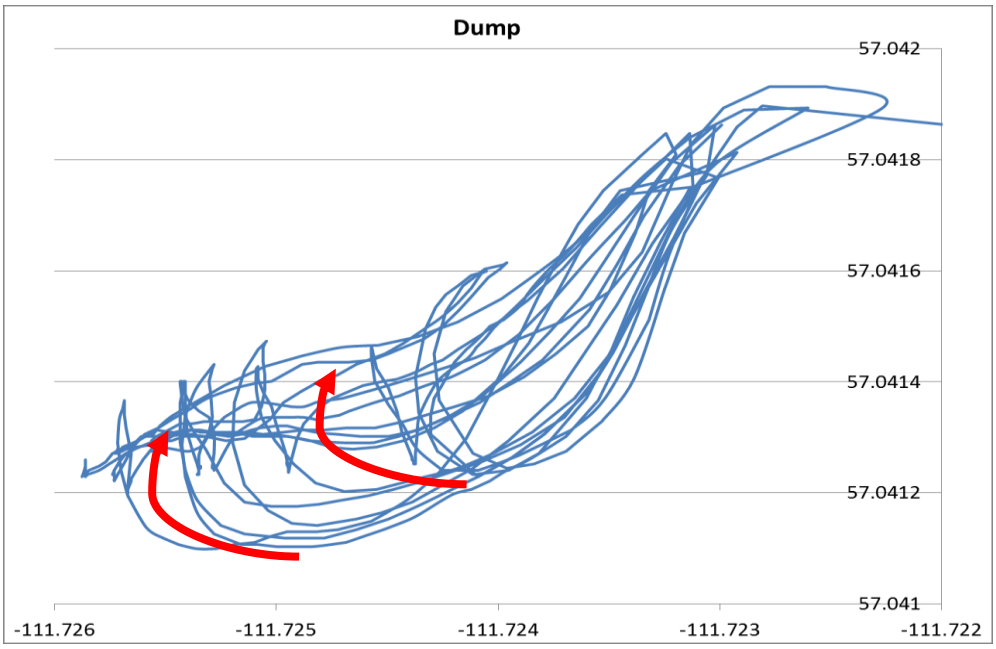

Figure 3-23 – Haul Truck GPS at Dump: Right Turns to Dump

3.8 Real Time Tire TKPH

As defined in section 2.3, tonne-kilometer per hour is a measure of the “workload” of a haul truck tire, or the work it has performed. If a threshold tkph estimated by the tire OEM is exceeded, the tire will likely overheat and succumb to heat failure by mechanical separation; interpreted as controllable by the tire OEM via operating the truck at a lower speed, at the expense of production. This makes it important for operations to not only monitor a more representative tire tkph than estimated by the tire OEM, but to incorporate it into their mine plan and work with tire OEMs to choose a more appropriate tire for a given haul application. In section 3.4 the tonnage loaded on each suspension cylinder was calculated, which is assumed to be translated to the tires. Multiplying the strut tonnage data by the hauler speed at any instant, we can determine a “real time” tkph for the tires, as shown in Figure 3-24.

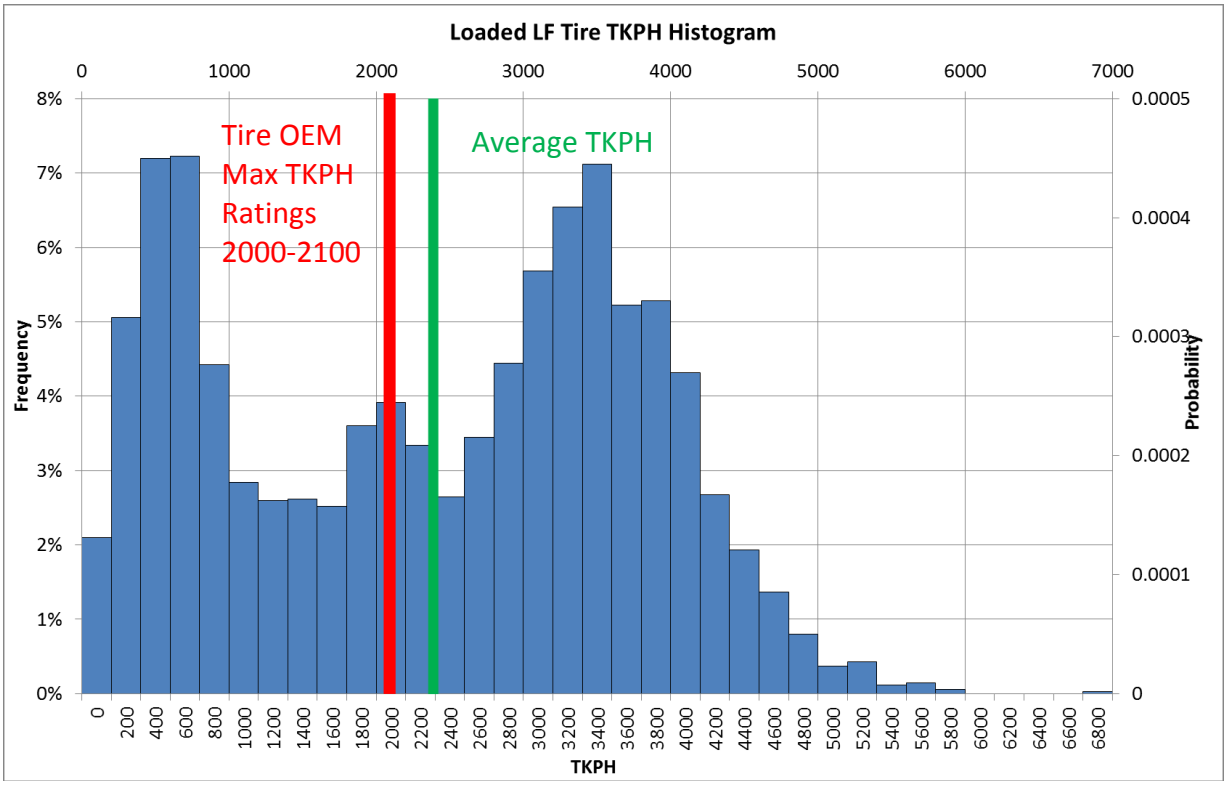

Figure 3-24 – Loaded Tire TKPH Distribution & Histogram – All Data

The histogram for “real time” tkph reveals that an average tire tkph for the oil sand data set surpasses the highest OEM tkph rating for a 59/80R63 heat resistance tire compound. It can be seen that the histogram for the full data set does not follow any idealized distribution, but if the data is broken down into different haul sections, normalized trends become evident; an example which is shown in Figure 3-25 for the main haul road section.

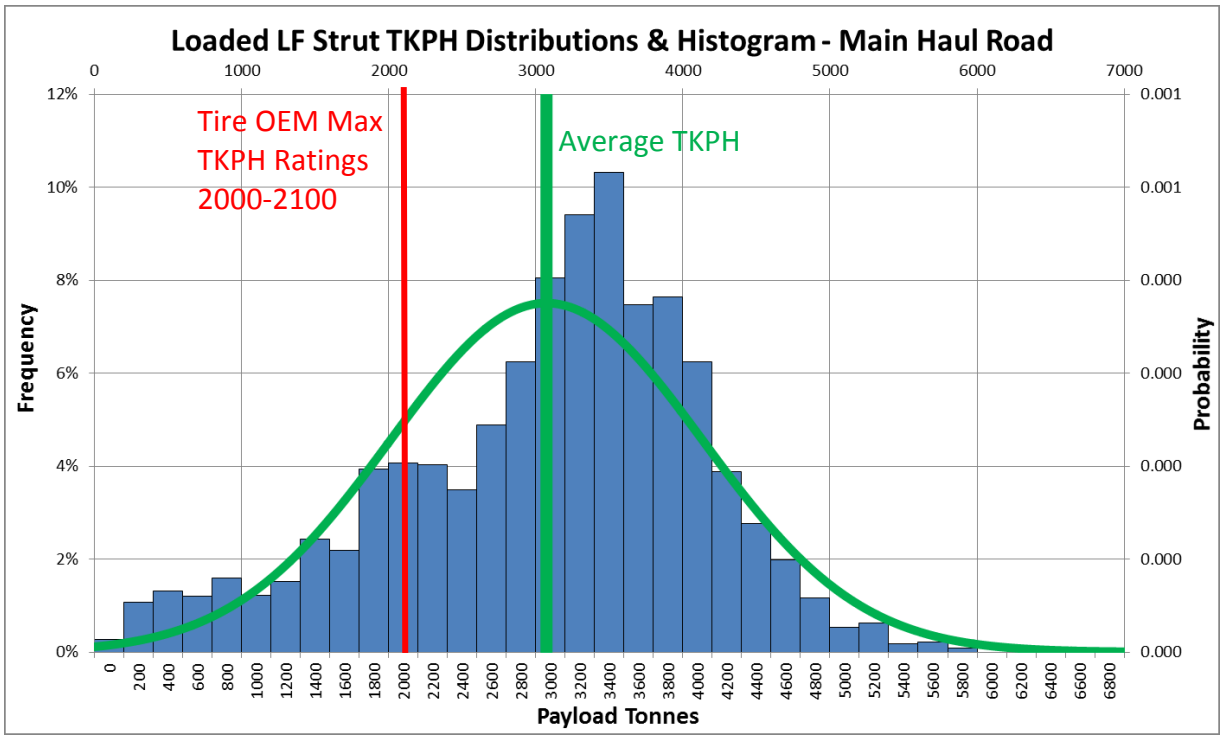

Figure 3-25 – TKPH Distribution and Histogram Example

As demonstrated in section 3.4, the suspension cylinder tonnage loading follows a normal distribution, and it would be expected that tkph follows a similar trend, however tkph is also proportional to truck speed. To determine the effect of speed on tkph, distributions were plotted of speed for each haul section to understand the relationship relative to the reaction to rolling resistance. Several other factors influence the speed of a haul truck, shown in Figure 3-26, including intersections, mine traffic, weather, accelerating/decelerating; but generally as rolling resistance decreases, haul speed will increase as revealed by the results in Figure 3-27.

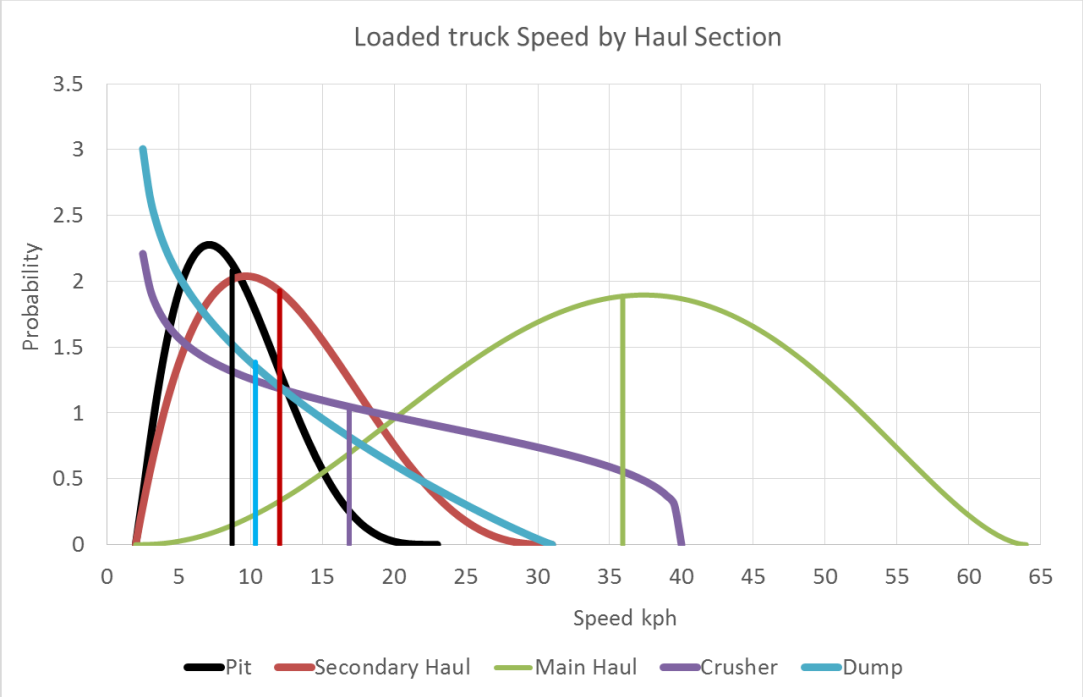

Main Haul = 2+62×Beta (3.3, 2.73)	SQ Error = 0.00908
Secondary Haul = 2+29×Beta (2.01, 3.8)	SQ Error = 0.152
Pit = 2+21×Beta (2.17, 4.62)	SQ Error = 0.0382
Crusher = 2+38×Beta (0.82, 1.28)	SQ Error = 0.0439
Dump = 2+31×Beta (0.84, 1.81)	SQ Error = 0.0259

Figure 3-26 – Loaded Haul Truck Speed Distribution by Road Section

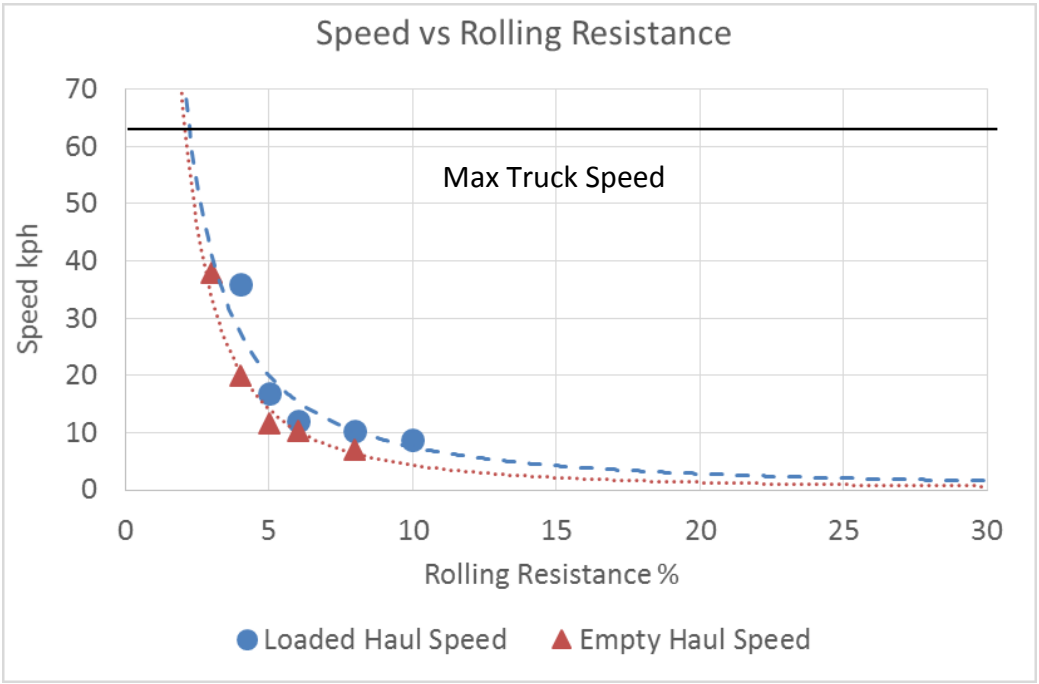

Figure 3-27 – Haul Truck Average Speed vs Rolling Resistance

It was determined that a beta distribution function provided a “best fit” model for truck speed, which when combined with the tonnage normal distributions, a gamma distribution function was determined to be a best fit for tkph, based on a lowest average square statistical error.

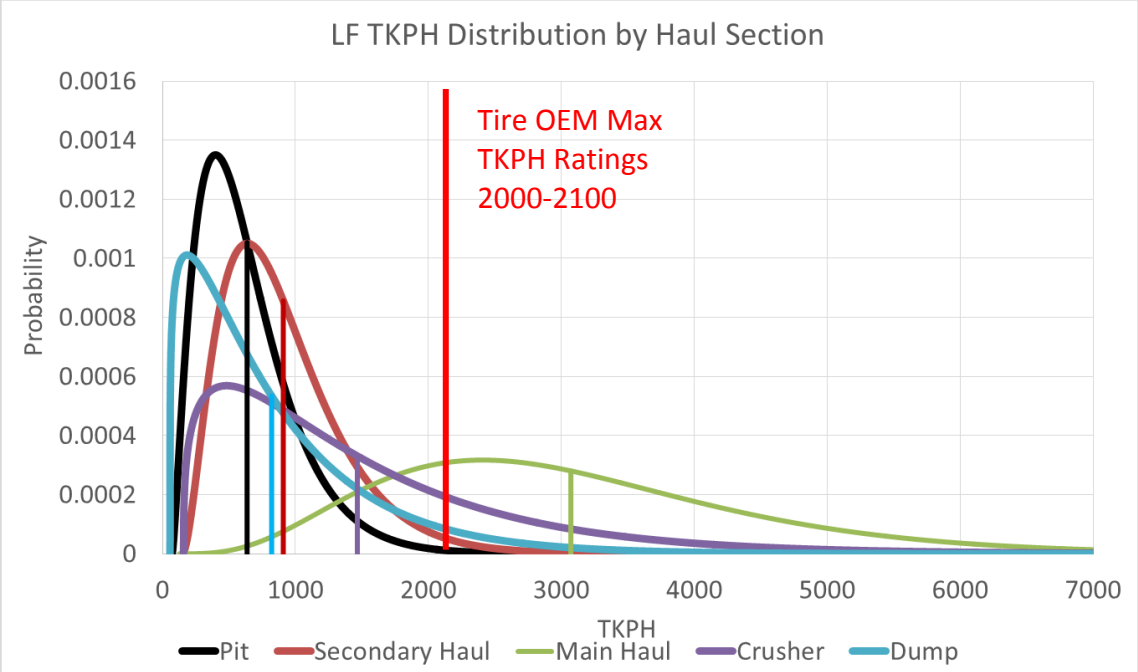

Main Haul = 128 + Gamma (4.45, 661)	SQ Error = 0.00569
Secondary Haul = 149 + Gamma (2.82, 269)	SQ Error = 0.0295
Pit = 72 + Gamma (2.38, 237)	SQ Error = 0.0124
Crusher = 159 + Gamma (1.33, 981)	SQ Error = 0.0244
Dump = 57 + Gamma (1.2, 639)	SQ Error = 0.00904

Figure 3-28 – Real Time TKPH Left Front Tire by Road Section

From Figure 3-28, only the main haul road real time tkph surpasses the OEM tkph recommended maximum rating of a heat resistance tire; mostly due to the haul trucks being able to operate at more than double speed on main hauls compared to other hauls. This suggests that the real time tkph will be driven by the length of the main haul road, but the tire load should not be ignored as a significant factor. Table 3-7 reveals the tkph for the entire data set, with front tires exposed to average values of 1900, which are just under the OEM maximum

tkph rating for a heat resistant tire. The ability to model speed and tonnage versus rolling resistance provides the ability for mines to predict real time tkph for a haul fleet, to minimize tkph influence on productivity.

Table 3-7 – Mine Real Time Tire TKPH per Haul Section by Speed

Section		LF tkph	LR tkph	RF tkph	RR tkph
Loaded	Main Haul	3072	2383	3100	2209
	Secondary Haul	909	826	820	691
	Crusher	1466	1264	1305	1001
	Pit	636	637	531	500
	Dump	821	576	719	448
	Average Loaded	2387	1873	2374	1707
Empty	Main Haul	1762	500	1565	507
	Secondary Haul	566	153	496	159
	Crusher	953	266	808	270
	Pit	321	96	317	104
	Dump	624	175	545	195
	Average Empty	1377	391	1226	399
Total Average TKPH		**1906**	**1166**	**1827**	**1083**

Previously it was discussed that exceeding a tire tkph rating may substantially shorten its life, but the repercussions are not limited to the capital price of a tire. Failure of the tire itself may be costly, but the truck will also need to be removed from operation to have its tire replaced, thereby reducing availability. If a failure is avoided and the heat issue is detected early, the truck may need to operate at lower speed, at a lower payload, or a combination of both; again decreasing production. An operation will need to find a balance between tire heat issues and productivity, possibly by rotating trucks from long to shorter haul cycles, during a given shift.

3.9 Actual Tonnage vs Suspension Cylinder Tonnage

To validate the proposed method of calculating truck payload utilizing the pressure of the four suspension cylinders from section 3.2, a comparison with actual manned scaled haul truck weights and payloads was completed. The scale and truck data was provided by a supplier, from a 797B operating in the oil sands, with 18 different payloads that were verified using industrial truck scales performed by the author. The data in Table 3-9 and Figure 3-29 reveal a significant difference of 16%, or 62 tonnes, between the scaled payload and calculated suspension cylinder payload.

Table 3-8 – 797B Scaled Weights vs Calculated Suspension Cylinder Weights

Parameter		Scale	Strut	Tonne Difference	Strut % Difference
Empty	LF Strut	65.7	49.97	15.7	23.9%
	RF Strut	63.1	44.80	18.3	29.0%
	LR Strut	70.4	25.10	45.3	64.4%
	RR Strut	69.6	22.95	46.6	67.0%
	EVW	**268.8**	**190.9**	**77.9**	**46.9%**
Loaded	LF Strut	119.6	97.8	21.8	18.3%
	RF Strut	120.4	103.2	17.3	14.3%
	LR Strut	214.6	129.1	85.5	39.9%
	RR Strut	197.0	134.1	62.9	31.9%
	GVW	**651.6**	**464.1**	**187.5**	**28.8%**
Payload		**382.8**	**321.3**	**61.5**	**16.1%**

If we are to apply this percent error to the original oil sands data in this thesis, the average payload would increase from 286 tonnes to 332 tonnes. As such it should be noted that the scaled strut groupings include weight that the struts are unable to account for, such as tires and rims. The VIMS payload also exhibits a -3% average error compared to the manned scale payload, which is aligned with a haul truck onboard payload system error experienced by the author in the oil sands. The average VIMS payload was 320 tonnes for the original oil sands

data, and adjusting for a -3% error brings the payload value to 330 tonnes, which is very close to the adjusted calculated strut payload of 332 tonnes.

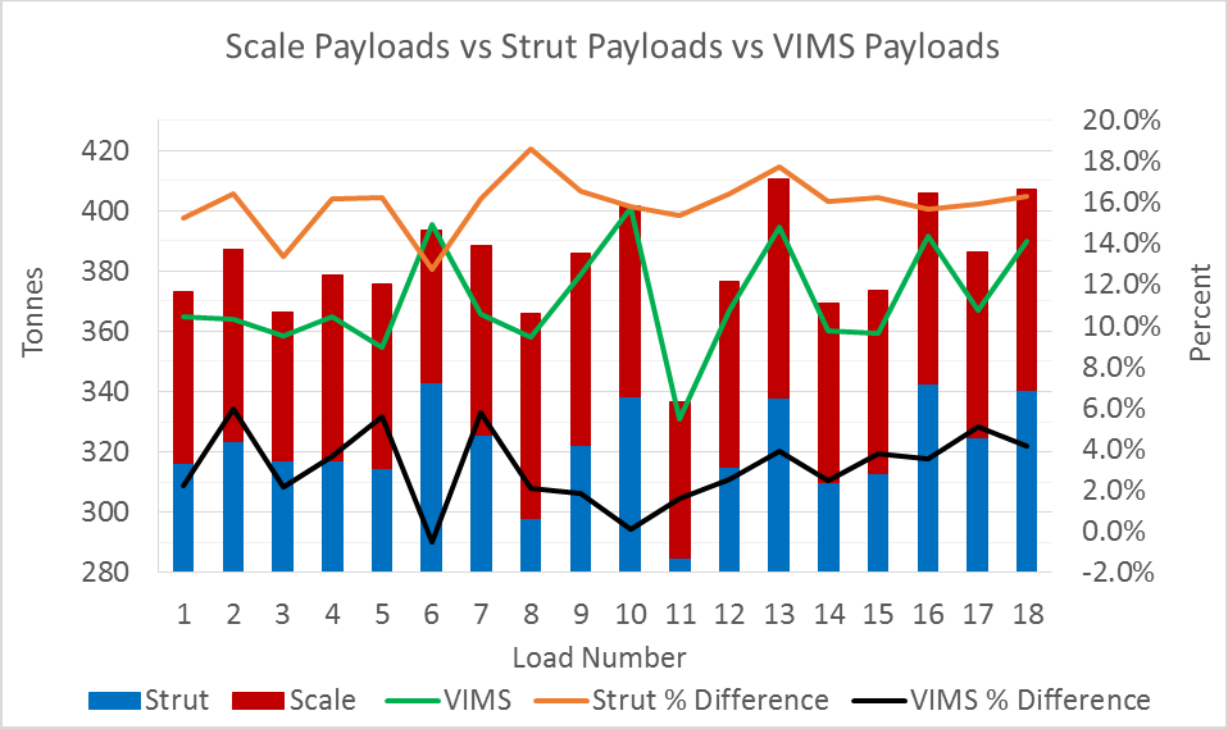

Figure 3-29 – 797B Scale Payload vs Strut Payload vs VIMS Payload

It cannot be confirmed that the error factors for the scaled truck data will be the same for the original oil sands data, but it does demonstrate a strong possibility that the calculated suspension cylinder tonnage method suggested here could be incorrect. An explanation for the potential error in the calculated suspension cylinder tonnage is that the calculation process assumes an ideal initial based charged suspension system, whereas in reality the system experiences inefficiencies such as friction, error from the suspension cylinder pressure sensor, damaged suspension cylinder, or the pressure in the cylinder is not correctly pre-charged to specified volumes of oil or gas. Another possibility is that the suspension cylinder experiences side loading due to a small camber and movement action on the cylinder itself, although pinned at both ends.

Any potential error of strut operation will predominantly only have a large effect on the tonnage analysis itself, as well as the real time tkph calculations. The g-level analysis is relative to the equilibrium conditions, thereby having the advantage of removing any possible large impacts due to error in the suspension cylinder pressure data.

The real time tkph analysis, presented in section 3.8, may be affected by an increase in additional tire loading due to inaccuracy in suspension cylinder tonnage calculation. Assuming the strut tonnage displays a 16% error, adjusting tkph to account for this error would generate the outcomes in Table 3-9, which potentially drives the front tire mine tkph above the OEM tkph threshold of ~2100.

Table 3-9 – Adjusted Mine Tire TKPH Based on Strut Tonnage Error

Section		LF tkph	LR tkph	RF tkph	RR tkph
Loaded	Main Haul	3564	2764	3596	2562
	Secondary Haul	1054	959	951	802
	Crusher	1701	1466	1514	1161
	Pit	738	739	616	580
	Dump	953	668	834	520
	Total	**2769**	**2172**	**2753**	**1980**
Empty	Main Haul	2044	580	1815	589
	Secondary Haul	656	177	575	184
	Crusher	1105	309	937	313
	Pit	373	112	368	121
	Dump	724	203	632	226
	Total	**1598**	**453**	**1422**	**462**
Total TKPH		**2211**	**1353**	**2119**	**1257**

4 Novel Application of G-level

4.1 Change in Suspension Cylinder G-level (Δg)

In section 3.6, it was demonstrated that a relationship between g-level and rolling resistance exists. While g-level is beneficial to record high g-level events, it doesn't fully illustrate the impact on the machine and suspension cylinders. An example of the limitations of simply taking the average g-level of a haul section can be seen in Figure 4-1, which exhibits that two sections with different magnitudes of change in g-level can have the same average g-level. Depending on the threshold for high g-level events, haul section 1 from Figure 4-1 may be classified as a similar road profile to haul section 2, even though the amplitude of g-level change is larger and more frequent in haul section 1.

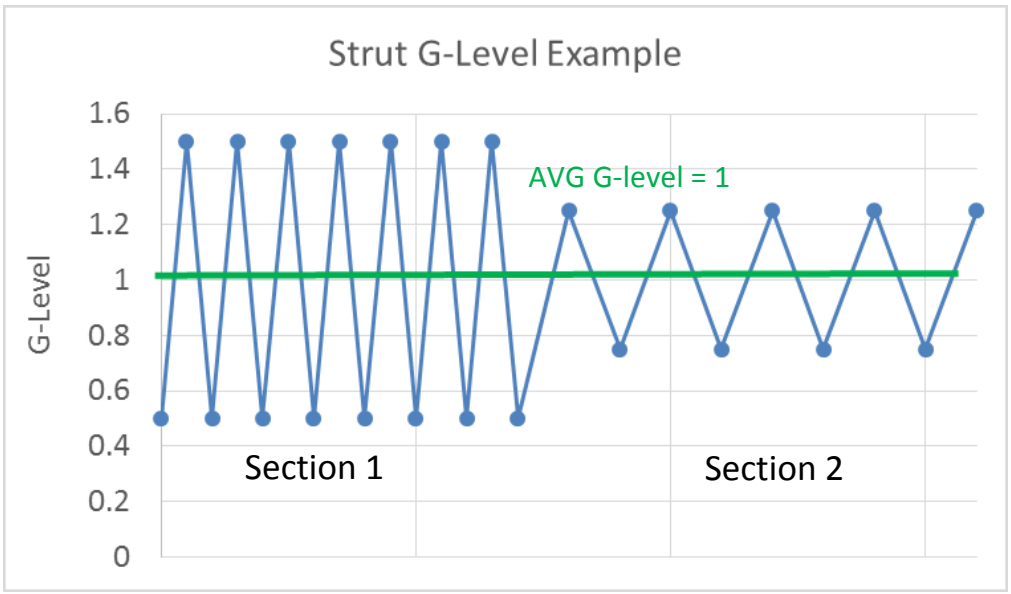

Figure 4-1 – Suspension Cylinder G-level Example

Shown in Figure 4-2 is this phenomenon of two road sections having the same average g-level, but the amplitude and frequency of the peaks is greater in the pit & haul road 2 section compared to that of the main haul road. If, for example, we are to only document events over 1.5g as high g-level events, neither of these sections would have a recordable event and from the performance indicators that we currently track, these two sections would be deemed similar.

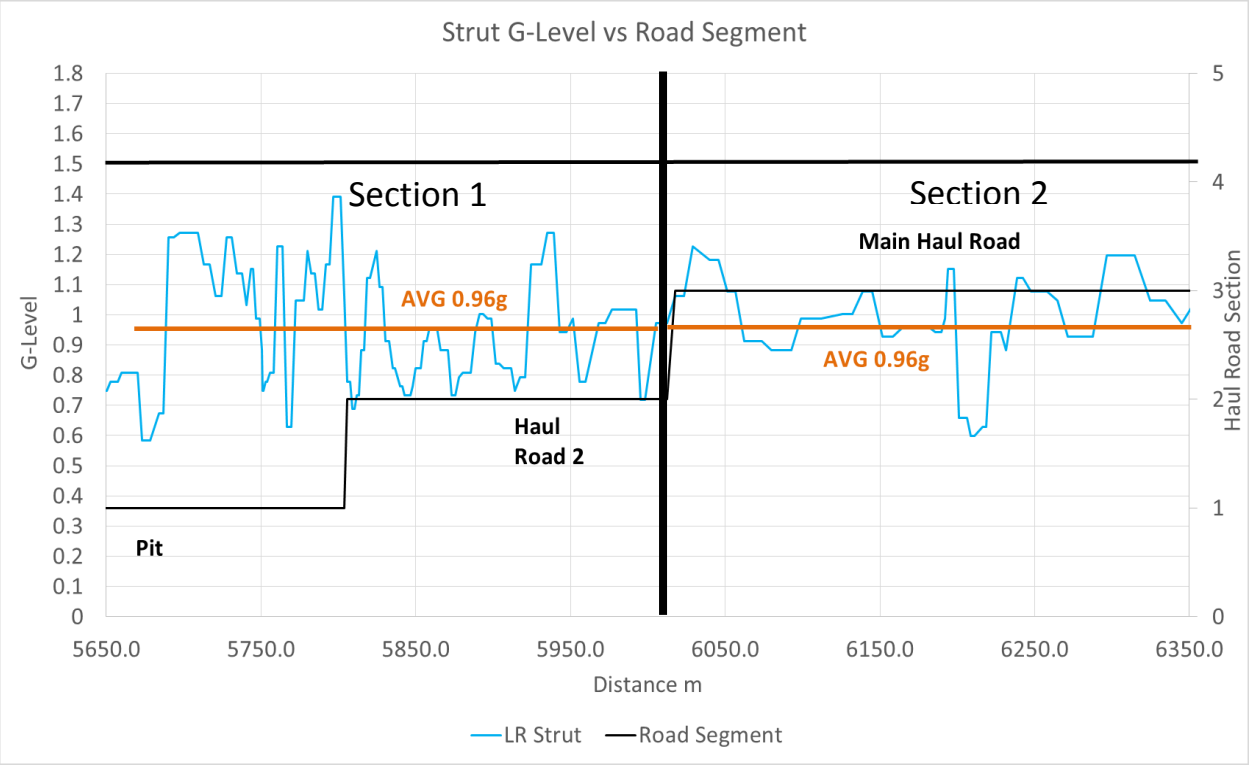

Figure 4-2 – Suspension Cylinder G-level Comparison: Base Example

One method to differentiate between sections with varying g-level amplitudes would be to measure and track this amplitude as a key performance indicator (KPI) relative to roughness of a haul road. Since the roughness of a haul road doesn't translate to a perfect wave motion through a suspension cylinder, thereby having an inconsistent amplitude in the data, the average absolute change (dg) in g-level from one point to the next may provide greater insight into the difference in haul road response.

The absolute of the change in g-level is utilized, as the combination of positive and negative values would cancel each other out, but the magnitude of this change provides equation 16.

$$Average\ dg = \frac{\sum_1^X ABS(g_x - g_{x+1})}{X} \qquad 16$$

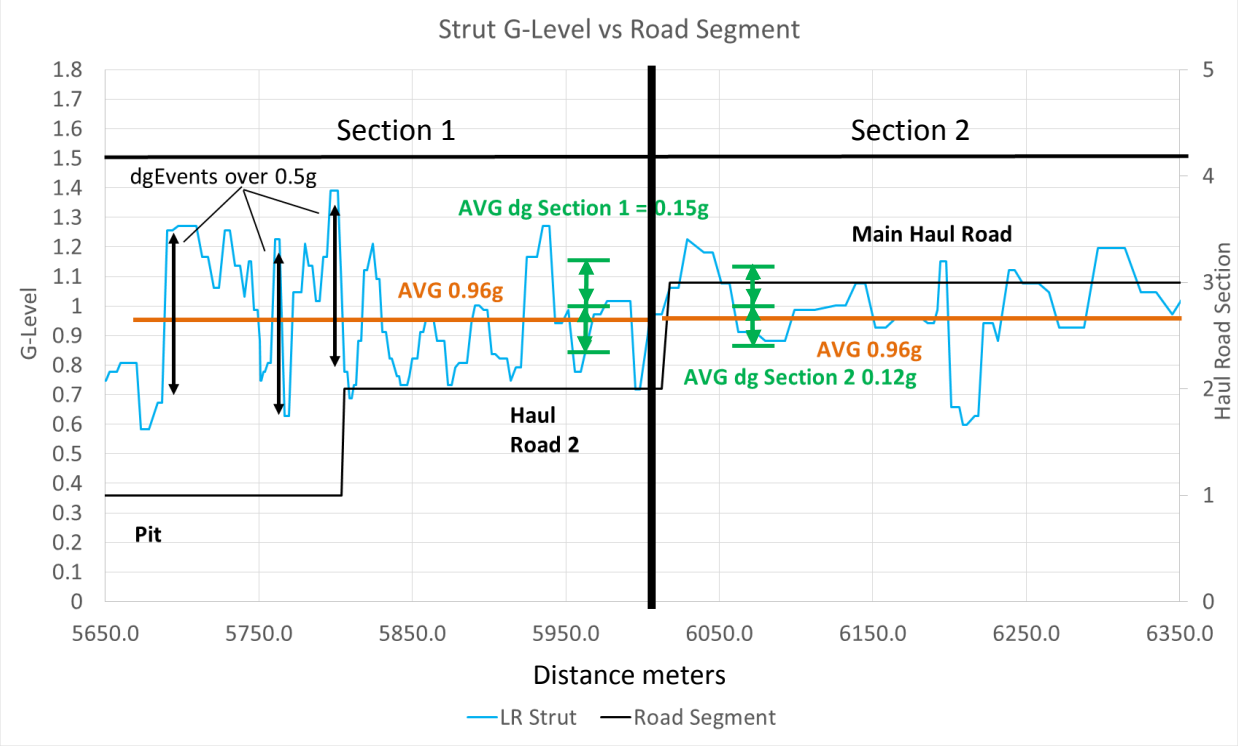

Figure 4-3 - Suspension Cylinder G-level Comparison: G-level Change Example

Using the same example in Figure 4-2, and accounting for change in g-level, we can see in Figure 4-3 that the g-level change in section 1 is approximately 27% higher than the change in g-level for section 2, thereby quantifying a difference between the two haul sections; which our previous KPI's did not. The average g-level change was calculated, equation 16, for each haul section in an attempt to correlate the g-level KPI to different road profiles, with the results shown in Figure 4-4.

The results show similar characteristics between the loaded and empty travel data for the respective haul sections, with only the crusher section displaying a noticeable difference. The rear struts have a noticeably larger g-level change value compared to the front struts, with some sections displaying changes over 0.2g on average.

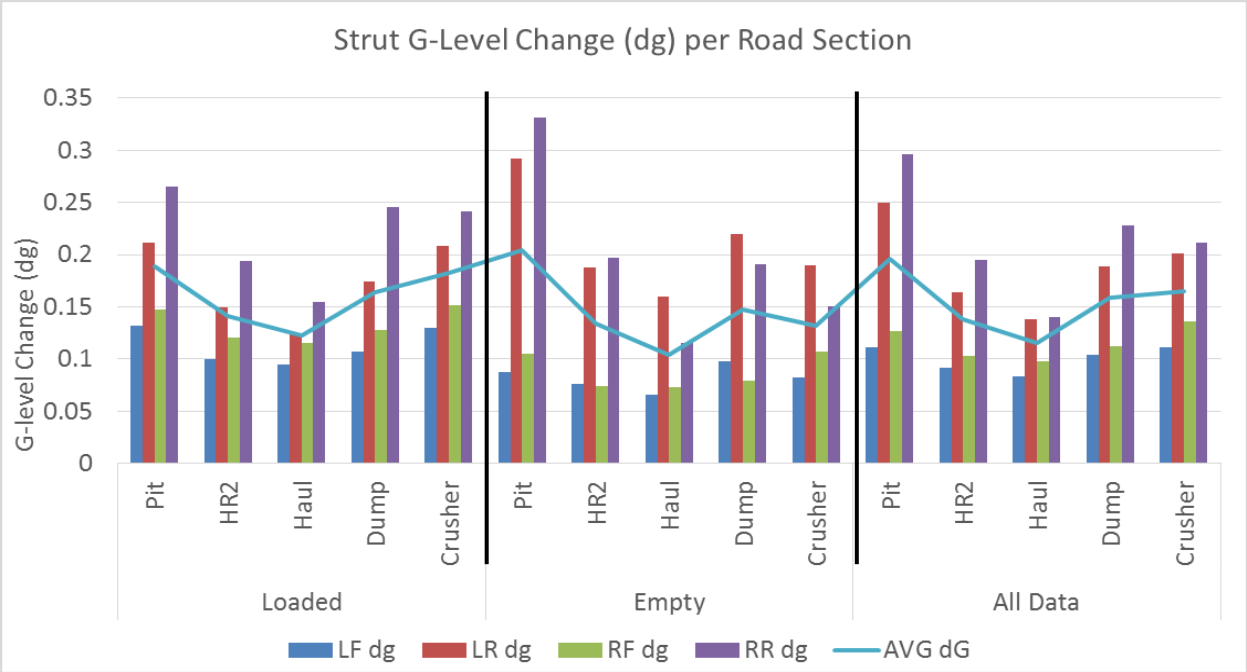

Figure 4-4 – Suspension Cylinder G-level Change (dg) per Road Section

Compared to the estimated rolling resistance, on average, those sections with lower rolling resistance display a lower change in g-level, which is demonstrated in Figure 4-5. The outlier to this hypothesis would be the "Crusher" section, which displays a higher g-level change than expected for the sections estimated rolling resistance. Since the author was not able to view the crusher pad during the time of data collection, the estimated rolling resistance may be higher, but a likely explanation is a combination of haul truck reversing and travelling with a raised dump body. Therefore a true correlation with the crusher area rolling resistance cannot be completed, and the data can be ignored in this analysis, Table 4-1.

Table 4-1 – Average G-level Change per Road Section
***Data Ignored in Further Analysis**

Section		Est. RR %	AVG dg Front Struts	AVG dg Rear Struts	AVG dg
Loaded	Pit	10.0	0.14	0.24	**0.19**
	Secondary Haul	6.0	0.11	0.17	**0.14**
	Main Haul	4.0	0.10	0.14	**0.12**
	Dump	8.0	0.12	0.21	**0.16**
	Crusher*	5.0	0.14	0.22	**0.18**
Empty	Pit	8.0	0.10	0.31	**0.20**
	Secondary Haul	5.0	0.08	0.19	**0.13**
	Main Haul	3.0	0.07	0.14	**0.10**
	Dump	6.0	0.09	0.21	**0.15**
	Crusher*	4.0	0.09	0.17	**0.13**
All Data	Pit	9.0	0.12	0.27	**0.20**
	Secondary Haul	5.5	0.10	0.18	**0.14**
	Main Haul	3.5	0.09	0.14	**0.11**
	Dump	7.0	0.11	0.21	**0.16**
	Crusher*	4.5	0.12	0.21	**0.16**

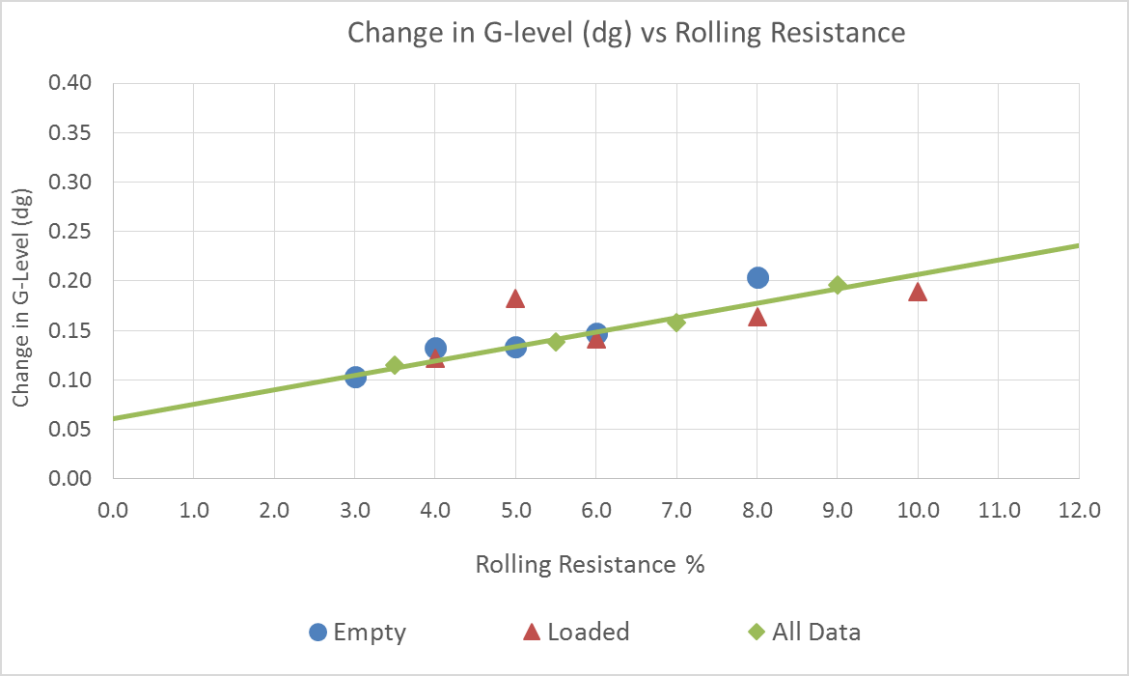

Figure 4-5 – Change in G-level vs Rolling Resistance

Another G-level KPI that can be conducted is summing large dg “change” events over plateau values, regardless of positive or negative values. Typically simple g-level events are tracked over 1.3g-1.5g, but when considering g-level change, haul trucks consistently experience dg events over 0.5g; which may not be documented as they fall below our current g-level tracking standards. This is demonstrated in the example in Figure 4-3, as there are 3 dg events over 0.5g, but no g-level events over 1.5g.

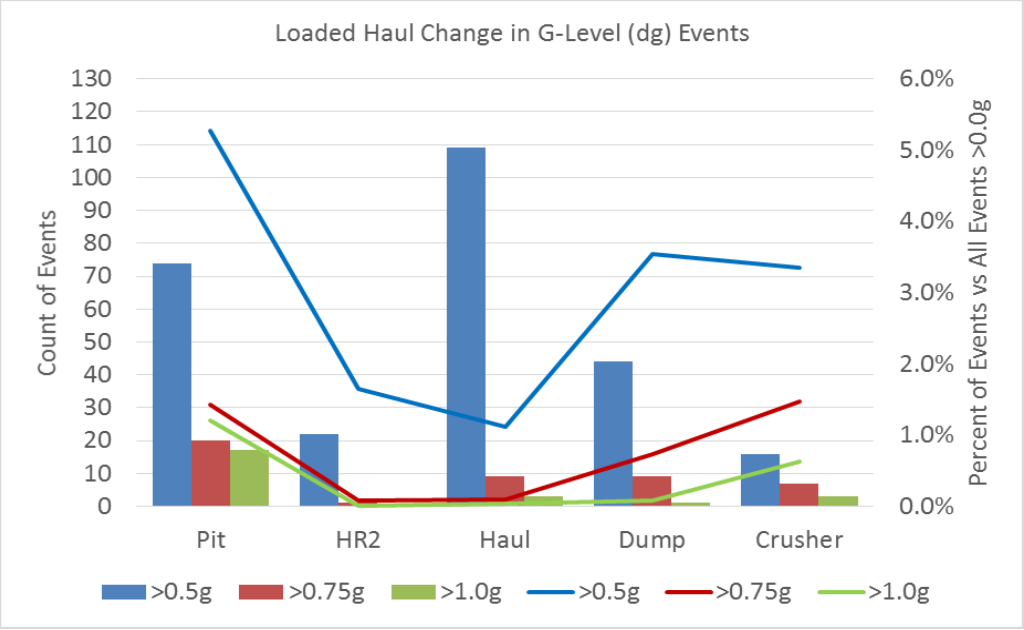

Figure 4-6 – Loaded Haul dg Events

Figure 4-6 displays the total number of dg events over 0.50g, 0.75g, & 1.00g for the loaded haul truck data, revealing g-level change events above 0.5g occur 2%-3% over the course of the loaded haul data. Comparing the frequency of simple g-level and dg events, Figure 4-7, they occur at roughly the same frequency for loaded conditions over similar increments of g-level. Figure 4-7 also demonstrates that total g-level events are roughly double that of total dg values, due to more data overall, but it also reveals that g-level change (dg) over 1g are more frequent than g-level events over 2g, which are both 1g increments above equilibrium their respective

values of 0g and 1g. Typically events over 0.5g above equilibrium, for simple g-level and other g-level parameters, can be defined as high stress events, whereas events near equilibrium are taken as low stress events. Figure 4-7 can then be viewed as proportional to a fatigue S-N curve relationship, and further research can explore the effect on g-level change on truck health.

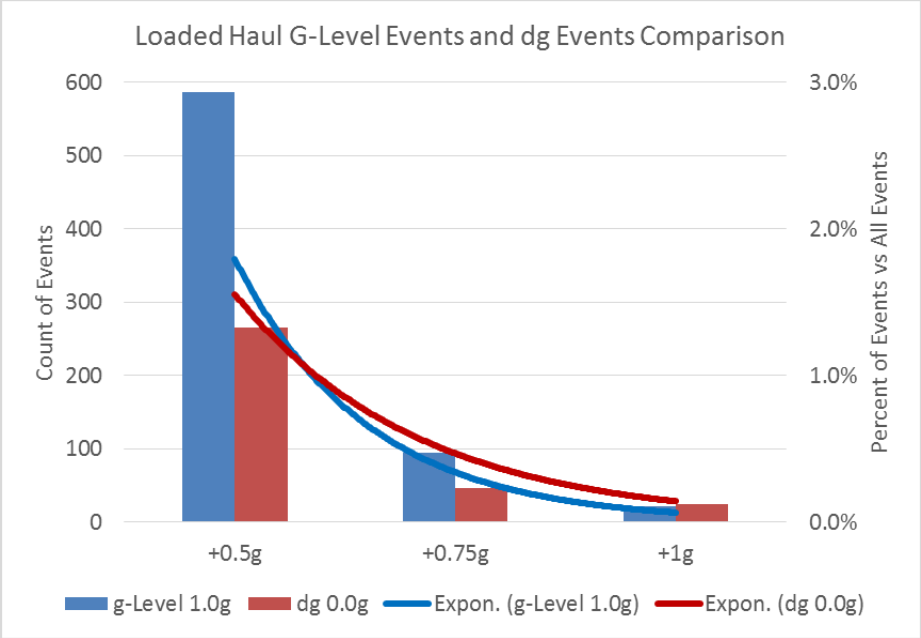

Figure 4-7 – Loaded Haul G-level & Change in G-level (dg) Events

4.2 Magnitude of G-level

When considering the magnitude of g-level, it is necessary to track the full amplitude of a g-level "wave", instead of point to point change in g-level, described in section 4.1. The difference between the two parameters can be seen in the example in Figure 4-8, where multiple changes (dg) in g-level can be included in the full amplitude or magnitude of the g-level wave.

Calculating the magnitude of g-level involves the summation of g-level change, as long as the events are of the same sign convention (positive or negative) or neutral. When the sign changes, the process is performed with the opposite sign convention.

$$\boldsymbol{Magnitude\ (mg)} = \sum_{-}^{+} \boldsymbol{dg} \qquad 17$$

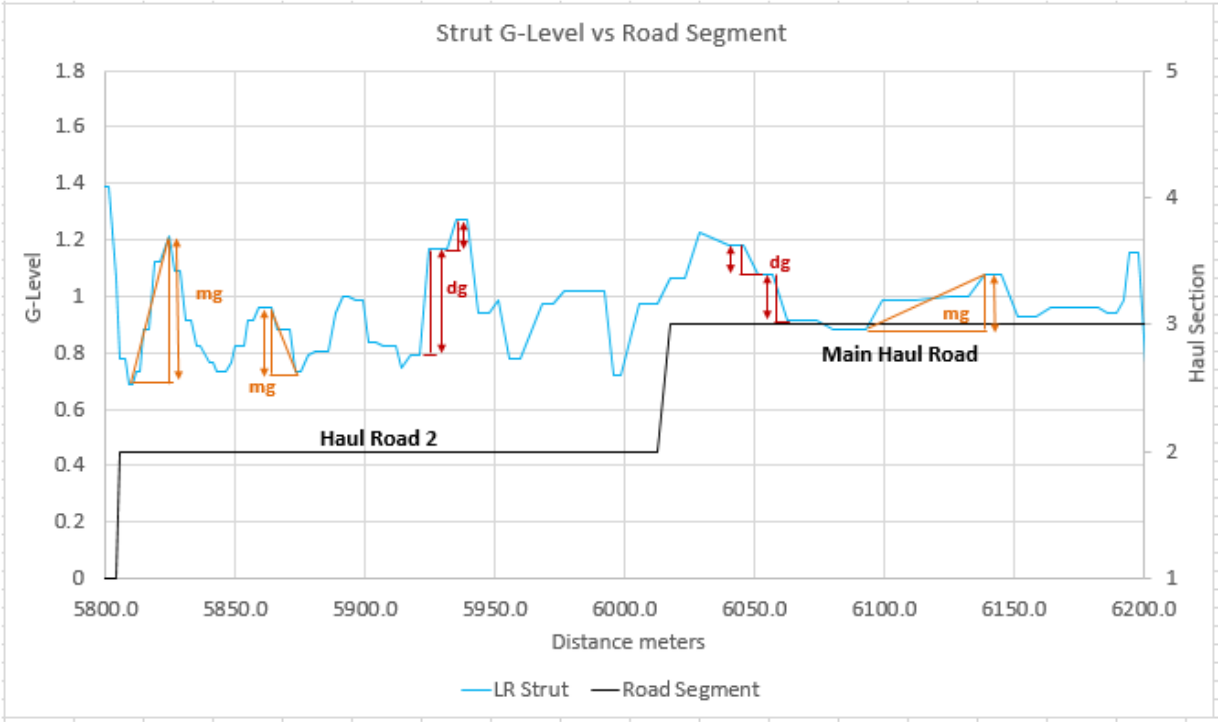

Figure 4-8 - G-level Change (dg) vs Magnitude (mg) Example

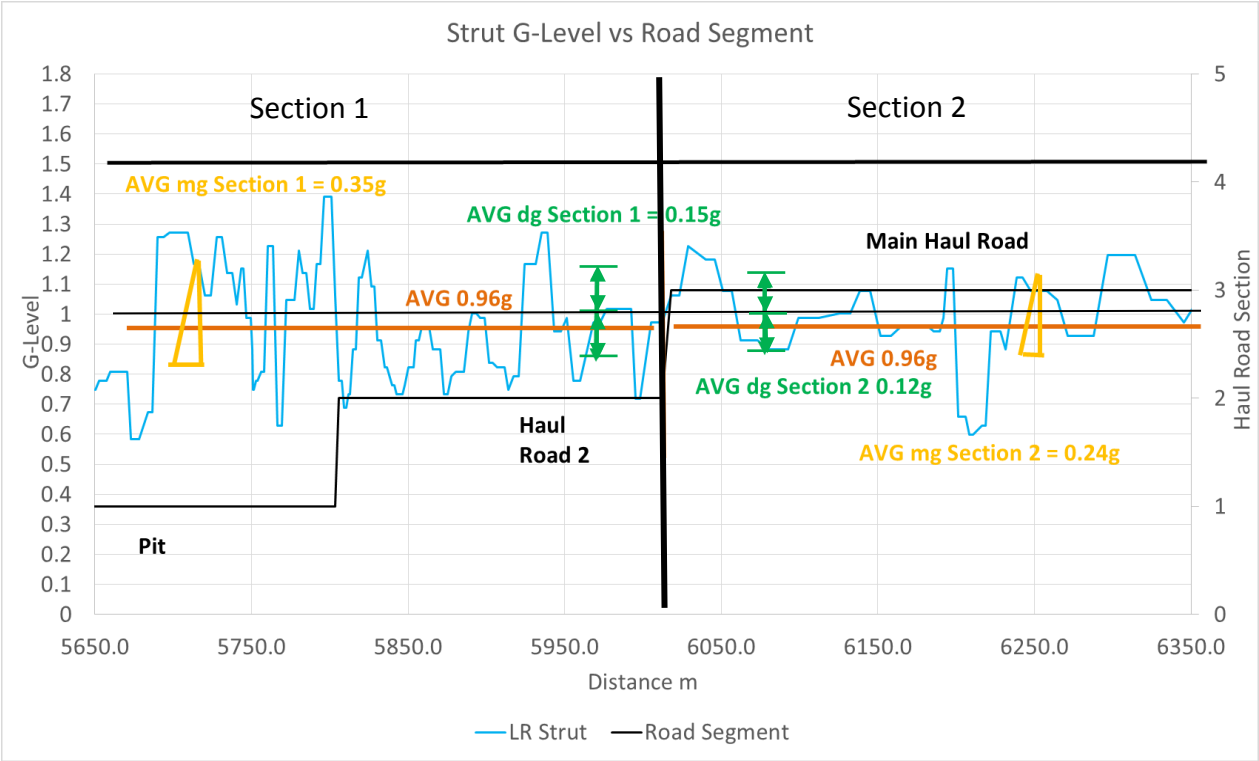

Figure 4-9 - Suspension Cylinder G-level Comparison: G-level Magnitude (mg)

The analysis of g-level change and magnitude can be described as modifications to miner's rule and a rainflow analysis (Fatemi, 2011), tracking individual macro and micro cycles, to determine the combined effects of various stress or loading cycles. Utilizing our previous example again in Figure 4-9, the magnitude difference between section 1 and section 2 is approximately 0.1g, or 47% larger, which quantifies a difference between the two haul sections, whereas an average of simple g-level does not reflect this.

The results in Figure 4-10 of g-level magnitude for the full data set show a similar trend to that of g-level change, and as expected, sections with lower rolling resistances display lower magnitudes. When we compare g-level change and magnitude versus rolling resistance in Figure 4-11, they follow similar trends, with magnitude of g-level having larger increments as rolling resistance increases. In parallel to g-level change (dg), the rear struts demonstrate a larger magnitude compared to the front struts, approaching 0.5g in a pit area, which is significant as this represents approximately 50% of the g-level equilibrium.

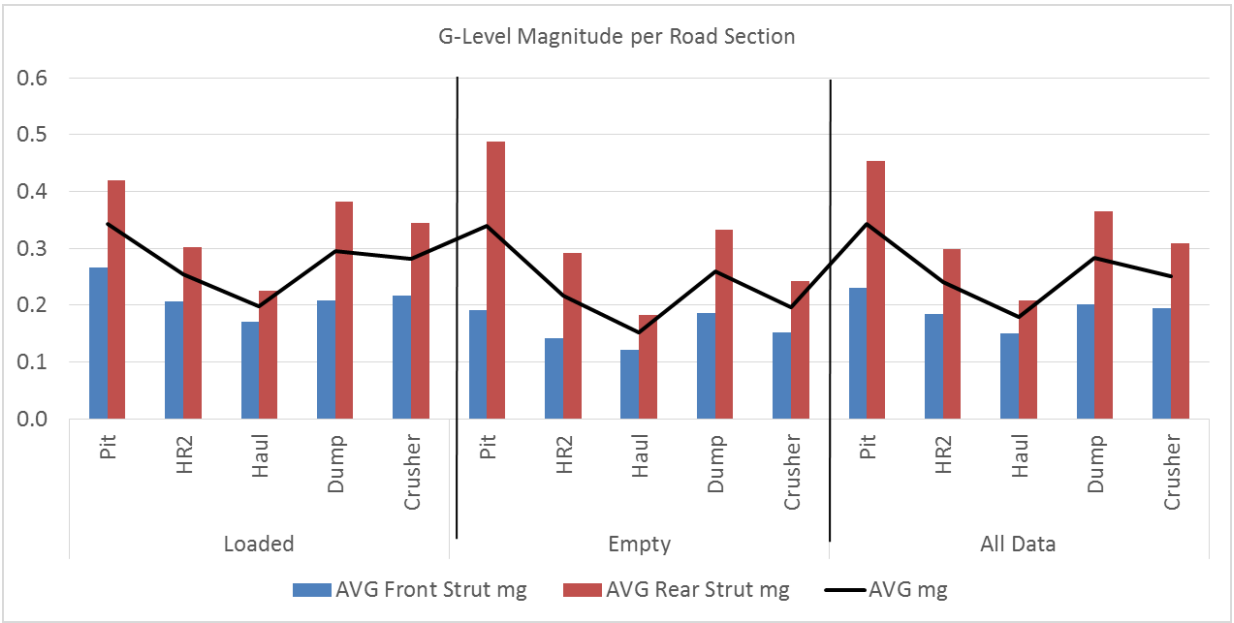

Figure 4-10 – G-level Magnitude (mg) per Road Section

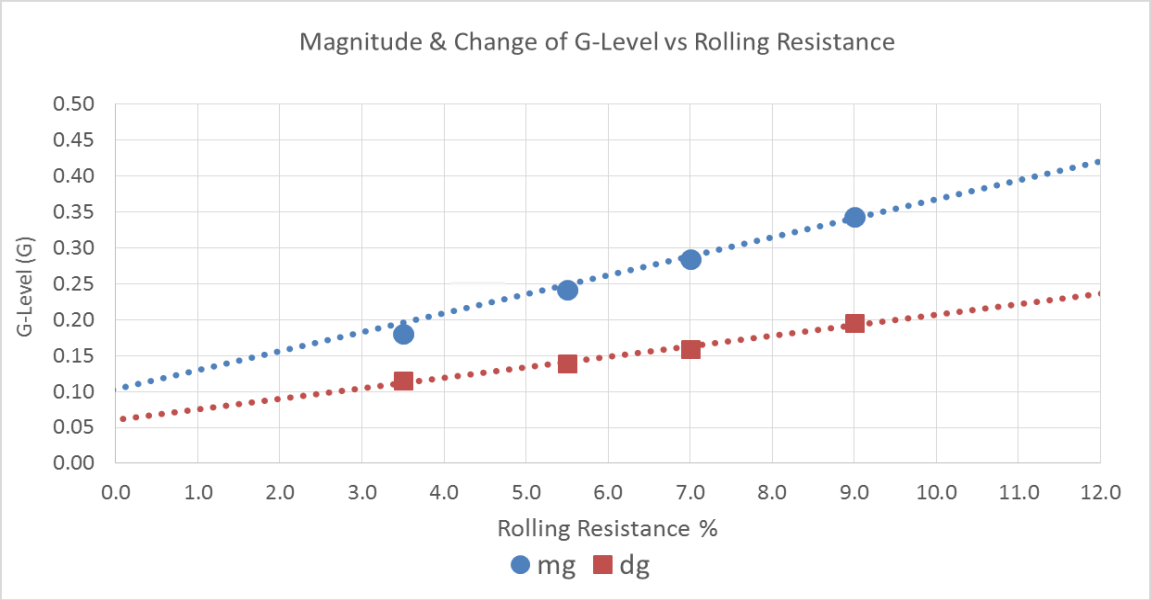

Figure 4-11 – G-level Magnitude (mg) & Change (dg) versus Rolling Resistance

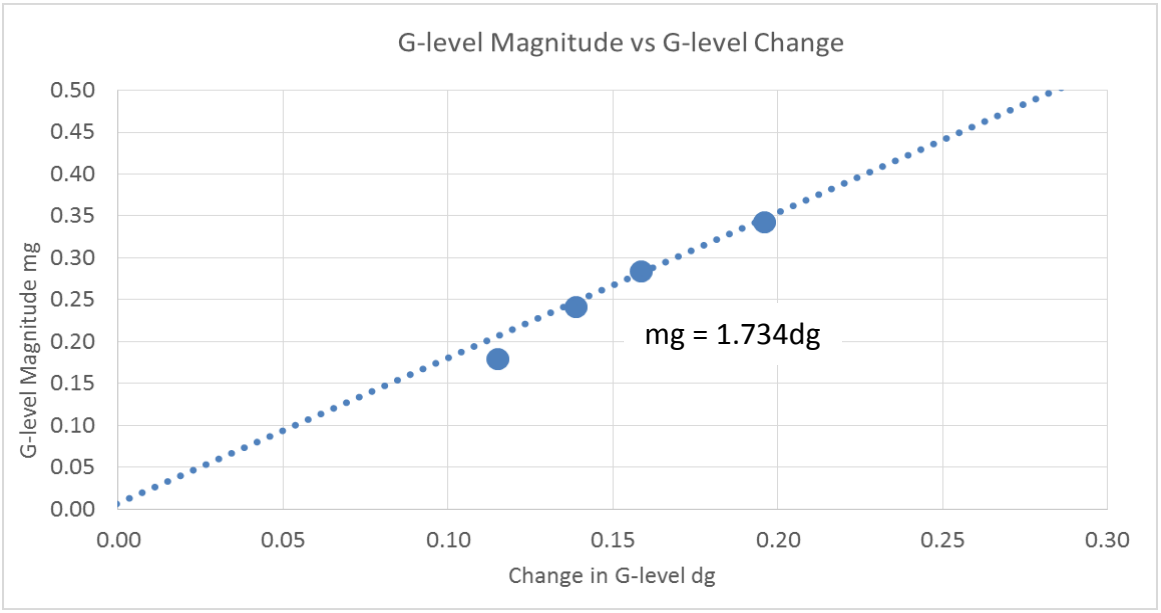

Figure 4-12 – G-level Magnitude vs G-level Change

In Figure 4-11, the g-level change and magnitude trends both suggest zero percent rolling resistance conditions still indicate a small amount of g-level motion. With g-level magnitude and change both exhibiting a strong correlation to rolling resistance, a comparison of the two values was plotted to understand their relationship. The linear trend was set to have an intercept of zero, as they should theoretically be directly related, suggested in equation 17.

4.3 G-level Wave

G-level tends to follow a wave motion, incrementing and decrementing around an equilibrium of 1g. The amplitudes and frequencies are inconsistent, therefore it cannot be considered a "stand out" wave, but when we compare a "rough" section of haul road to a smoother section, a visual difference of amplitude and frequency can be seen. In the previous section 4.2, the amplitude or g-level magnitude (mg) of these "waves" was estimated by conducting a modified rainflow analysis. For wave frequency, time and distance are the most reasonable variables to examine, but speed could also be considered as it contains both of these parameters, such that equations 18 through 20 are proposed:

$$\boldsymbol{G - Level\ Wave\ by\ Distance} = \frac{\sum_{-}^{+} \boldsymbol{dg}}{\boldsymbol{D_{+} - D_{-}}} = \frac{\boldsymbol{mg}}{\boldsymbol{dD}} \qquad 18$$

$$\boldsymbol{G - Level\ Wave\ by\ Time} = \frac{\sum_{-}^{+} \boldsymbol{dg}}{\boldsymbol{T_{+} - T_{-}}} = \frac{\boldsymbol{mg}}{\boldsymbol{dT}} \qquad 19$$

$$\boldsymbol{G - Level\ Wave\ by\ Speed} = \sum_{-}^{+} \boldsymbol{dg} \div \frac{\boldsymbol{D_{+} - D_{-}}}{\boldsymbol{T_{+} - T_{-}}} = \boldsymbol{mg} \times \frac{\boldsymbol{dT}}{\boldsymbol{dD}} \qquad 20$$

All three equations' parameters can be evaluated via positive and negative values reflective of the g-level wave. Distance seems to be a logical parameter for mapping a road profile via determining the magnitude of g-level per meter of haul road, with the one issue being that at a sample rate of 1 hertz, when our speed increases so does the length of distance covered in a 1 second interval; this is discussed in section 3.3 via the Nyquist theory. On the faster haul roads where our trucks are travelling over 30kph, roughly 8 meters are covered per second.

When considering time as a function of a g-level wave, the speed of the haul unit has a large impact, as time continues to increase, even as the haul truck approaches a balanced condition; which will decrease the overall "wave" value significantly. An intriguing parameter is speed as a function of g-level wave, as it includes both time and distance, but can display large bias in g-level wave values if a haul truck operator is inconsistent in operating speed throughout a haul route.

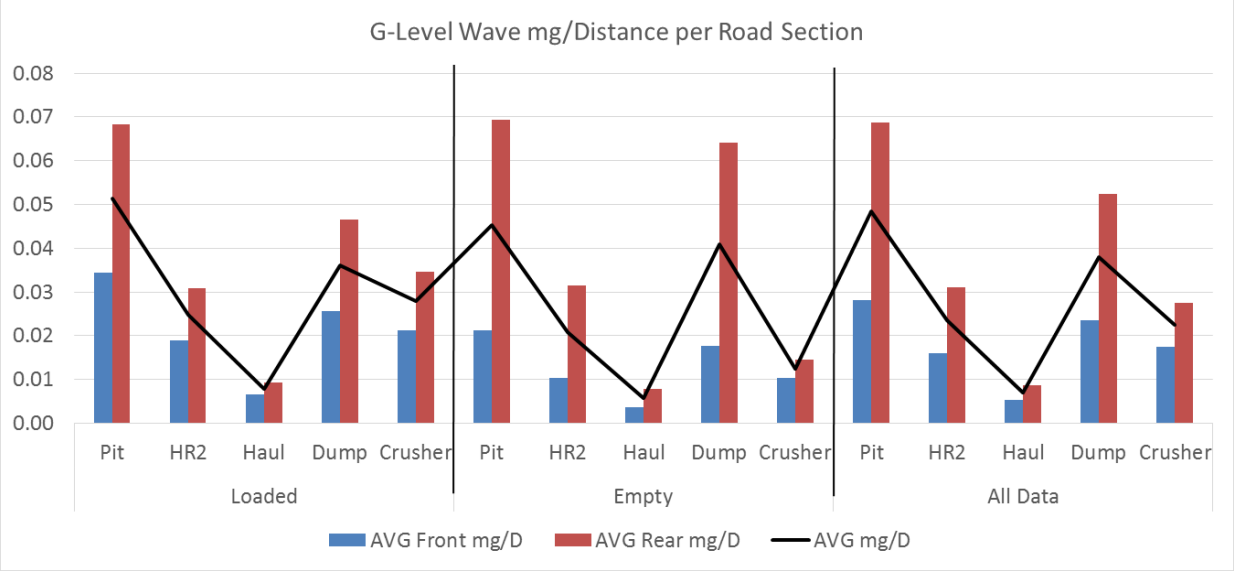

Figure 4-13 – G-level Wave by Distance (mg/D) per Road Section

The comparison of g-level wave magnitude by distance per haul section is shown in Figure 4-13, confirming the hypothesis that "rougher" sections produce a larger g-level wave response compared to smoother road surfaces. The main haul road g-level wave is approximately a fifth of the value of the pit area, which is a substantial difference. The comparison between loaded and empty hauls are consistent by specific road section, with the average empty haul g-level wave being slightly lower than that of a loaded haul.

The results for g-level wave with respect to time, shown in Figure 4-14, shows a lower response for empty vs loaded hauls for a given section. This is most likely driven by the magnitude of g-level between empty and loaded hauls, as empty haul trucks do not experience the same G-force levels as for a loaded haul truck.

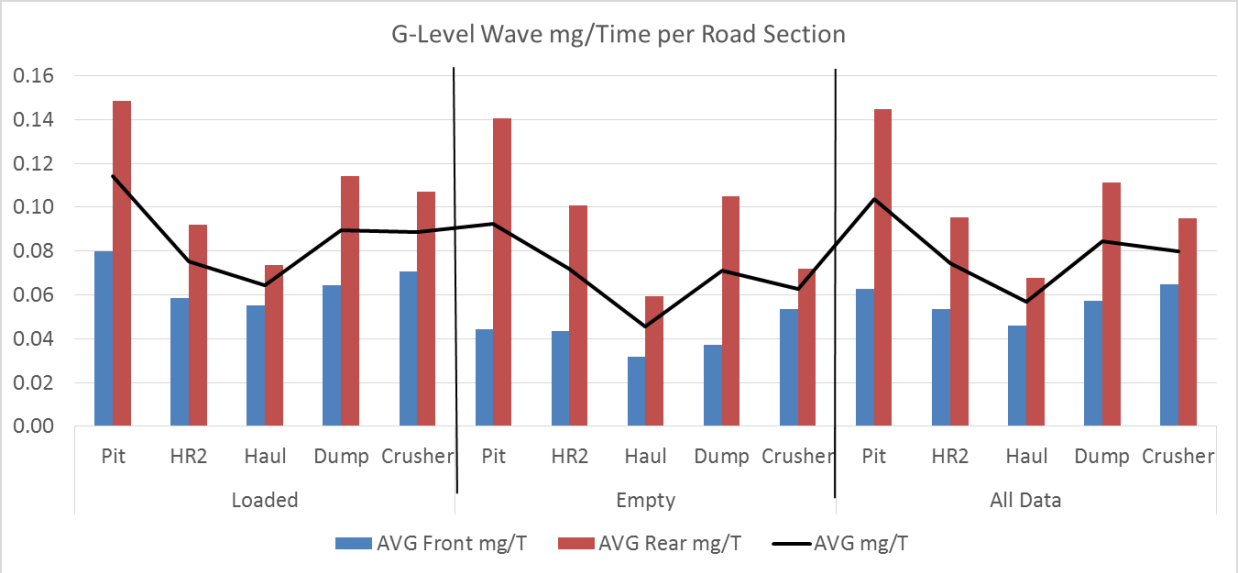

Figure 4-14 – G-level Wave by Time (mg/T) per Road Section

The final parameter involving g-level wave employs speed of the haul truck as a comparison. In Figure 4-15, a similar trend to g-level wave by distance is evident, Figure 4-13, but when compared to averages of all g-level classifiers in Figure 4-16, the magnitude of change between the two parameters is very different.

All classifiers generally show a strong correlation to road roughness by haul section, with some displaying larger similarities than others. The magnitude of g-level and g-level wave as a function of truck speed exhibits comparable magnitudes by haul section, which implies that speed has a minimal effect on g-level magnitude.

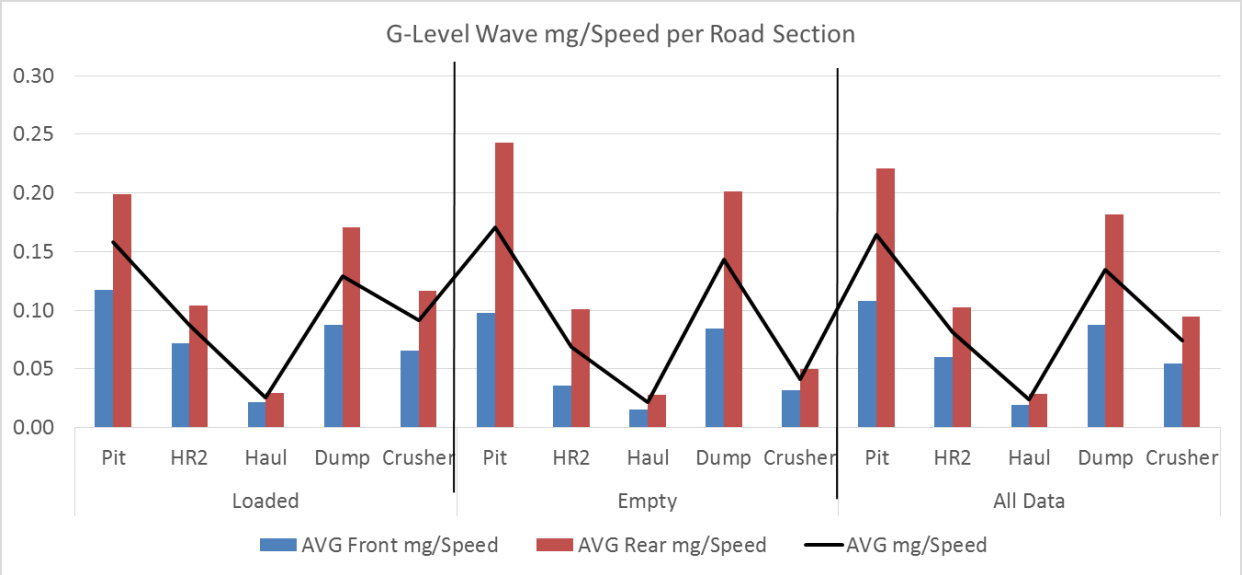

Figure 4-15 – G-level Wave by Speed (mg*s/m) per Road Section

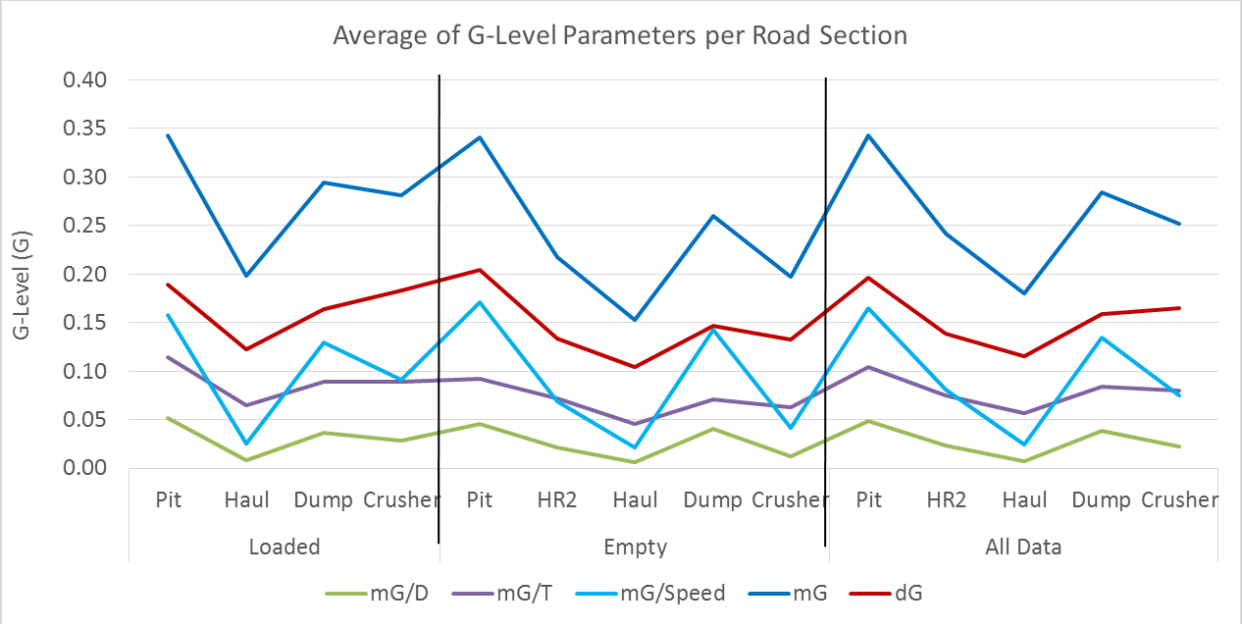

Figure 4-16 – Comparison of G-level Parameters by Road Section

To understand the true relationship between g-level and haul road conditions, the g-level KPI results were plotted against estimated rolling resistance for specific hauls to discern any

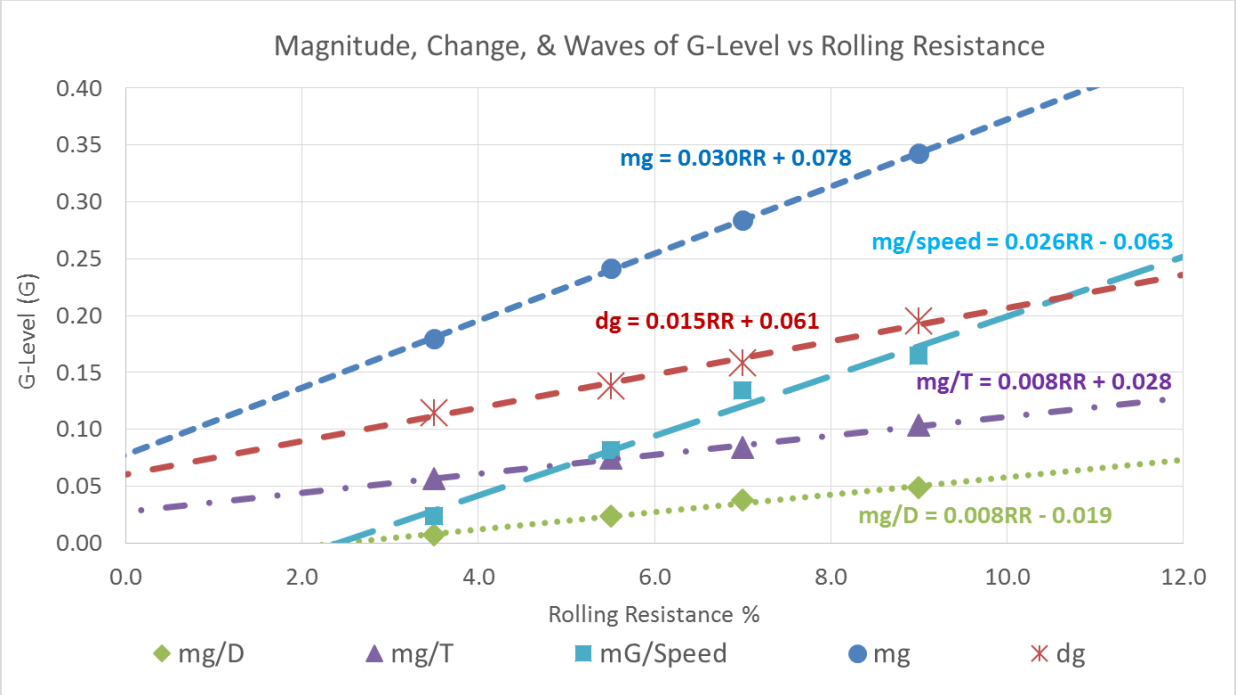

Figure 4-17 – G-level Parameters vs Rolling Resistance

correlation, in Figure 4-17. All classifications are displayed as linear relationships, by increasing g-level as rolling resistance, RR, increases. As mentioned previously, g-level magnitude and g-level wave by speed have comparable slopes relative to rolling resistance, at 0.0295g and 0.0262g slopes respectively, endorsing the suggestion that speed has a minimal influence on g-level magnitude. G-level wave by distance and g-level wave by time also have similar slopes, inferring that both distance and time have a relatively similar impact on g-level magnitude.

G-level wave then provides a measure to begin monitoring road roughness, incorporating both amplitude and frequency. When considering haul truck tires, a large g-level wave should correlate to an increased hysteresis and heat generation in the tire, possibility causing overheating issues as described in section 2.4. This is suggested as a future work direction for direct monitoring.

4.4 Rack, Pitch, Bias & G-level Classifiers

A similar analysis as completed on suspension cylinder g-level change, g-level magnitude, and g-level wave, was also conducted on rack, pitch, and bias g-levels to determine the impact of events occurring on a haul truck frame. In section 3.7, a statistical analysis was completed on RPB events with the focus being on large events typically over 1.5g. When we consider change in g-level for RPB events, the potential for a large swing in value exists as RPB can fluctuate from negative to positive around 0g, whereas the strut g-level remains relatively around +1g. Given the g-level calculation for RPB negate g, where the 4 struts in each RPB equation 12 to 15, the unit g is cancelled out and the norm for RPB is then 0g.

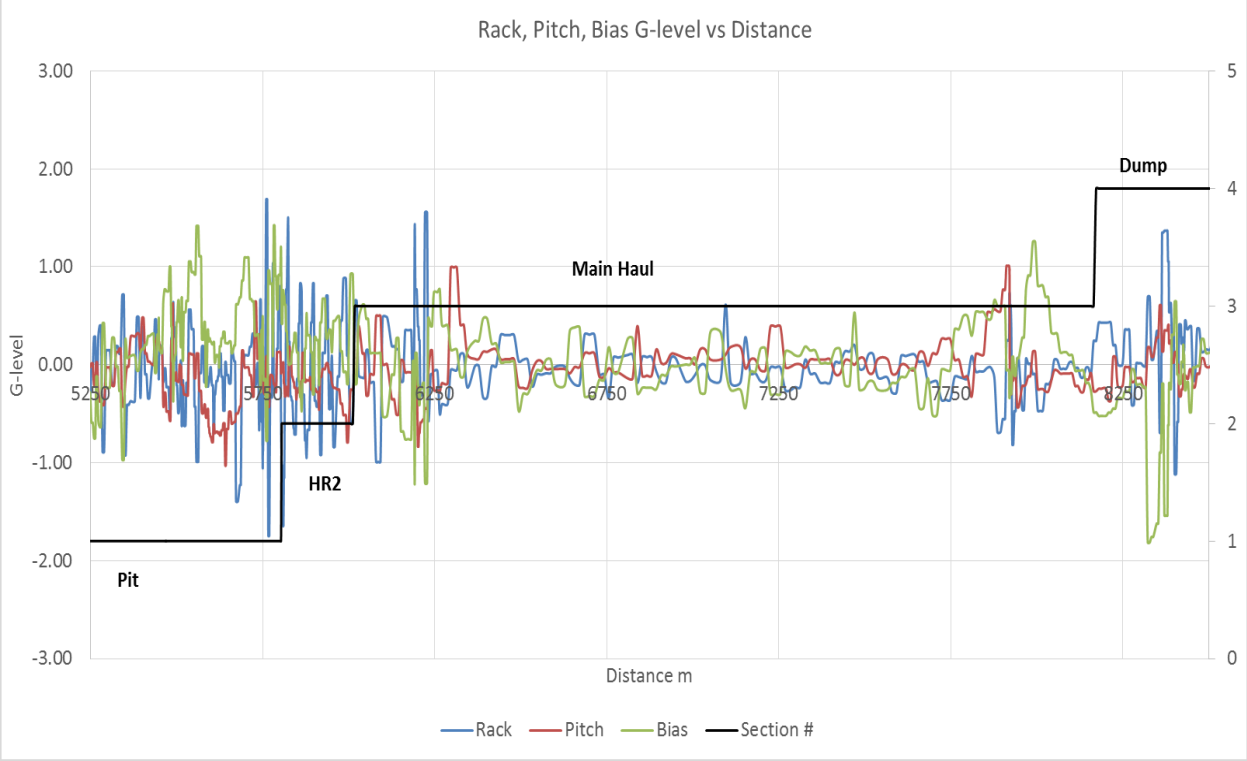

Figure 4-18 – Example of Rack, Pitch, Bias G-level

A plot of rack, pitch, & bias g-level for a haul truck as it performs its duty cycle is very similar to the g-level of a suspension cylinder, except at equilibrium the RPB g-level is at 0g, as opposed to 1g for struts. It can be observed that rack and bias typically trend opposite from one another, whereas pitch is independent. Joseph (2003) described them as natural rack events, which are negative one third bias events due to the geometry of the rack and bias calculations; thus opposite in sign but not the same in magnitude. In the results in Figure 4-19, rack events display the highest values of g-level change compared to pitch and bias events, which can also be visually confirmed in the example in Figure 4-18. The average change in rack g-level approaches or exceeds 0.5g, specifically for all loaded hauls excluding the main haul. It's interesting to note that the average bias g-level change is highest on the dump & crusher areas, which could be a product of tight turning as the haul truck positions to dump, per the dumping operational motion patterns shown in Figure 3-23.

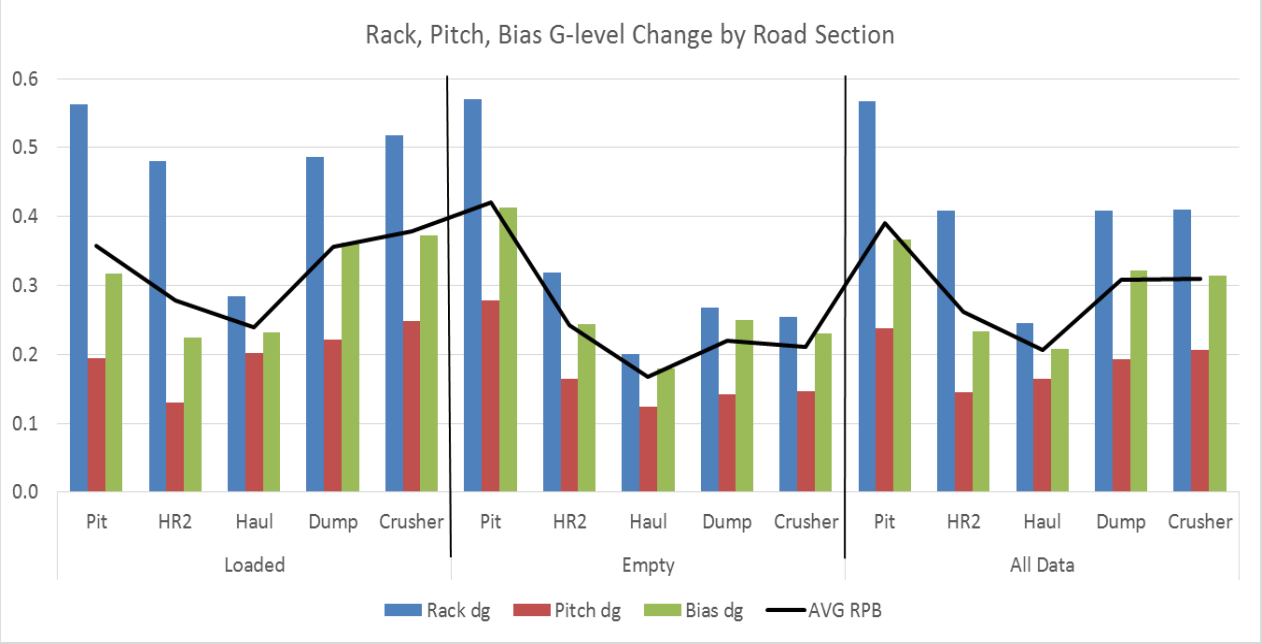

Figure 4-19 – Rack, Pitch, Bias G-level Change by Road Section

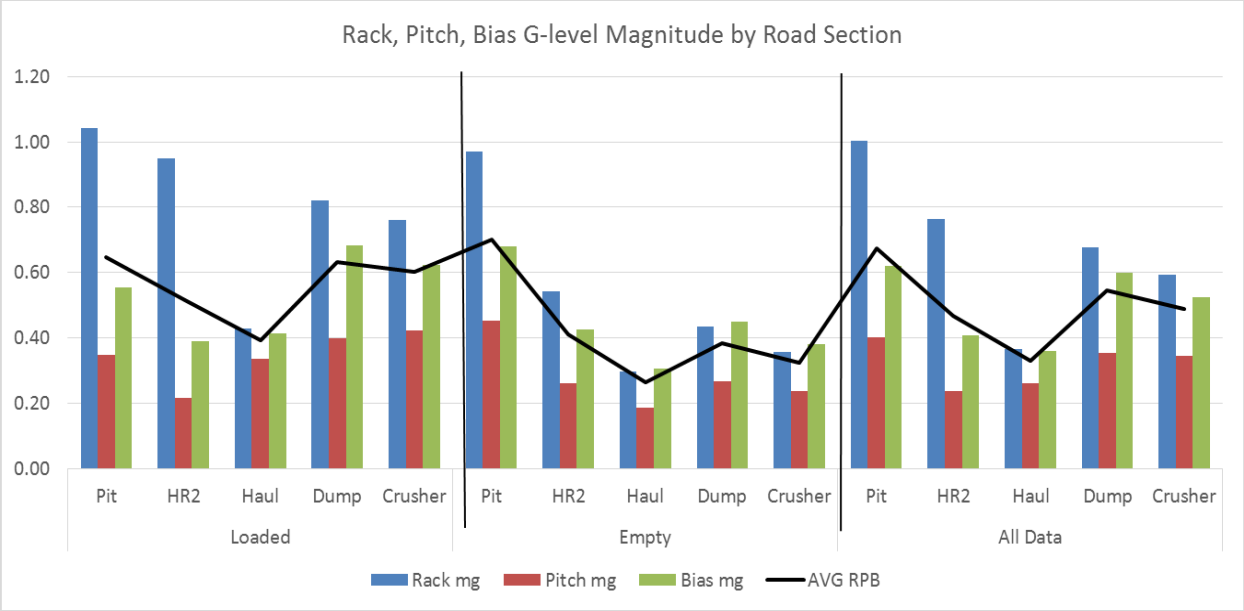

Figure 4-20 – Rack, Pitch, & Bias G-level Magnitude per Road Section

When we consider the magnitude of g-level, the RPB values are almost double compared to g-level change, with some road sections consistently reaching a wave magnitude of 1g. This becomes concerning as the data demonstrates large shifts in g-level, from positive to negative or vice-versa, in a short period of time. Specifically when considering rack events, which exhibit a twisting motion to the truck frame, the data demonstrates that the truck is experiencing on average a change of 1g roughly every 4 seconds of operation on specific haul road sections.

The number of RPB g-level change events over certain threshold values were tabulated for the data set, with the results shown in Figure 4-21. The largest percent of events occurring in the pit and dump/crusher areas, with rack g-level change events over 1g occurring approximately 10% of the time in the pit area. This includes rack changes greater than 2g over a one second period, which account for 2% of the duration in some sections. This is a major concern in regards to frame life, as the data set demonstrated on average 1 to 2 of these events per haul, with the largest g-level change recorded at -3.44g rack.

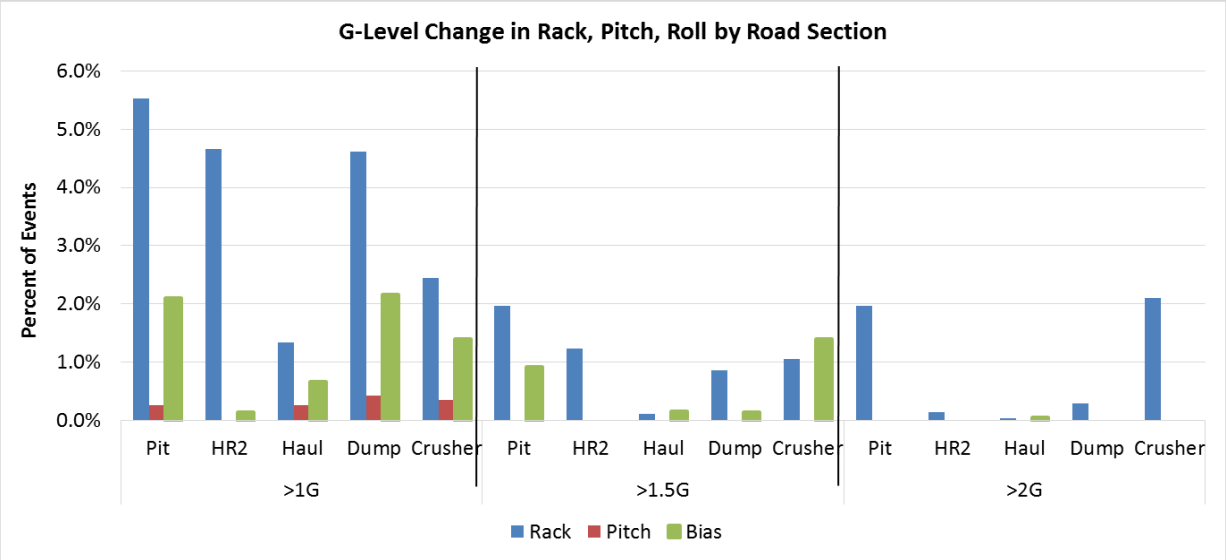

Figure 4-21 - RPB G-level Change (dg) by Road Section

An analysis of g-level wave can also be completed for rack, pitch, and bias, as it was established in Figure 4-18 that RPB g-level acts as inconsistent waves, with varying amplitudes and frequencies by road section, similar to the g-level of a suspension cylinder. Figure 4-22, Figure 4-23, and Figure 4-24 demonstrate g-level wave by distance, time, and speed respectively, with the results following the hypothesis that higher rolling resistance roads exhibit a larger g-level wave.

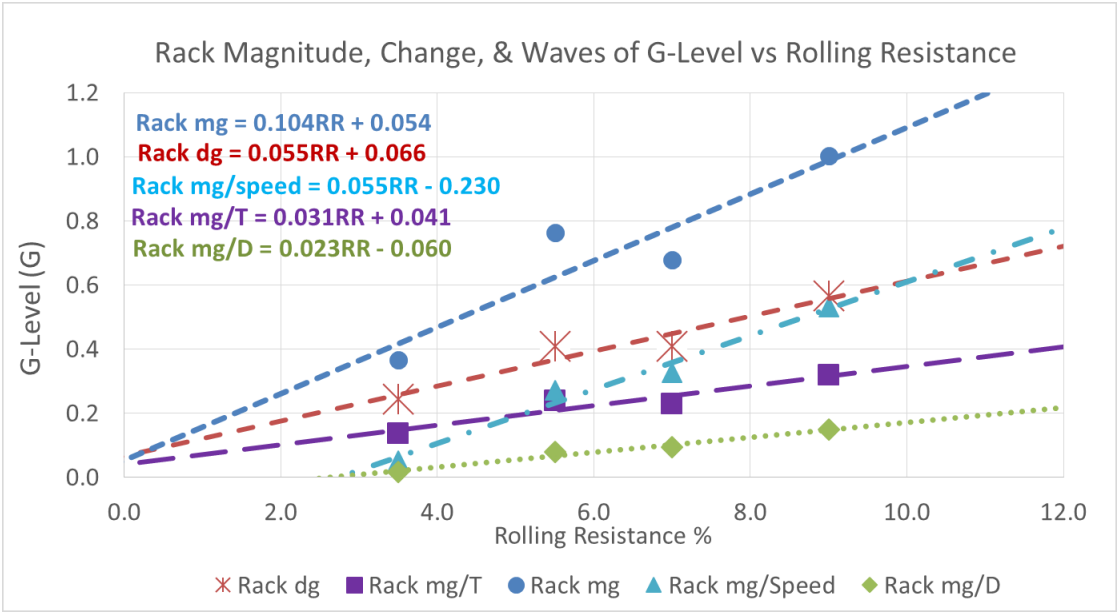

Figure 4-22 - Rack Magnitude, Change, & Waves of G-level vs Rolling Resistance

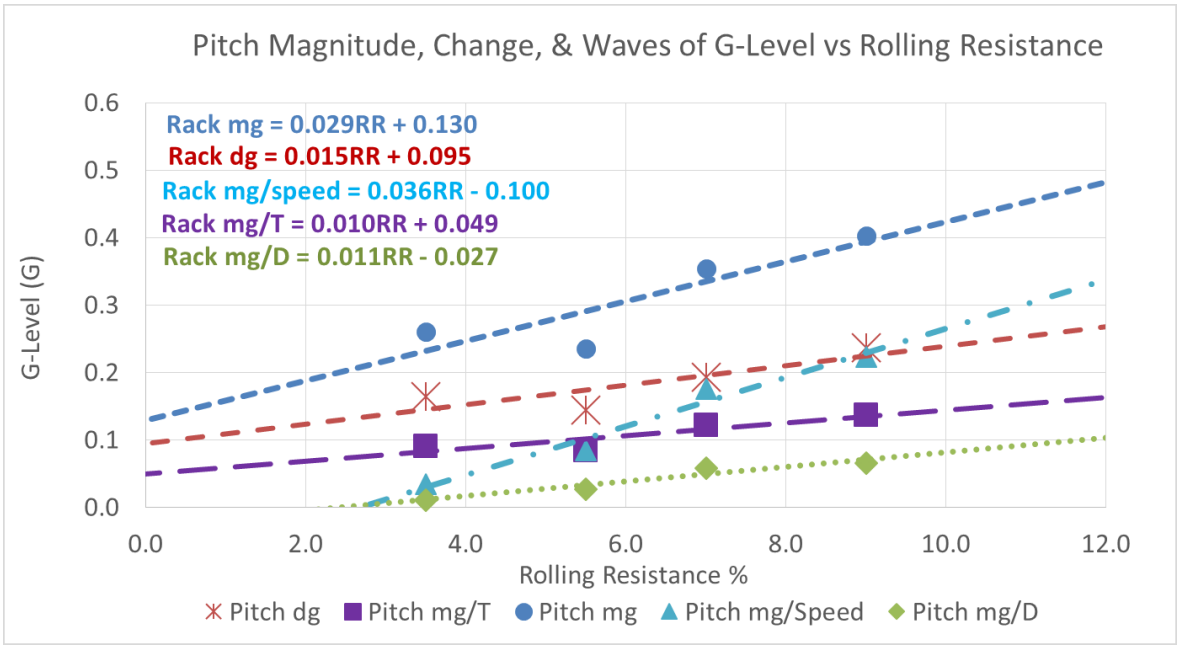

Figure 4-23 - Pitch Magnitude, Change, & Waves of G-level vs Rolling Resistance

An interpretation of the comparison between rolling resistance and RPB g-level parameters suggests that two different relationship exists, g-level wave by distance and time, as well as magnitude and g-level wave by speed, as they display similar slopes. The same relationships were also evident in the strut g-level parameters vs rolling resistance in Figure 4-17.

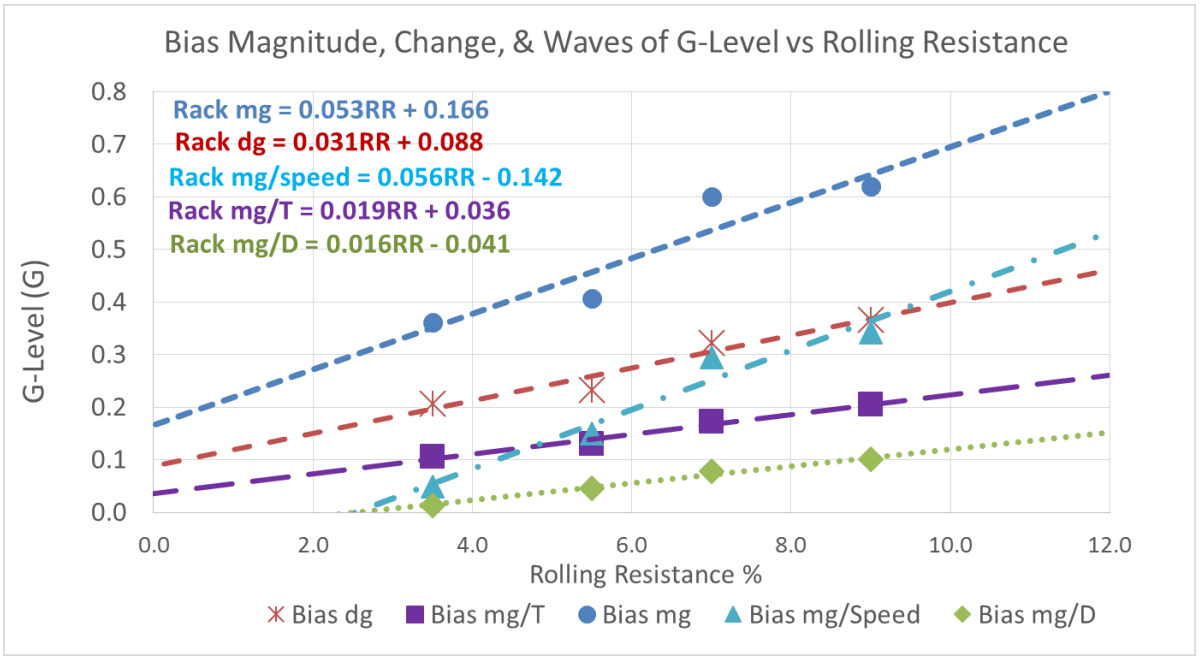

Figure 4-24 - Bias Magnitude, Change, & Waves of G-level vs Rolling Resistance

5 Haul Road Profiling through Suspension Cylinder Data

5.1 Current Haul Road Benchmarking Methods

Section 4 provided a thorough analysis of haul truck suspension cylinder and frame RPB g-levels during hauling. By comparing the magnitudes and values of the g-level events by haul sections, the analysis provided a basis for profiling the roughness of haul roads to better understand damaging frame and component impact sources. Section 5 continues this investigation, but instead of looking at the data from the perspective of the suspension cylinder performance, as per the previous section 4, the analysis will focus on the haul road conditions.

The previous chapters analyzed g-level via the suspension cylinder deflection, and broke down g-level into different criteria such as change in g-level, magnitude of g-level, and g-level wave. Manufacturers design haul trucks, including frames and components, to withstand a certain level of structural fatigue before failure. If we were able to classify haul roads by the number of events they produce on a truck, it can provide the ability to predict the life of a truck frame structure and associated components.

As previously mentioned in section 3.7, Caterpillar utilizes a system called FELA to determine the life of haul truck frame, illustrated in Figure 5-1. This system utilizes the average of the rack and pitch pressures over a set period of time to determine haul road severity, and translates the FELA value to an estimate in component life. The main limitation of the Caterpillar FELA system is that it takes an average over the haul, and is unable to break down into individual haul sections that are of high concern, and thus with an average dilutes such impacts. The system triggers an alert when a certain threshold RPB event occurs; which can be tracked to the

location of the occurrence; but FELA does not account for events by strut location or g-level change and magnitude for RPB events.

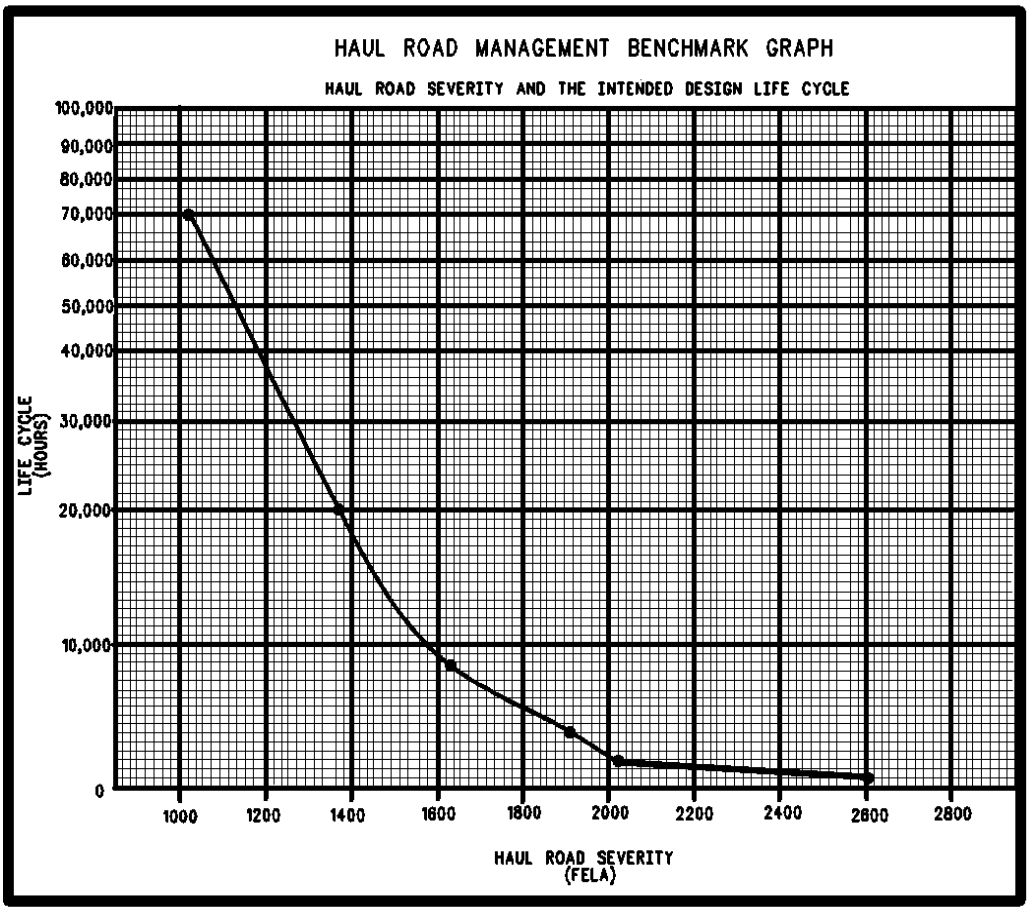

Figure 5-1 – Caterpillar FELA Haul Road Benchmark System (Caterpillar Inc., 2017)

When large g-level events occur at a singular suspension cylinder, it typically triggers a RPB event as well, but if a road was to cause a haul truck to "bounce" with an even strut distribution, this would cause large strut events without registering a RPB event. This is demonstrated by the example shown in Table 5-1.

Table 5-1 – Large Suspension Cylinder G-level vs Lack of Rack, Pitch, Bias Event

Scenario 1 – Normal g-level				Scenario 2 – High Strut g-level			
LF g	RF g	Rack g	0	LF g	RF g	Rack g	0
1	1	Pitch g	0	2	2	Pitch g	0
1	1	Roll g	0	2	2	Roll g	0
LR g	RR g			LR g	RR g		

Scenario's that can generate occurrences as exemplified in Table 5-1 include the bottom of a ramp or a rolling wave road section, which can be common in oil sand applications due to the changing material stiffness properties of the road. An example of a rolling wave road section causing bouncing of a haul truck in oil sand can be seen in Figure 5-2 below.

Figure 5-2 – Haul Truck Bouncing in Oil Sand (Joseph & Barton, 2000)

5.2 Macro Haul Road Profiling

If a haul truck is outfitted with GPS, the location of the truck can be plotted proportional to suspension and frame events, allowing operations to view sections of road causing potential truck damage. The methods of investigating g-level change and magnitude from section 4 prove valuable when plotting road events by these g-level KPI's, as simple g-level of strut and RPB tend to overlook poor road conditions. This is demonstrated in the following examples, as Figure 5-3 reveals 6 locations of poor haul condition triggering suspension cylinder g-level or RPB g-level events greater than 2g.

Figure 5-4 displays the proposed methodology utilizing g-level change and magnitude for suspension cylinders and RPB, which highlights 7 additional poor haul sections over similar g-level thresholds, for the same data set that are not highlighted in Figure 5-3.

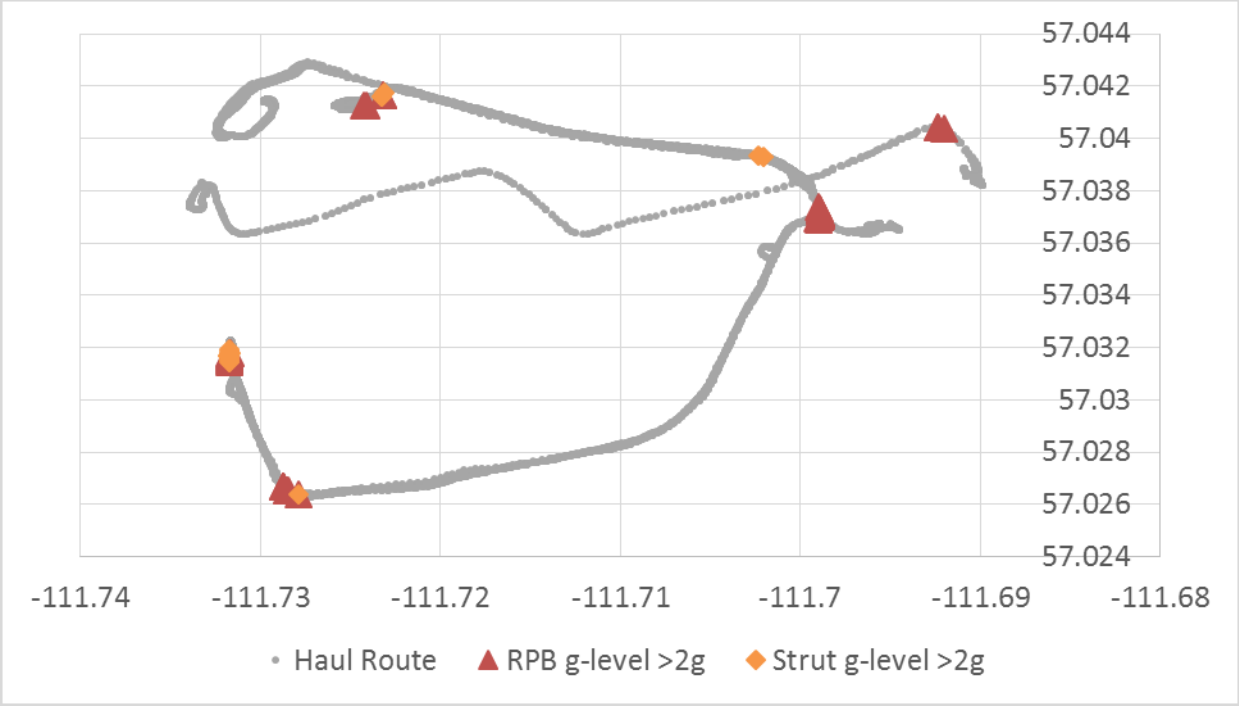

Figure 5-3 – Haul Road Suspension Cylinder & RPB G-level Event Plotting

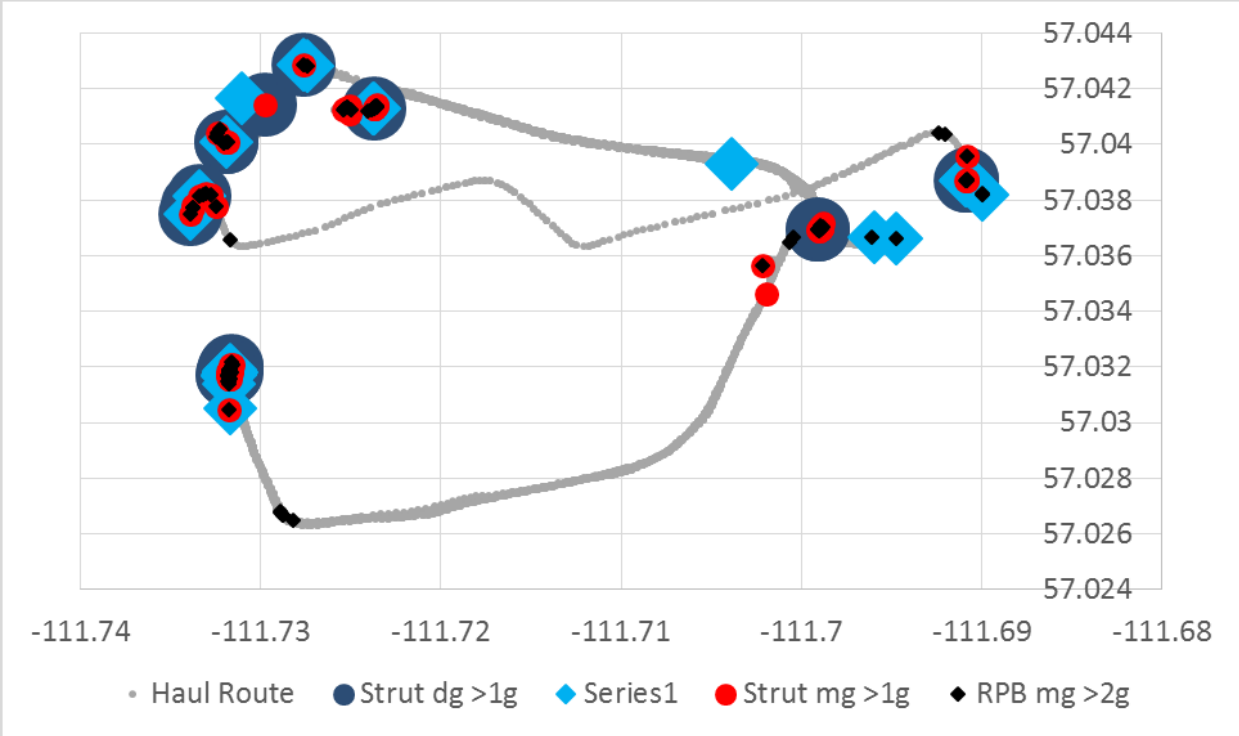

Figure 5-4 – Haul Road Suspension Cylinder & RPB G-level Change & Magnitude Event Plotting

Comparing g-level change and g-level magnitude to understand the most appropriate metric for evaluating haul roads, Figure 5-4 suggests that both parameters reveal almost the same poor road conditions, with only a couple differences. Utilizing the impact events, an experienced mine operations engineer would be able to interpret the data and visit the on-site location to determine the root cause of the g-level event, and provide a road remediation solution. Without the benefit of visiting on-site locations, the author conducted an interpretation based on his experience of typical oil sands operating conditions, to provide an example of such a g-level analysis, Figure 5-5.

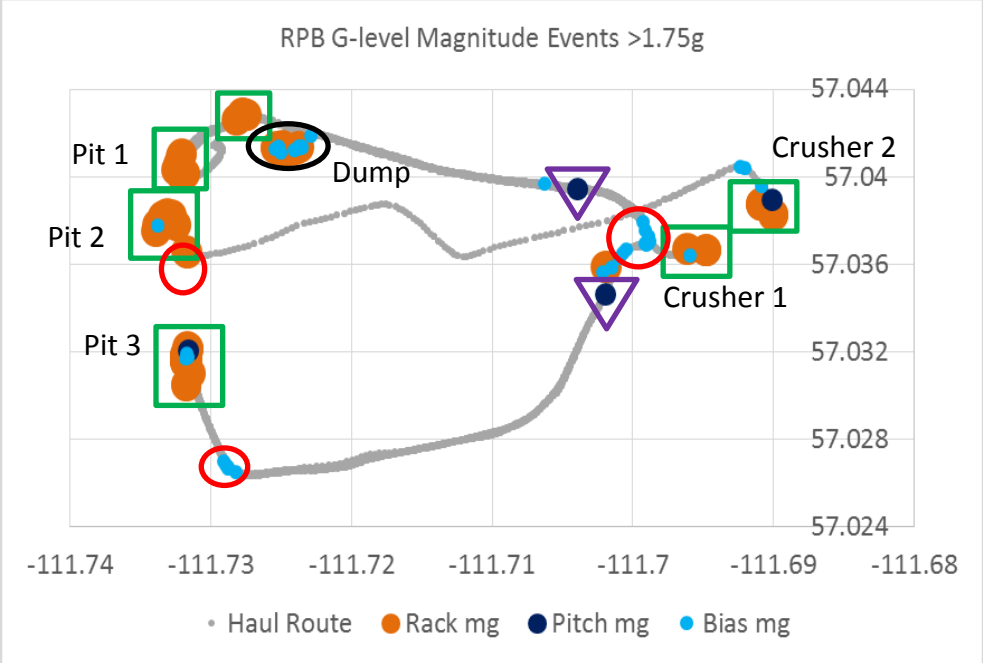

Potential Causes of RPB Events

- Poor ramp transition leading to pitch event
- Lack of super-elevation around corner causing bias event
- Poor/soft road conditions producing RPB events
- Tight turning on dump leading to bias, poor underfooting causing rack

Figure 5-5 – Haul Road Condition Analysis Utilizing RPB G-level Magnitude

The example in Figure 5-5 utilized RPB g-level magnitudes, but as mentioned above, g-level change would also be adequate. Ideally a combination of suspension cylinder and RPB g-level data would be incorporated into such an analysis.

5.3 Micro Haul Road Profiling

In addition to plotting g-level parameter events for suspension cylinders and RPB, a further in-depth analysis may be conducted with respect to road conditions, causing the events featured in section 5.2. This analysis may be used to validate the accuracy of g-level change in comparison to the Joseph (2003) g-level analysis, and indicate its significance to become a metric to measure haul road conditions. In Figure 5-6, a detailed plot of g-level and g-level change can be seen for an impact event over two different cycles, "7" and "11" on a main haul road.

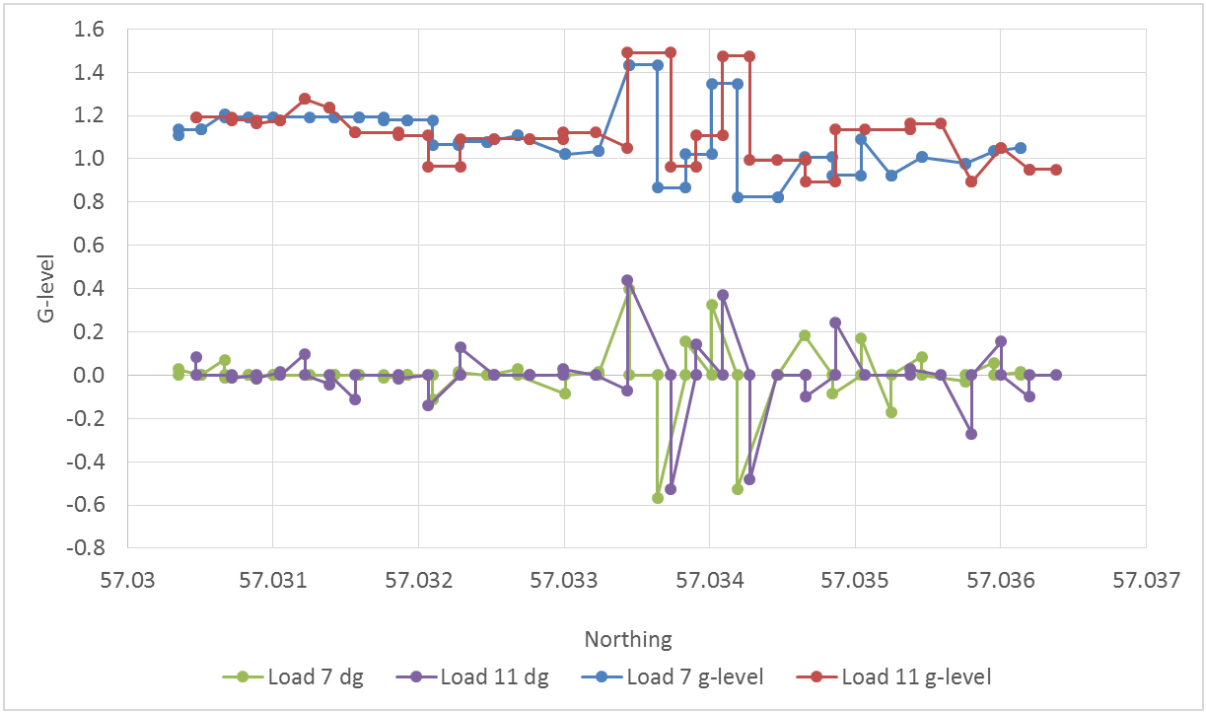

Figure 5-6 – G-level vs G-level Change Example: Left Front Suspension Cylinder

When the two hauls are overlain, Figure 5-6, we can see they almost mimic one another, specifically for g-level change. The simple g-level plots are comparable, with similar increments of change (dg), but tend to be offset by a small magnitude of 0.1g to 0.2g. G-level change tracks the similar increments from the g-level plot, and demonstrates that these increments are indeed almost the same values.

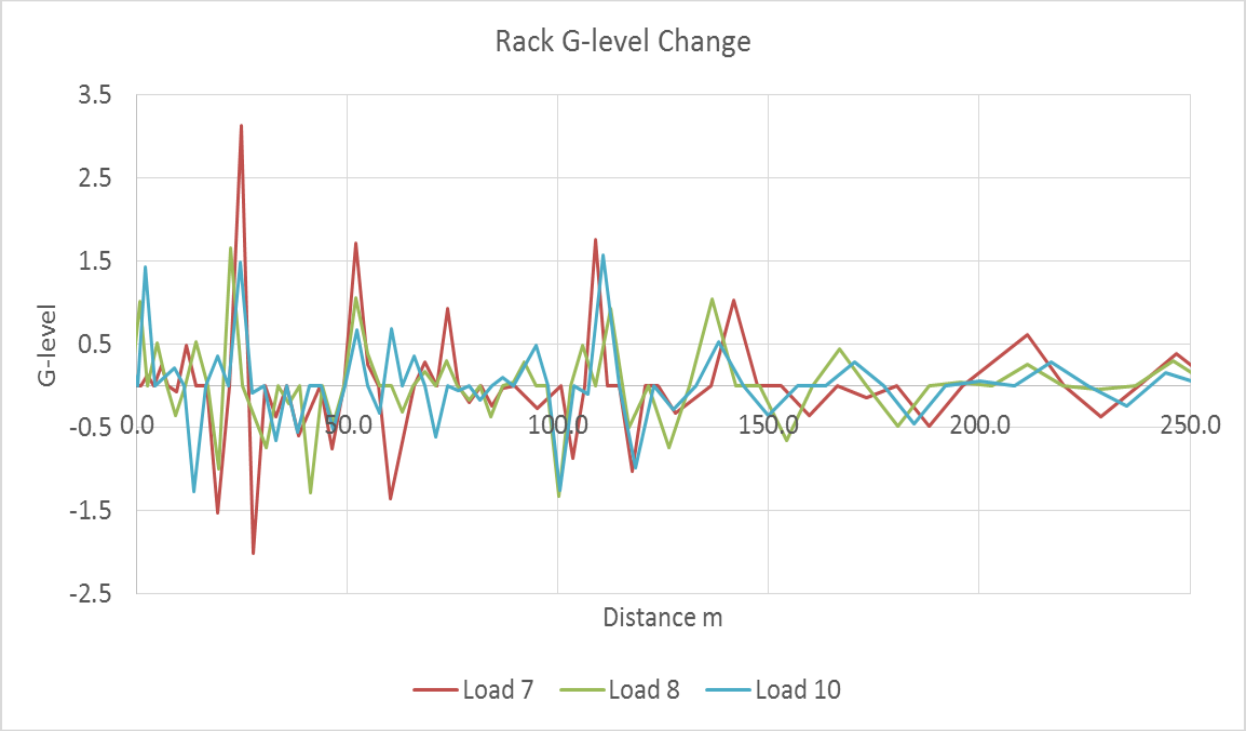

Figure 5-7 – Rack G-level Change Example: Pit Area

Another example of the accuracy of g-level change can be seen in Figure 5-7, which shows the rack g-level change for three different loaded haul cycles travelling in a pit area after being loaded with a payload. This particular haul section displays several large rack events, specifically at a distance of 25m, where 3 rack events over 1.5g occur within ~20 meters of travel, with one event registering over 3g's.

This analysis permits specific road conditions causing large frame and strut events to be reflected clearly in a quantifiable manner, so the impact of the events can be understood. Further detailed examples of strut and RPB g-level change can be found in appendix B.

5.4 Road Condition Mapping

Section 5.2 investigated mine haul conditions, determining problem zones that produce potential component damaging events, but the analysis did not quantify the road conditions for the remaining haul sections. Utilizing our analysis for g-level, g-level change, and magnitude of g-level, the full mine haul route may have its roads categorized based on their specific g-level parameter values. This can be accomplished by calculating local g-level averages, which is to trim down the data into "floating average" sections of hundreds of GPS points instead of tens of thousands, such as Figure 5-8.

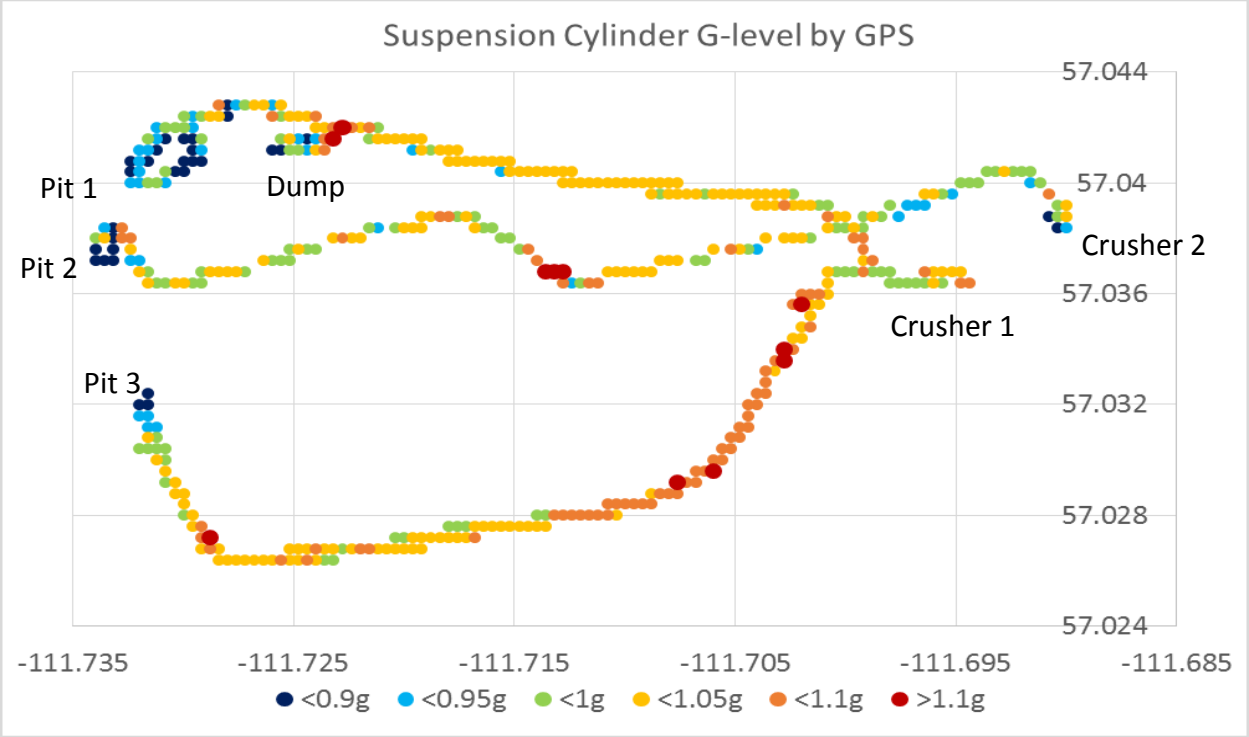

Figure 5-8 – Mine Road Condition Map by Suspension Cylinder G-level

Figure 5-8 exhibits the strut GPS g-level analysis for an entire oil sand mine, confirming what was determined in section 3, with areas of high rolling resistance displaying lesser strut g-level values, and vice-versa. This can be confusing, as it solicits the question of whether hauls producing high average g-level values, which is typically expected from poor road conditions, are causing damage to truck structure. The unclear analysis from simple strut g-level validates the value of g-level change and magnitude, as they provide clarity when quantifying haul roads, by following the base hypothesis of decreasing road quality correlating to higher g-level values.

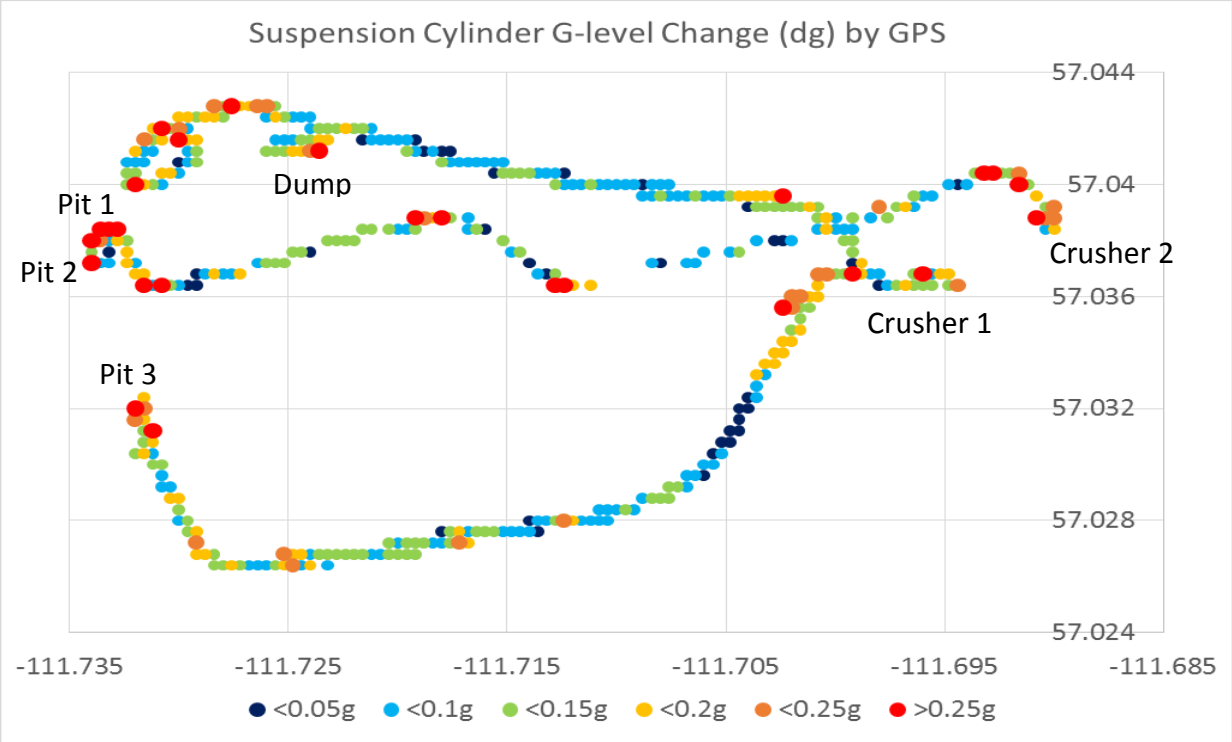

Figure 5-9 – Mine Road Condition Map by Suspension Cylinder G-level Change (dg)

The resulting road condition haul map example with corresponding strut g-level change is shown in Figure 5-9 through Figure 5-11, with similar road condition maps being produced by suspension cylinder g-level magnitude, g-level wave, as well as RPB g-level parameters, which can be seen in appendix C. The most consistent and accurate g-level parameters tend to be g-level change and magnitude for suspension cylinders and rack events in particular.

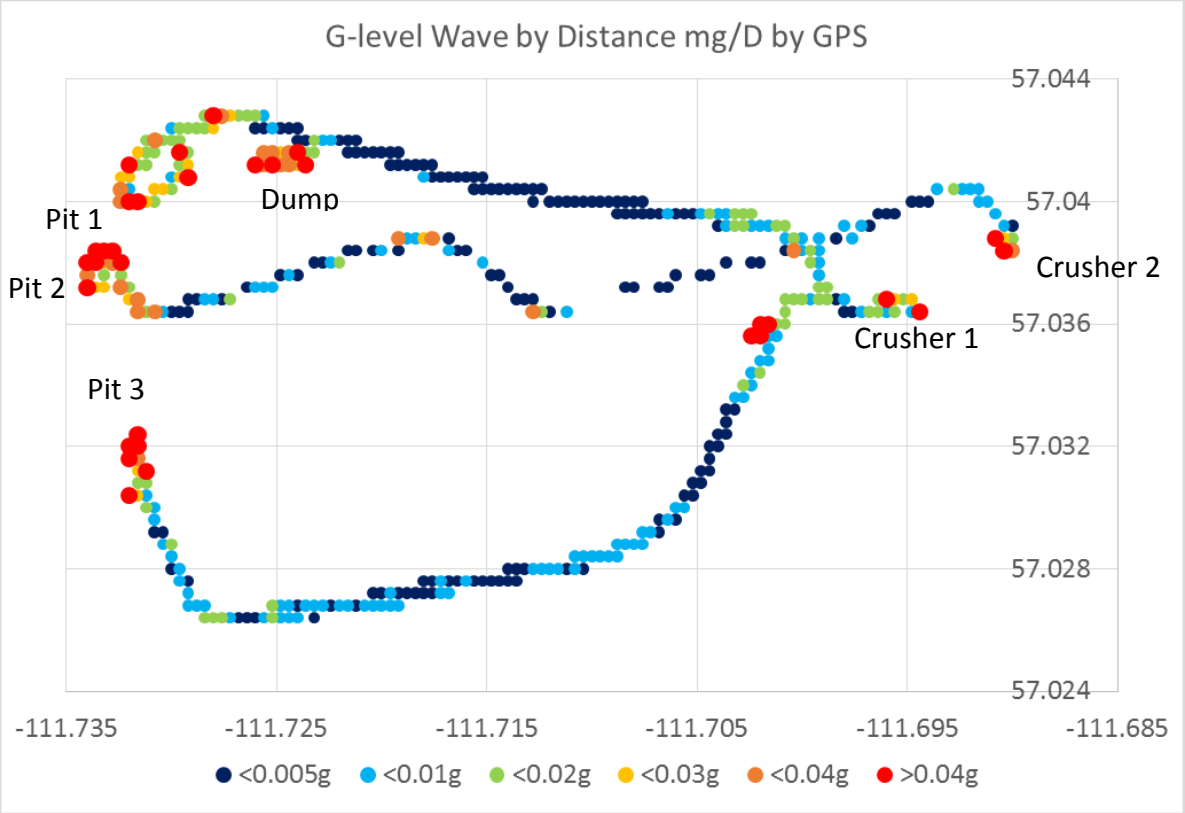

Figure 5-10 – Mine Road Condition Map by Suspension Cylinder G-level Wave mg/D

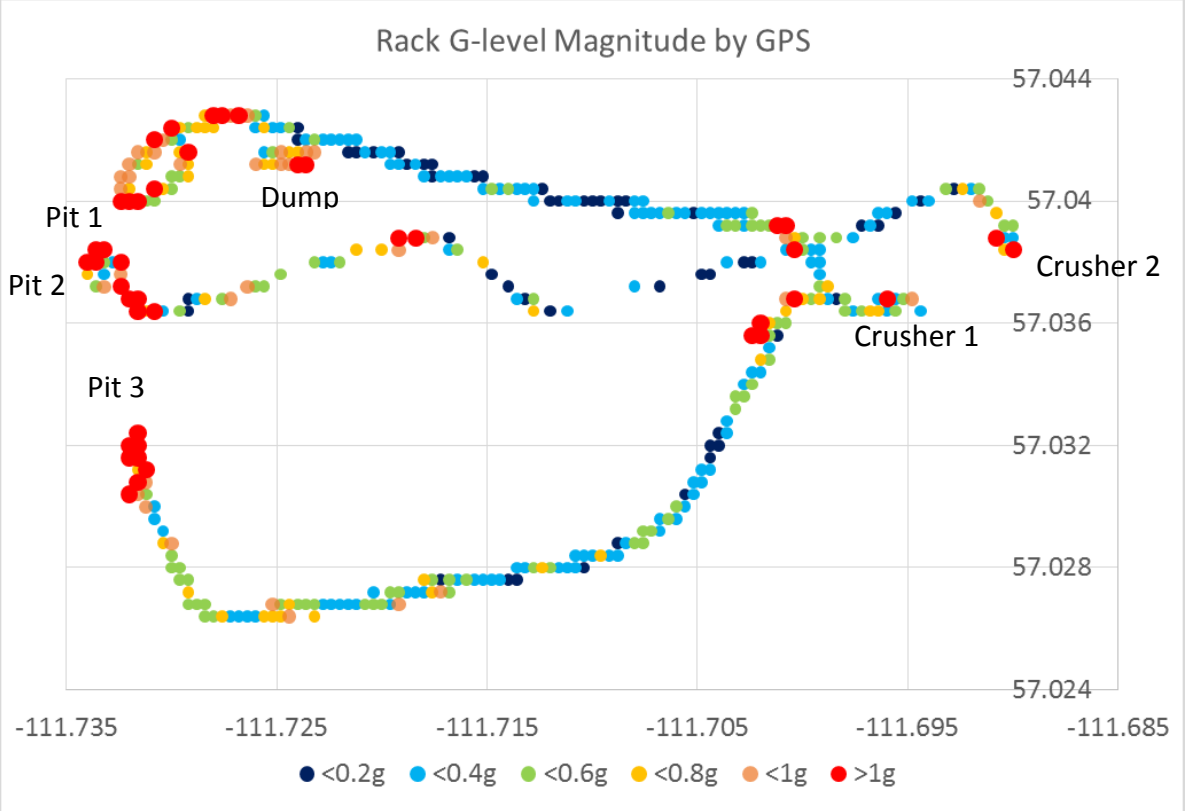

Figure 5-11 – Mine Road Condition Map by Rack G-level

5.5 G-level Wave Frequency

When discussing g-level wave, it has been determined that amplitude and frequency are the two key variables to determine the impact of the wave. The focus in this thesis has been on the amplitude of the wave, but the attention will now shift towards frequency, as this permits the evaluation of events per length of haul road. Frequency can be calculated for g-level magnitude and change for both suspension cylinder and RPB data. The units of frequency deemed valid for the analysis are distance and time. G-level wave is not included in the analysis as it is already incorporated by frequency in the calculation.

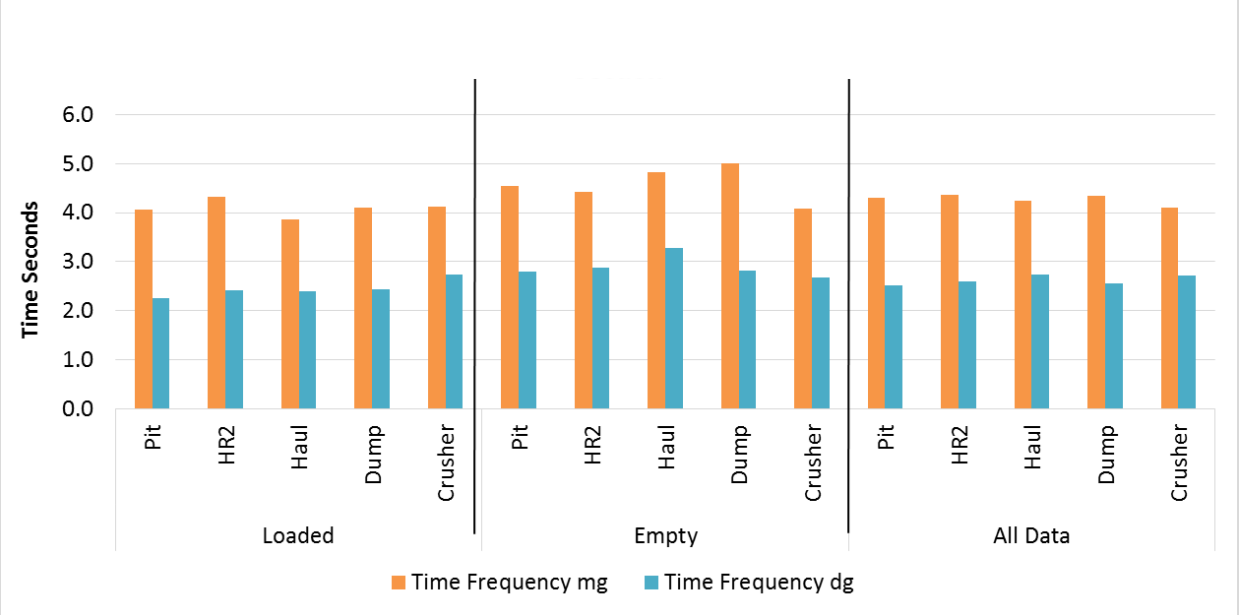

Figure 5-12 – Time Frequency of Suspension Cylinder G-level Change & Magnitude

Time as a frequency does not provide any useful detail in terms of classifying road sections, as no trend can be found in the data, Figure 5-12. It does however demonstrate that on average, a haul truck suspension cylinder experiences a g-level change event every 2-3 seconds, and the strut will reach a high g-level magnitude approximately every 4-5 seconds.

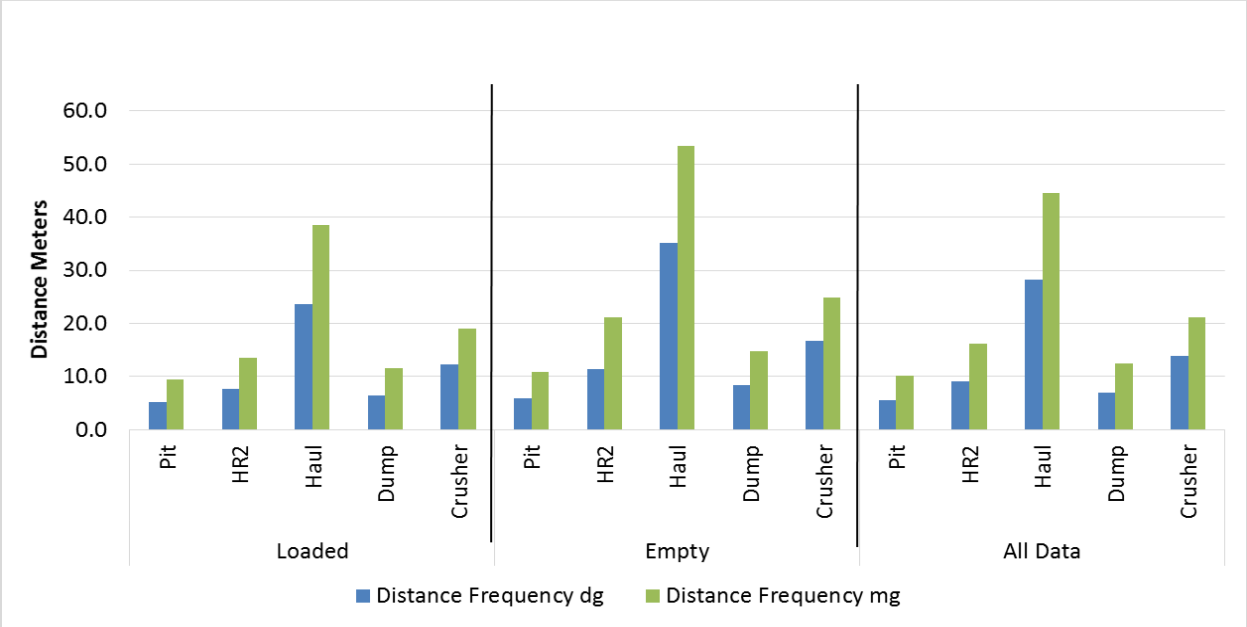

Figure 5-13 –Distance Frequency of Suspension Cylinder G-level Parameters by Road Section

As expected, the main haul road displays a lower frequency, or larger distance between events, than the remaining haul sections with higher rolling resistance by a multiple of 3 to 6. It can be noted that the wheelbase of the Cat 797B used in this analysis is 9.6m, and has a natural frequency of 1 to 3 hertz, such that 9.6m to 29m may represent a large number of events. The results from Figure 5-13 include all events, but the data can be filtered to only include events of significance or past a certain threshold, which may prove to be more useful when estimating haul truck component life based on the operating conditions. This is demonstrated in Figure 5-14, which includes an example for frequency of loaded g-level change above 0.2g.

Roiling resistance and frequency by distance were plotted to determine the relationship that exists between the two variables in Figure 5-14 & Figure 5-15. The trend suggests that frequency significantly increases as rolling resistance approaches zero, for both g-level change and magnitude. In theory, this trend would hold true, as zero rolling resistance should entail no road undulations or any roughness to the road, thereby providing no opportunity for the strut

pressure to change. Frequency of g-level is important to monitor, as it provides a measure of road undulations and roughness. Even though smaller g-level changes and magnitudes may not cause substantial damage on a haul truck, consistent bouncing will theoretically increase the hysteresis in a haul tire, raising its temperature and potentially leading to an overheat scenario that would pull the truck out of production or cause it to slow down.

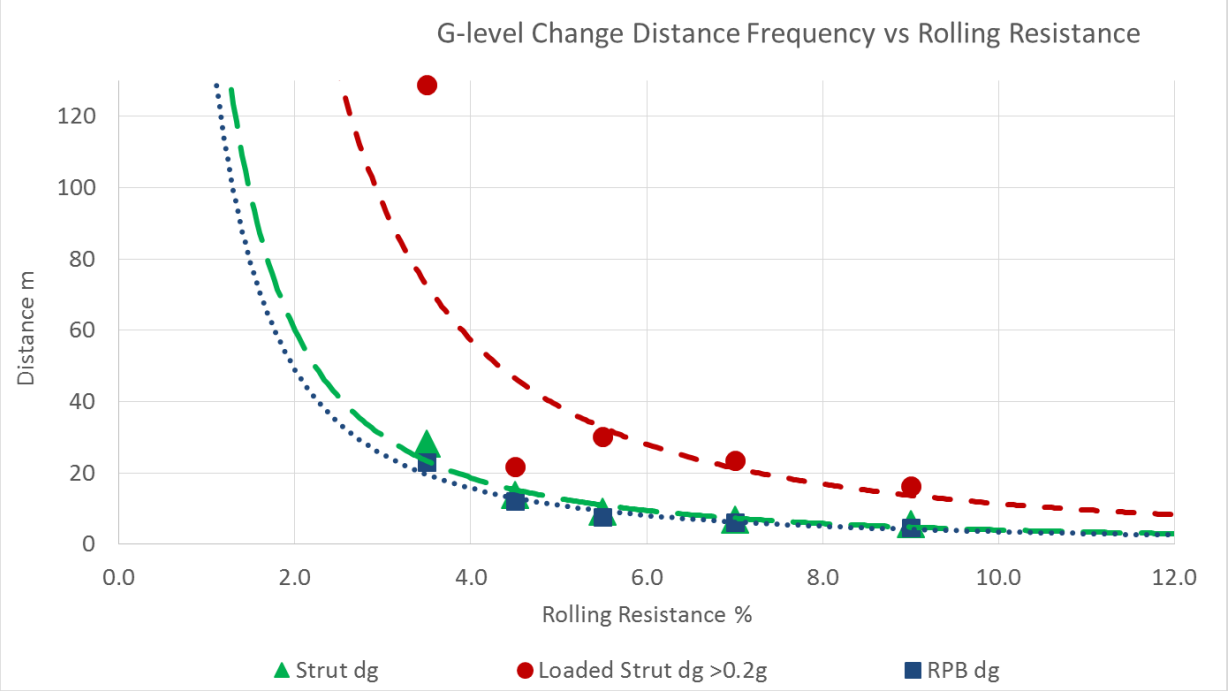

Figure 5-14 – Distance Frequency of G-level Change vs Rolling Resistance

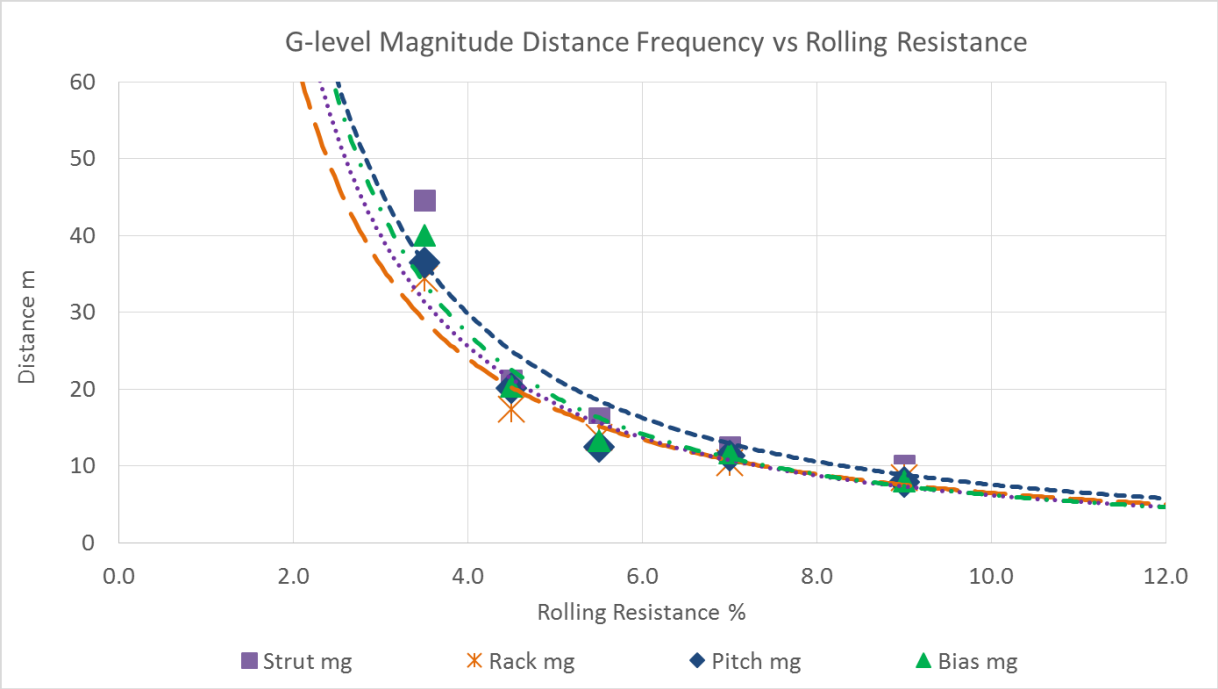

Figure 5-15 – Distance Frequency of G-level Magnitude vs Rolling Resistance

6 Conclusion and Future Work

6.1 Conclusion

Given Caterpillar 797 haul truck operational data from an oil sands mine near Fort McMurray, Alberta, an analysis was conducted to determine the relationships between haul truck motions and the surface course over which they operate. The analysis focused specifically on the components of a quarter vehicle model, which include a truck oleo-pneumatic suspension system, corresponding truck tires, and the ground profile. The strut pressure data was converted into a mass and an acceleration factor, termed g-level.

With respect to suspension cylinder mass, a payload was determined by subtracting the empty mass on the suspension cylinders from the loaded mass, which resulted in an average payload of 286 tonnes for the Caterpillar 797 data. A Caterpillar 797 haul truck is designed to accommodate 345 to 363 tonnes, depending on machine configuration and empty vehicle weight, which in conjunction with an average VIMS payload of 320 tonnes, presented a significant difference in comparison to the calculated payload. To validate the calculated mass calculations, separate data was provided from another Caterpillar 797, and paired with actual scaled weights, revealing a 16.1% difference between actual payload and suspension cylinder calculated payload.

While this error cannot be confirmed to be the same for the original truck data, it does advocate that the calculation method may include inaccuracies, in not accounting for inefficiencies experienced due to setup, friction or mechanical operation. In terms of the analysis, a potential error would only affect the real time tonne-per-kilometer-hour (tkph)

calculation for a tire, as the workload rating of the tire determined from the strut loading and speed at which it travels. Originally, the real time tkph was found to be 5% to 7% below the OEM ratings, but if adjusted for a 16% increased load as determined by the scale study data, the real time tkph will exceed the manufacturer threshold by 4% to 7%.

One objective of this thesis was to utilize the suspension cylinder g-level data as a classification metric for the quality of a haul road, with the results generally showing high rolling resistance areas correlating to lower g-level values. This proved contrary to what was expected, as plots of g-level demonstrate large fluctuations in short frequencies for high rolling resistance sections, contrasting smoother and less volatile relationships for low rolling resistance hauls. This led to considering g-level as a wave, defining the amplitude and frequency of the suspension cylinder data, as well as the rate of change.

G-level change and magnitude (amplitude) then provides another metric to track large, potentially damaging g-level events of suspension cylinders; with these parameters recording a higher percentage of events than simple g-level averages, as proposed by Joseph (2003). G-level change and magnitude presented strong linear correlations to rolling resistance, demonstrating higher g-levels with increased rolling resistance. When considering the full g-level wave, three different parameters were utilized to track frequency; distance, time, and speed, with all 3 parameters demonstrating positive linear relationships with rolling resistance. Frequency was also calculated as its own metric, holding true to the hypothesis of higher rolling resistance profiles presenting greater frequencies. It was exhibited that on average, a haul truck experiences a magnitude change every 4 to 5 seconds, which varies from a distance of 10

meters in a pit area to 45 meters on a main haul road. These results are roughly halved when considering g-level rate of change, with respect to both time and distance.

The g-level analysis also incorporated stress events on the truck frame, specified as rack, pitch, and bias events, derived from the g-level of the four individual struts. The truck frame events bring further clarity of the haul course, as they make a distinction between front to rear and side to side motions, and twisting of the frame. The results for frame rack, pitch, and bias (RPB) g-level change and magnitude revealed numerous large events, with values larger than the Joseph (2003) simple g-level.

When investigating g-level change in finer detail, it was determined that the results are repeatable across several different hauls, demonstrating similar g-level change values over the same haul sections. At a macroscopic level, utilizing GPS coordinates to graph large events and average g-level values for suspension cylinder and RPB frame parameters, validated the importance of recording g-level change and magnitude. Profiled maps for g-level change and magnitude provided more insight into the haul conditions of the mine than simple g-level.

This thesis details the process to extract greater value from haul truck suspension cylinder data, resulting in methods to profile haul road conditions at a mine site and the corresponding potential availability ramifications for a haul truck. The haul profile has a large effect on the life of a haul trucks components, with the resultant force transferred through the tire and the suspension cylinder with some energy absorption, and eventually producing an impact on the haul truck frame.

Being able to forecast the g-level or force and subsequent motion impact event on a frame, correlated to haul conditions, would give mine maintenance manager's the ability to estimate the life of frame welds, and proactively signal when a more thorough hands-on inspection is needed. With respect to tires, measuring the road roughness via suspension cylinders provides a better understanding of the hysteresis the tire may experience during its duty cycle, and help explain the occurrence of heat related failures when the apparent site measured tkph is below the OEM standard.

Typically, the current method of road condition monitoring at many mines is based on visual assessments by operators and supervisors, who then call for support equipment for road maintenance. Utilizing the suggested calculation procedure in this thesis, mine operations can classify the haul sections based on severity, followed by dispatching support equipment to the locations determined relative to the road condition GPS maps. This methodology can potentially boost production at a mine, as it allows the ability to prioritize road sections with the highest rolling resistance and road roughness; which have the largest impact on cycle time and machine health. Removing large g-levels induced by road profiles will aid in improving tire life and machine availability, thereby maximizing the production potential of a haul fleet and minimizing the cost to operations, overall generating a lower cost per tonne for the mining operation.

6.2 Future Work

This thesis demonstrated an extended g-level process utilizing haul truck data from a "soft rock" oil sand mine, in which the ground bearing capacity of the underfoot is low in comparison to a hard rock mine. It is suggested that further analysis be conducted into the suspension cylinder g-level response from a hard rock mine or coal mine, to compare the results to the oil sand data set reported here. The concept then would be to collect a database of g-level parameters from several different mine sites, to permit comparison of each site against one another, with the goal of aspiring to best practice in haul road management. It is imperative to document haul road conditions from mine sites as data is provided; as an ongoing comparison of rolling resistance to eventually develop a comprehensive predictive model.

Further research should also be conducted on a possible relationship between rolling resistance and road roughness. Although the terms are sometimes used interchangeably, and road roughness is considered to be a variable of rolling resistance; but it is evident from the field that soft rock deforms and it can be argued that the parameters should be considered separate from one another.

Thompson and Visser have conducted research into haul road design and evaluation, developing a road defect score which relates road roughness and rolling resistance in hard rock mines (Thompson & Visser, 2006). The model involves twelve evaluation criteria including potholes, corrugations, cracking, and rutting. Research should be completed validating such a model for soft rock mines, and establishing a relationship with the road defect score versus truck g-level parameters. Undoubtedly given the g-level versus rolling resistance relationship

for empty versus loaded trucks in this work, the relationship for a soft rock mining operation would not be the same as a hard rock operation.

Ideally the models developed in this thesis will be implemented into a simulation system, capable of inputting road material properties, as per Thompson and Visser's road defect score, to predict the operational and maintenance performance of a haul fleet. As the database of suspension cylinder pressure data is expanded, the simulation model will need to be continually updated for a wide range of different mines and rolling resistances. The potential exists for a simulation system that can track suspension cylinder g-level KPI's, truck frame RPB events, and the real time tkph of haul truck tires utilizing road properties, so that operations and maintenance can improve their predictive capabilities to increase production and lower costs.

7 References

Anon. (2004, October 21). Field Data Collection, Supplied by Oil Sand Site Operations.

Anzabi, V. R., Nobes, D., & Lipsett, M. (2012). Haul Truck Tire Dynamics due to Tire Condition. *25th International Congress on Condition Monitoring and Diagnostic Engineering.* IOP Publishing.

Bridgestone Corporation. (2011). *Bridgestone Data Book - Off The Road Tires.*

Caterpillar Inc. (2008). *Caterpillar® Truck Tire Management.*

Caterpillar Inc. (2012). *Caterpillar Performance Handbook 42.* Peoria, Illinois, U.S.A: Caterpillar Inc.

Caterpillar Inc. (2013). *797F Mining Truck.* Caterpillar Inc.

Caterpillar Inc. (2017, 07 09). *Off Highway Trucks*. Retrieved from Caterpillar: http://www.cat.com/en_US/products/new/equipment/off-highway-trucks.html

Caterpillar Inc. (2017). *Road Analysis Control*. Retrieved from Caterpillar : http://www.cat.com/en_US/support/operations/technology/fleet-management-solutions/road-analysis-control.html

Caterpillar Inc. (2017, 05 26). *Trends: Road Analysis Control (RAC) For Off-Highway Truck/Tractors Caterpillar.* Retrieved from AVSpare: https://avspare.com/catalog/cat/content/i01376573/

Colquhoun, A., Dains, M., Villalobos, O., Noon, T., Gladieux, S., & Clifton, K. (2012). *Caterpillar Payload Management.* Caterpillar Inc.

Fatemi, A. (2011). *Fatigue From Variable Amplitude Loading.* Toledo: The University of Toledo.

Goodyear. (2003). *Global Off-The-Road Tire Engineering Data Book.*

Hajizadeh, M., & Lipsett, M. G. (2015). Anomaly detection in mining haul truck suspension struts. *International Journal of Condition Monitoring Vol. 5, Num 1.*, 9-11.

Harris, W. (2005, May 11). *How Car Suspensions Work*. Retrieved June 26, 2014, from How Stuff Works: http://auto.howstuffworks.com/car-suspension.htm

Hitachi Construction Machine Co. (2017, 07 09). *Haul Trucks*. Retrieved from Hitachi: http://www.hitachiconstruction.com/product-categories/haul-trucks/

Joseph. (2003). Large Mobile Mining Equipment Operating on Soft Ground. *International Mining Congress and Exhibition of Turkey*, (pp. 143-147). Turkey.

Joseph, T., (2012). *MINE 622 Lecture - Tires, Rims, & Real Time TKPH.*

Joseph, T., & Barton, J. (2000). Is Bigger Better. *SMART Conference - OsEIP Program Presentation.* Edmonton.

Joseph, T., & Welz, M. (2011). Revisiting Ground Vibrations due to Mining Equipment Motion. *CIM Journal, Metal Mining Society, Canadian Institute of Mining, Metallurgy & Petroleum Vol. 2, Num. 2*, 72-78.

Joseph, T., Duncan, S., & Curley, M. (2017). The impact of broken rock behaviour on shovel dipper capacity, truck body design and tire life. *International Journal of Geological and Geotechnical Engineering*.

Knights, P., & Boebner, A. (2001, August). Statistical correlation of off-highway tire failures with open pit haulage routes. *Mining Engineering*, 51-56.

Komatsu America Corp. (2017, 07 09). *Mining Electric Trucks*. Retrieved from Komatsu America Corporation: http://www.komatsuamerica.com/mining/electric-trucks

Liebherr. (2017, 07 09). *Mining Trucks*. Retrieved from Liebherr: https://www.liebherr.com/en/deu/products/mining-equipment/mining-trucks/mining-trucks.html

Lipsett, M., & Anzabi, R. (2011). Seasonal Effects on Haul Truck Tire Life. *Maintenance Performance, Measurement, & Management* (pp. 157-162). Luleå, Sweden: Luleå University of Technology.

MacMahon; Rhino Tyres; Tyre Innovations Ltd. (2009). *Eaglefield Site Study.*

Magna Tyres Group. (2014). *Technical Databook 2014.*

McGarry, P. (2007). *Haul Truck Tires and Open Pit Mining Applications.*

Michelin. (2010). *Technical Data Book - Earthmover and Industrial Tires.*

Michelin. (2011). *Rolling Resistance - Basic Foundation By Randall Clark.*

Netscher, N., Aminossadati, S., & Hooman, K. (2008). *A Review of Patents in Tyre Cooling.*

Otraco. (1993). *Development in Tyres for Quarrying.*

Parreira, J. (2013). *An Interactive Simulation Model to Compare an Autonomous Haulage Truck System with a Manually-Operated System.* Vancouver: University of British Columbia.

Rasche, T. (2001). *Establishing Preventative Safety and Maintenance Strategies by Risk Based Management – The Tools of the Trade.* Brisbane: Minerals Industry Health and Safety Centre.

SAE International. (1995). *J1098 - Surface Vehicle Standard.* Warrendale, PA.

Stumpf, H. W., & Hohl, G. (2000, June). Military Off-The-Road Tires. *Seoul 2000 FISITA World Automotive Congress.* Seoul.

Tannant, D. D., & Regensburg, B. (2001). *Guidelines for Mine Haul Road Design .*

Thompson, R. J., Visser, A. T., Heyns, P. S., & Hugo, D. (2006). Mine road maintenance management using haul truck response measurements. *Mining Technology, Institute of Materials, Minerals and Mining, Vol. 115, No. 4*, 123-128.

Thompson, R., & Visser, A. (2006). Selection and Maintenance of Mine Haul Road Wearing Course Materials. *Mining Technology Volume 115*, 140-153.

Tire Maintenance Council. (1994). *Radial Tire Conditions Analysis Guide.*

Van de Loo, P. (2003). *Trucks, The Development of the Smart Strut Improved Sliding Pillar Front Active Suspension System for Mining.* Birrana Engineering Pty Ltd.

Werner, J. T., & Barrowman, K. (2001). *Remote Real-Time Tire Monitoring in Open Pit Mines.*

Zhou, J. (2007). *Investigation into the Improvement of Tire Management Practices.*

Zhou, J., Hall, R., Huntingford, K., & Fowler, G. (2008). Effect of off-the-road tyre rotation practices on tyre life: a case study. *Mining Technology, 117*(3), 101-110.

8 Appendix

8.1 Appendix A – Haul Truck Speed Distributions

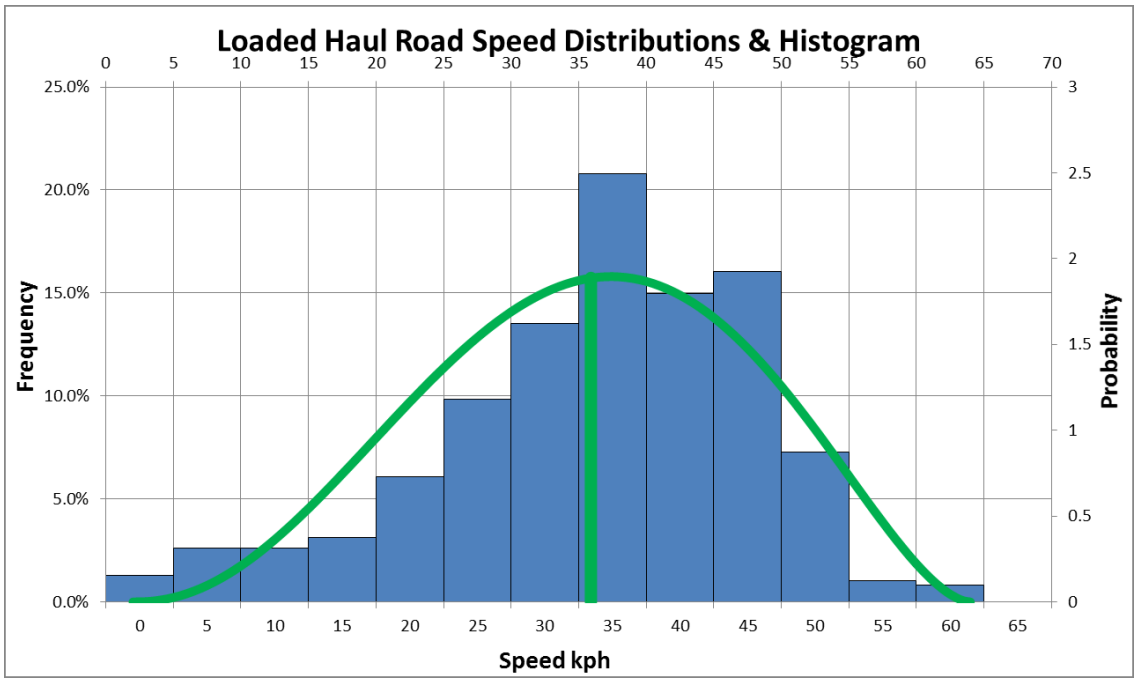

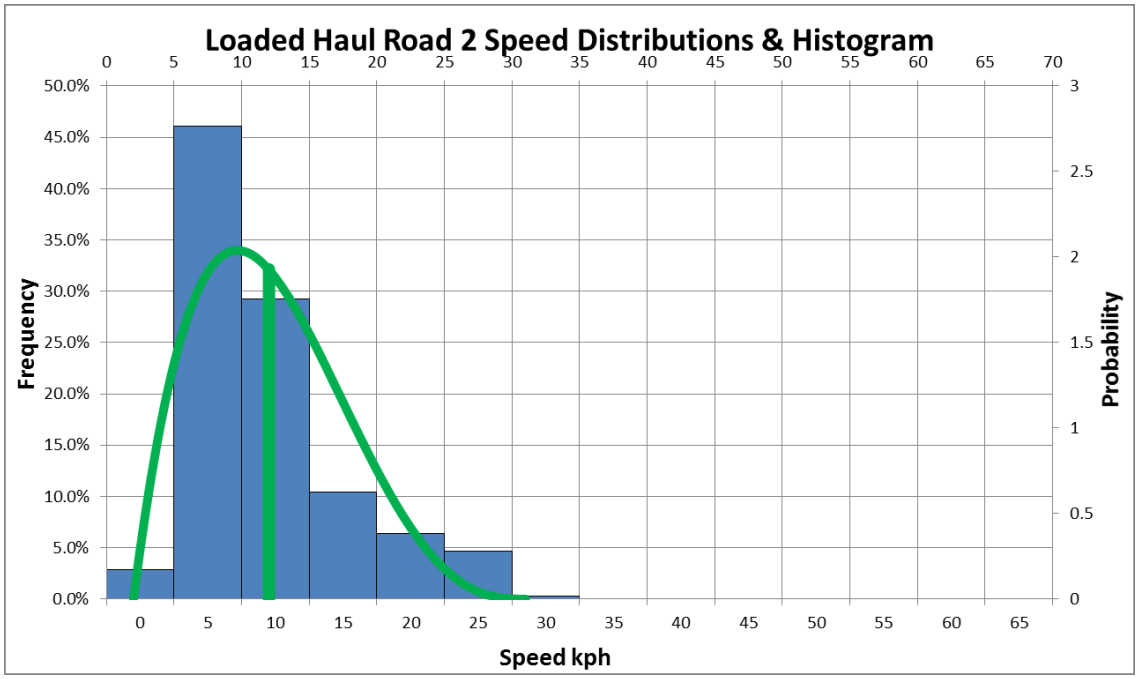

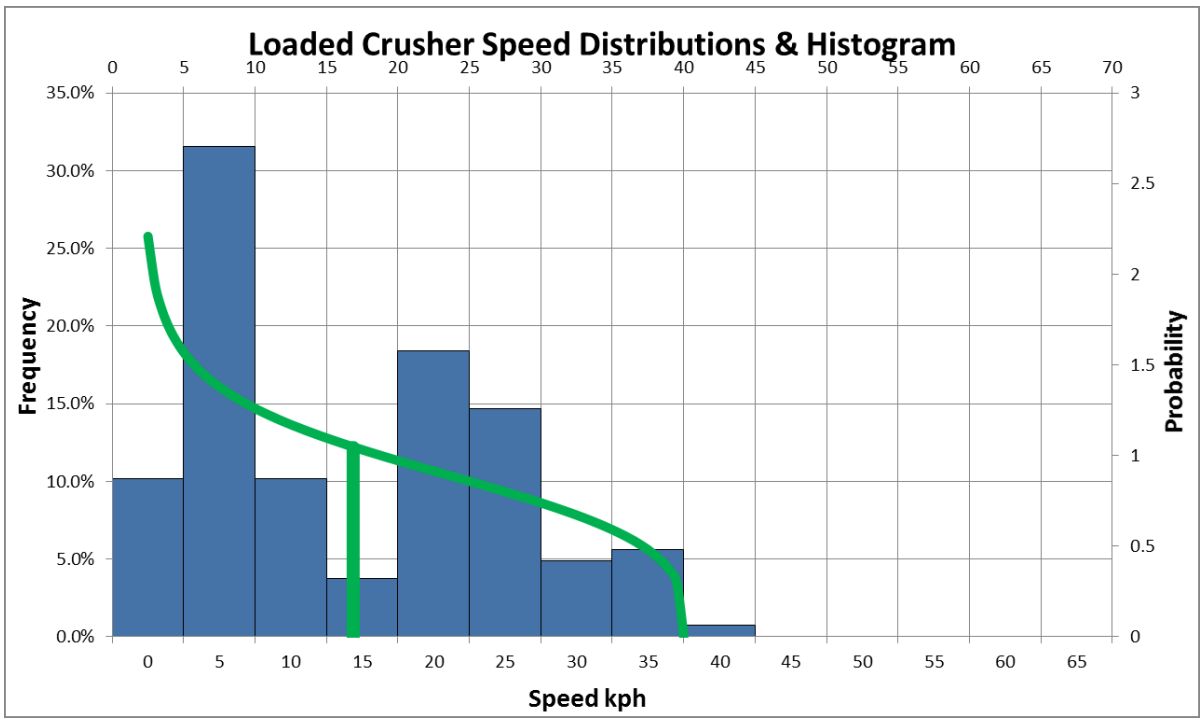
Loaded Crusher Speed Distributions & Histogram
Frequency
Probability
Speed kph
0 5 10 15 20 25 30 35 40 45 50 55 60 65 70
35.0% 30.0% 25.0% 20.0% 15.0% 10.0% 5.0% 0.0%
3 2.5 2 1.5 1 0.5 0

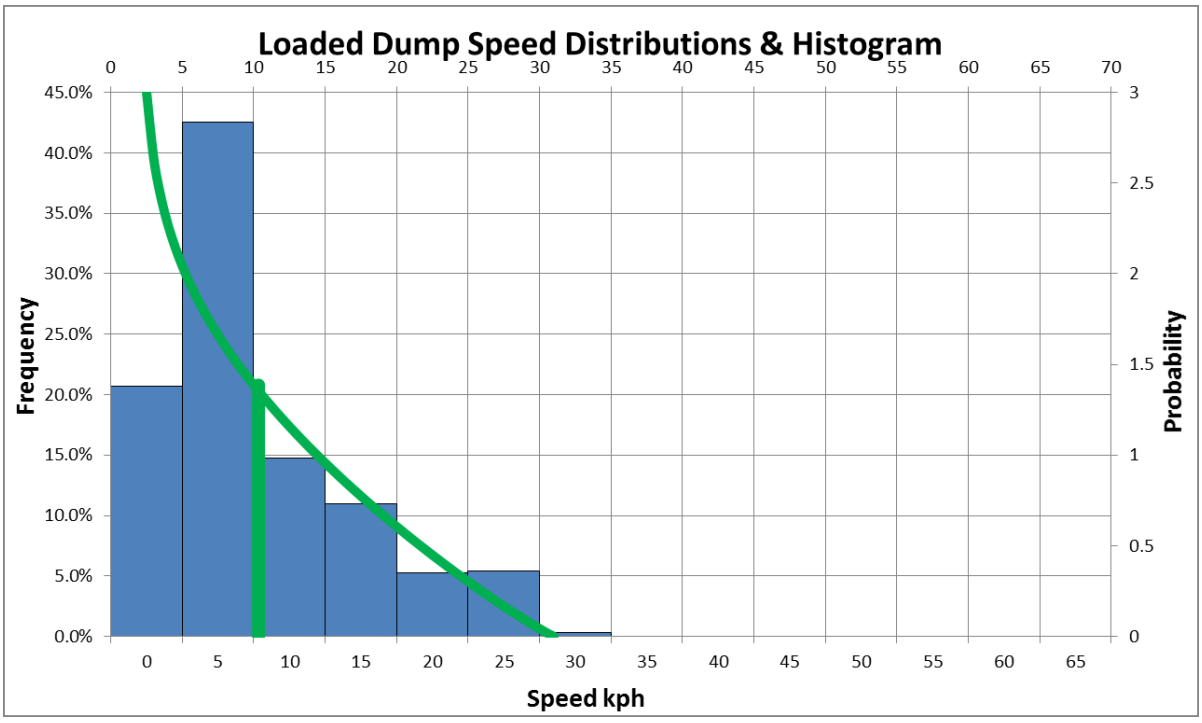
Loaded Dump Speed Distributions & Histogram
Frequency
Probability
Speed kph
0 5 10 15 20 25 30 35 40 45 50 55 60 65 70
45.0% 40.0% 35.0% 30.0% 25.0% 20.0% 15.0% 10.0% 5.0% 0.0%
3 2.5 2 1.5 1 0.5 0

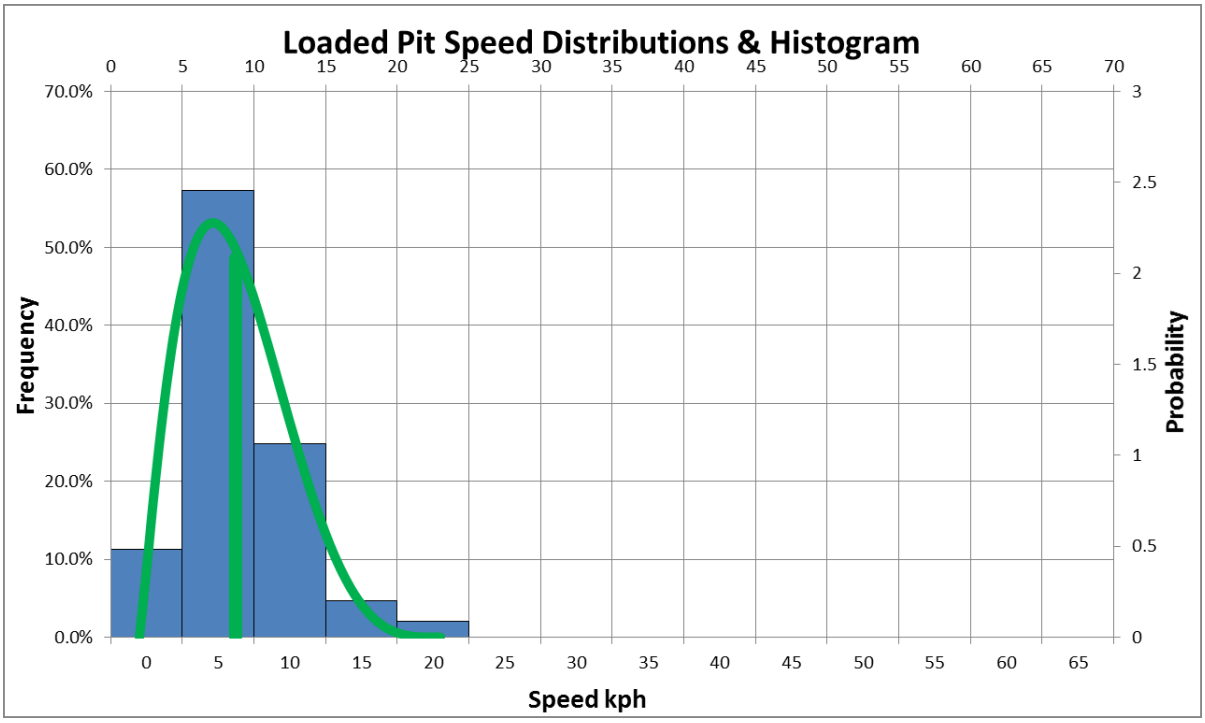
Loaded Pit Speed Distributions & Histogram
Frequency
Probability
Speed kph
0 5 10 15 20 25 30 35 40 45 50 55 60 65 70
70.0% 60.0% 50.0% 40.0% 30.0% 20.0% 10.0% 0.0%
3 2.5 2 1.5 1 0.5 0
0 5 10 15 20 25 30 35 40 45 50 55 60 65

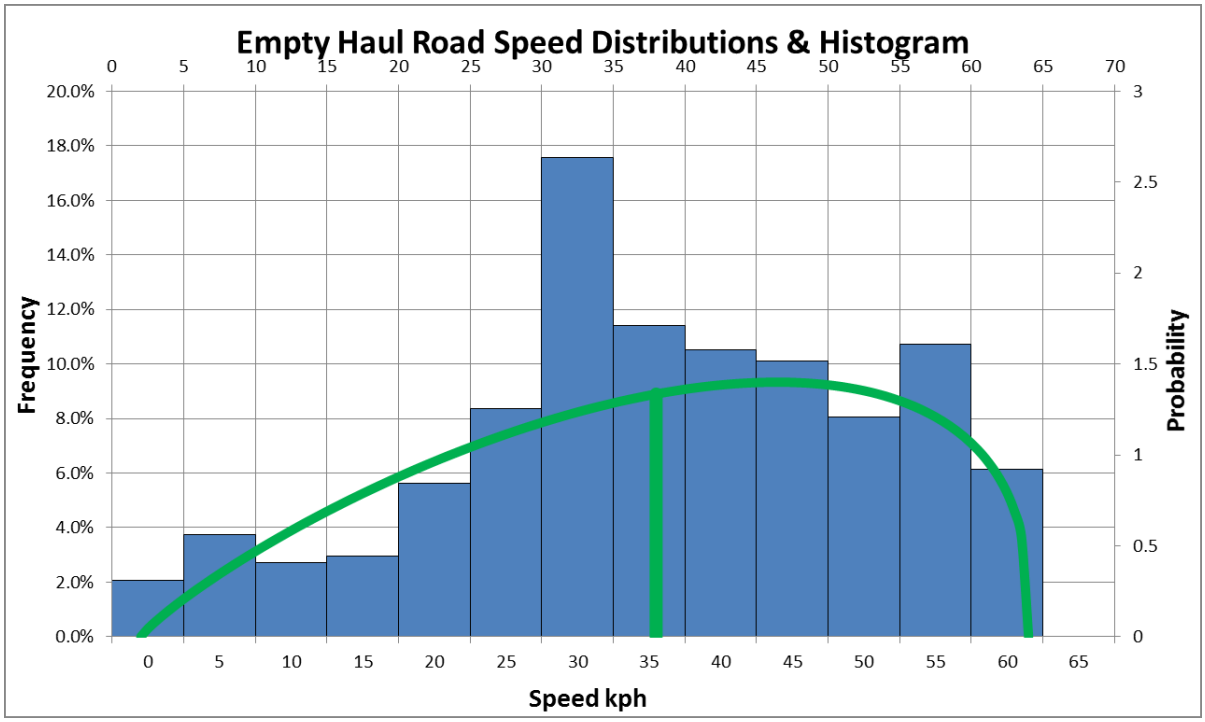
Empty Haul Road Speed Distributions & Histogram
Frequency
Probability
Speed kph
0 5 10 15 20 25 30 35 40 45 50 55 60 65 70
20.0% 18.0% 16.0% 14.0% 12.0% 10.0% 8.0% 6.0% 4.0% 2.0% 0.0%
3 2.5 2 1.5 1 0.5 0
0 5 10 15 20 25 30 35 40 45 50 55 60 65

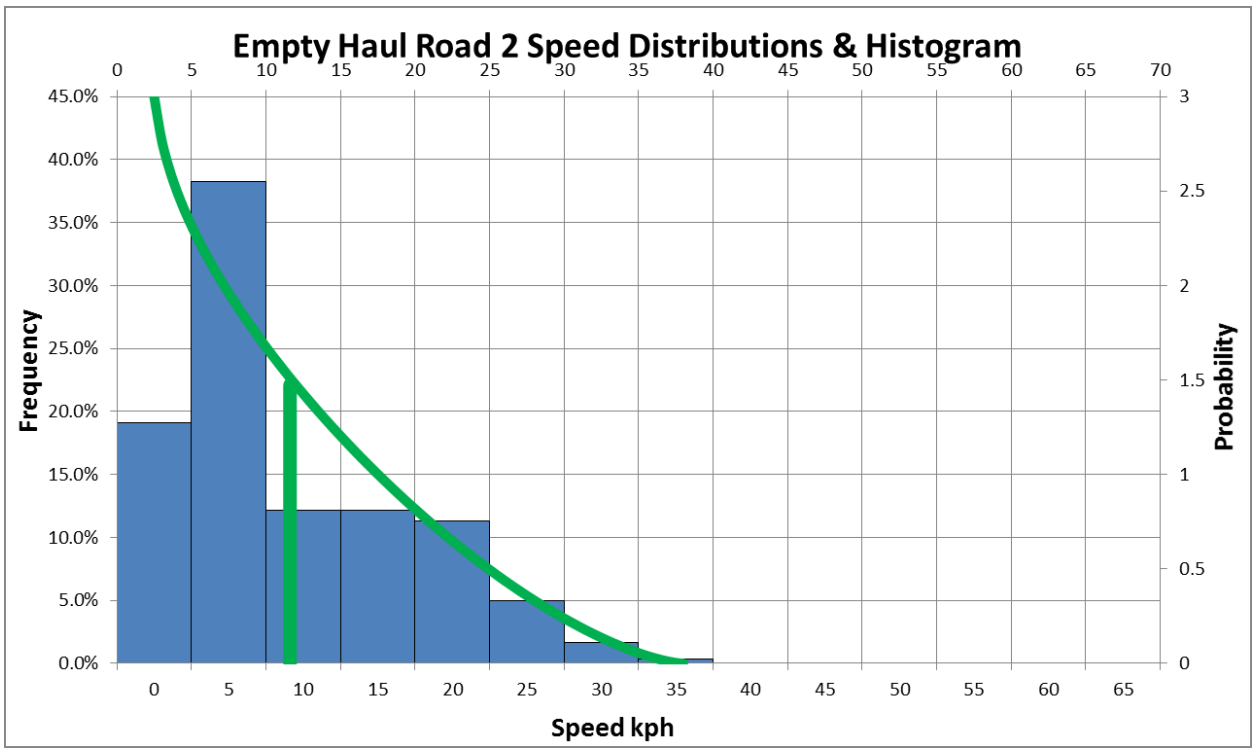
Empty Haul Road 2 Speed Distributions & Histogram
Frequency
Probability
Speed kph
0 5 10 15 20 25 30 35 40 45 50 55 60 65 70
45.0% 40.0% 35.0% 30.0% 25.0% 20.0% 15.0% 10.0% 5.0% 0.0%
3 2.5 2 1.5 1 0.5 0

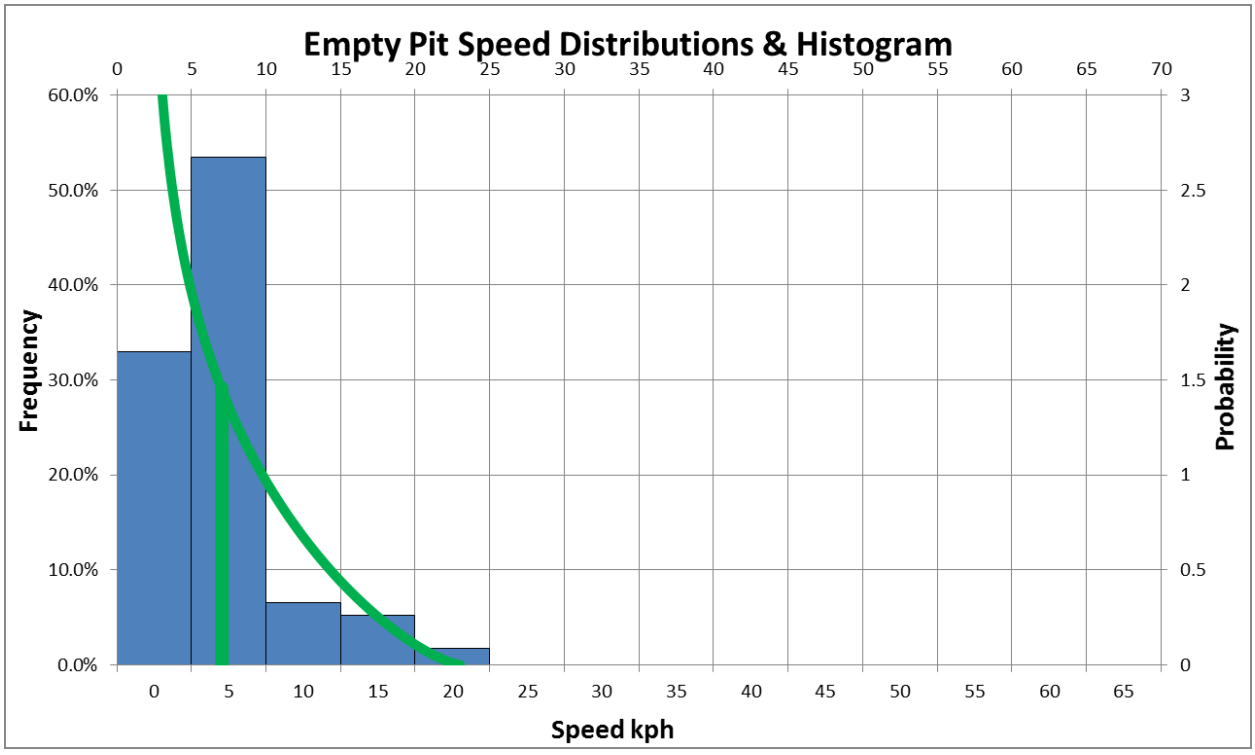
Empty Pit Speed Distributions & Histogram
Frequency
Probability
Speed kph
0 5 10 15 20 25 30 35 40 45 50 55 60 65 70
60.0% 50.0% 40.0% 30.0% 20.0% 10.0% 0.0%
3 2.5 2 1.5 1 0.5 0

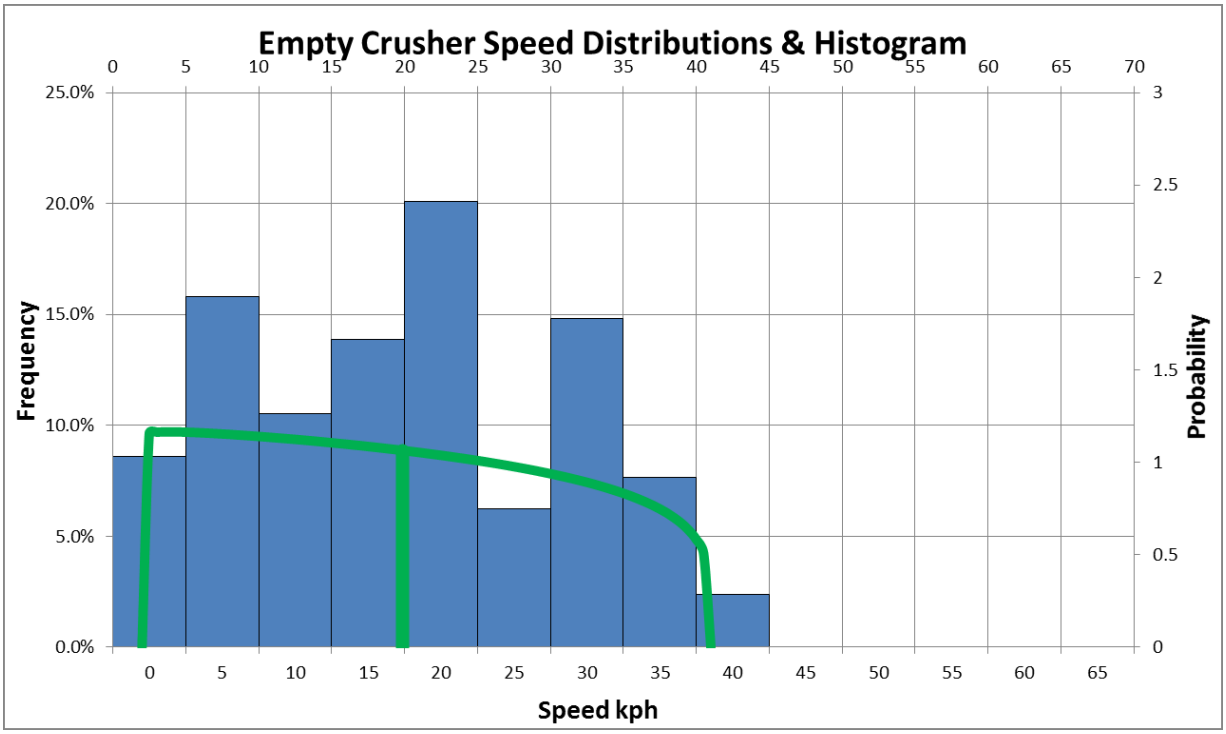
Empty Crusher Speed Distributions & Histogram
Frequency
Probability
Speed kph
0 5 10 15 20 25 30 35 40 45 50 55 60 65 70
25.0% 20.0% 15.0% 10.0% 5.0% 0.0%
3 2.5 2 1.5 1 0.5 0

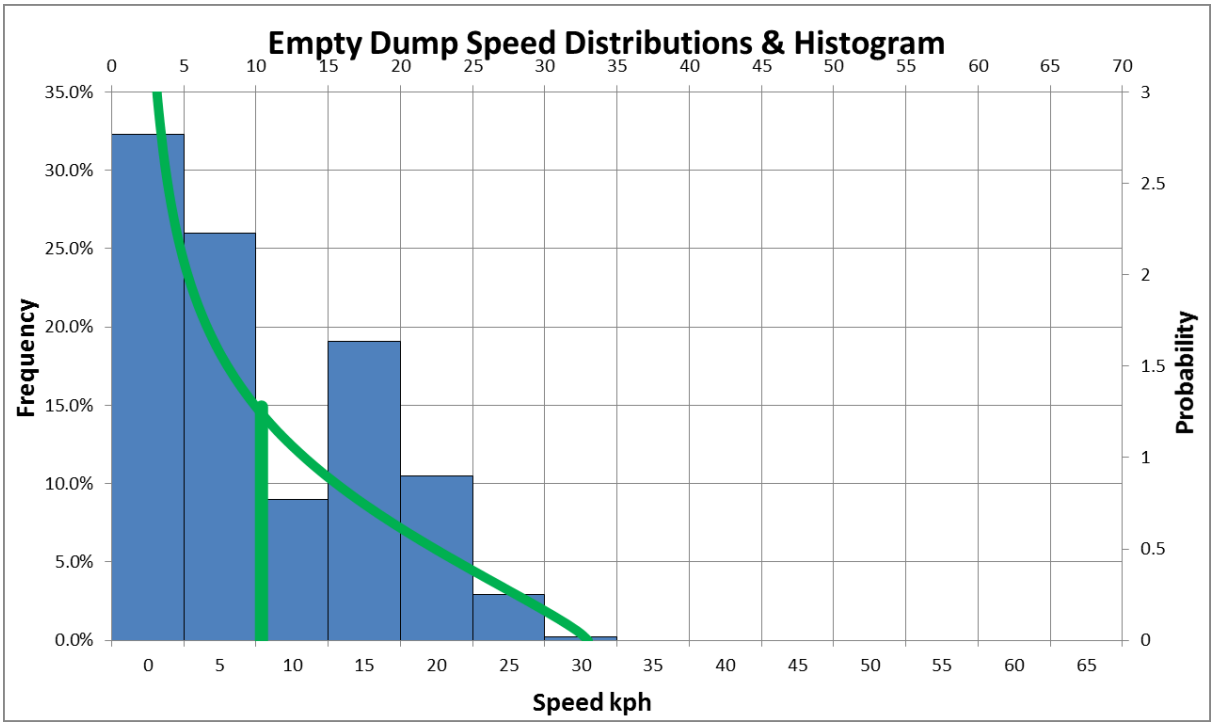
Empty Dump Speed Distributions & Histogram
Frequency
Probability
Speed kph
0 5 10 15 20 25 30 35 40 45 50 55 60 65 70
35.0% 30.0% 25.0% 20.0% 15.0% 10.0% 5.0% 0.0%
3 2.5 2 1.5 1 0.5 0

8.2 Appendix B – Micro Haul Road Profiling

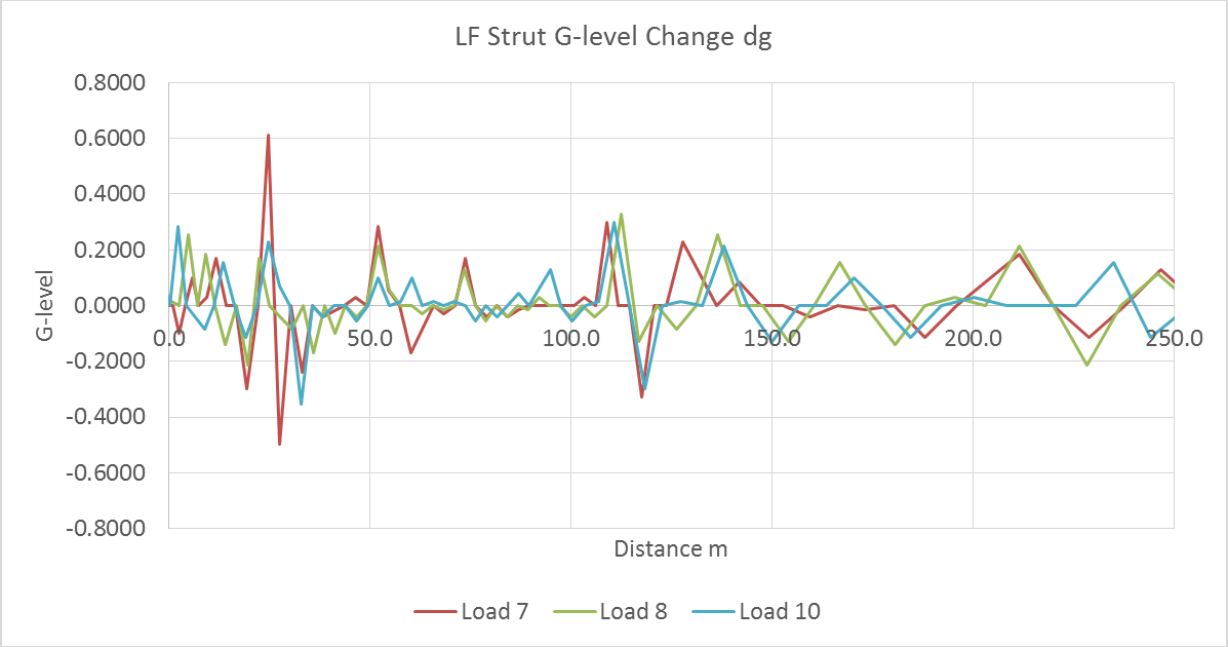

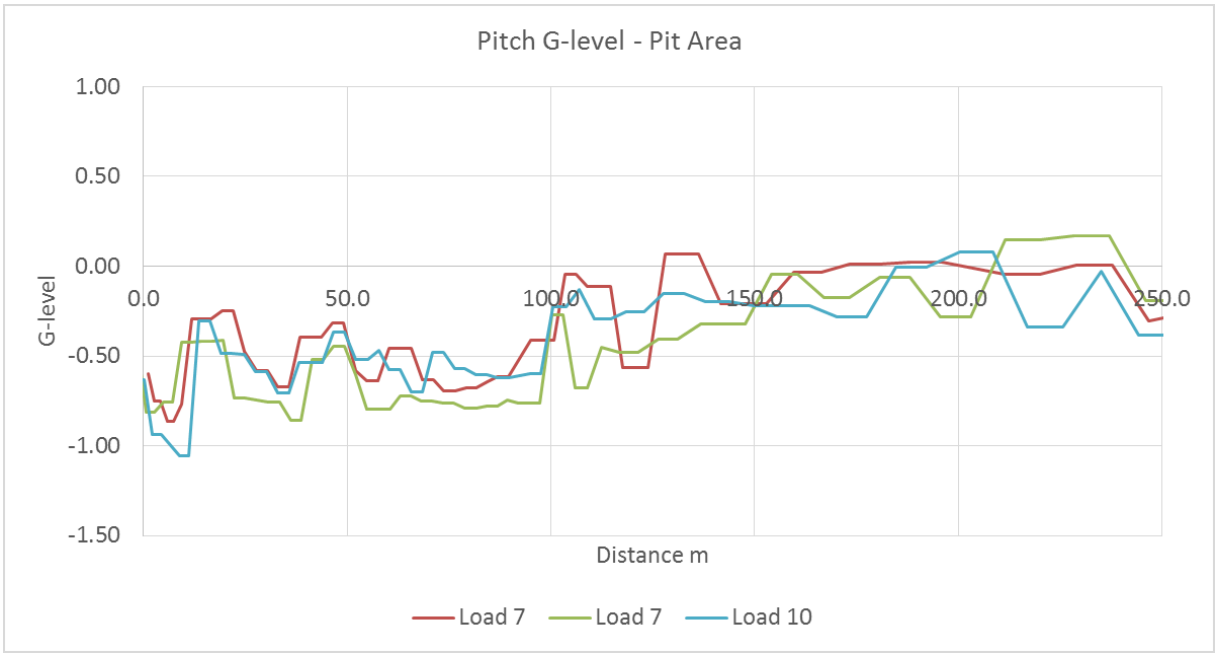
Pitch G-level - Pit Area
1.00
0.50
0.00
-0.50
-1.00
-1.50
G-level
0.0
50.0
100.0
150.0
200.0
250.0
Distance m
Load 7
Load 7
Load 10

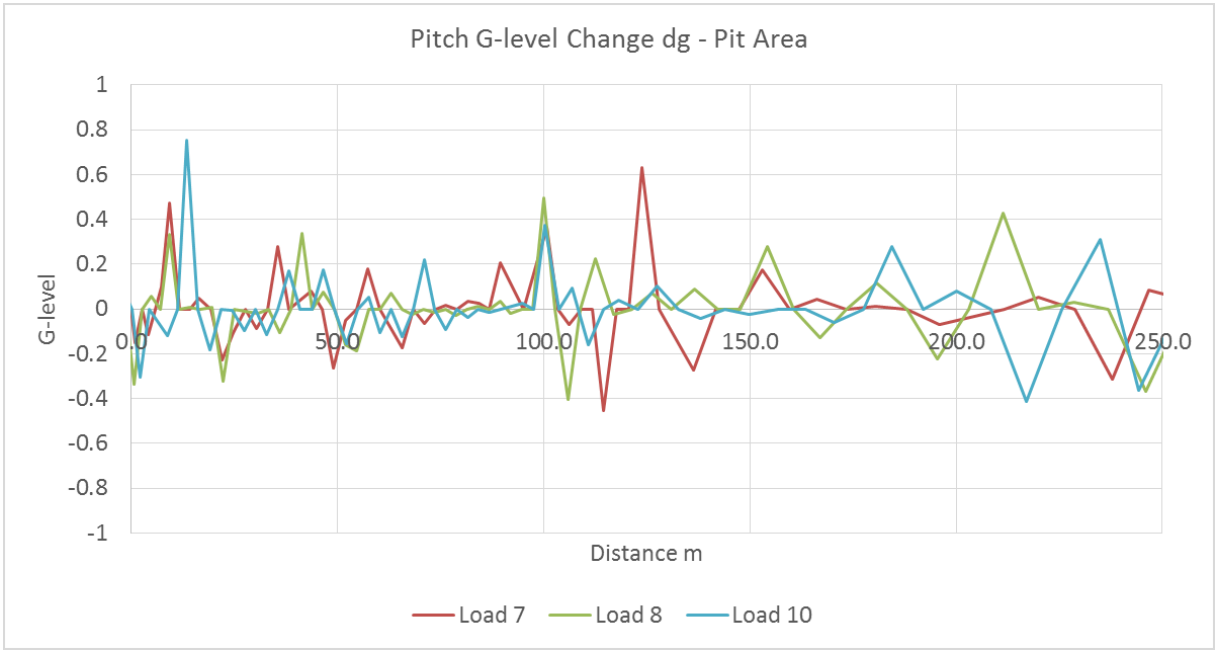
Pitch G-level Change dg - Pit Area
1
0.8
0.6
0.4
0.2
0
-0.2
-0.4
-0.6
-0.8
-1
G-level
0.0
50.0
100.0
150.0
200.0
250.0
Distance m
Load 7
Load 8
Load 10

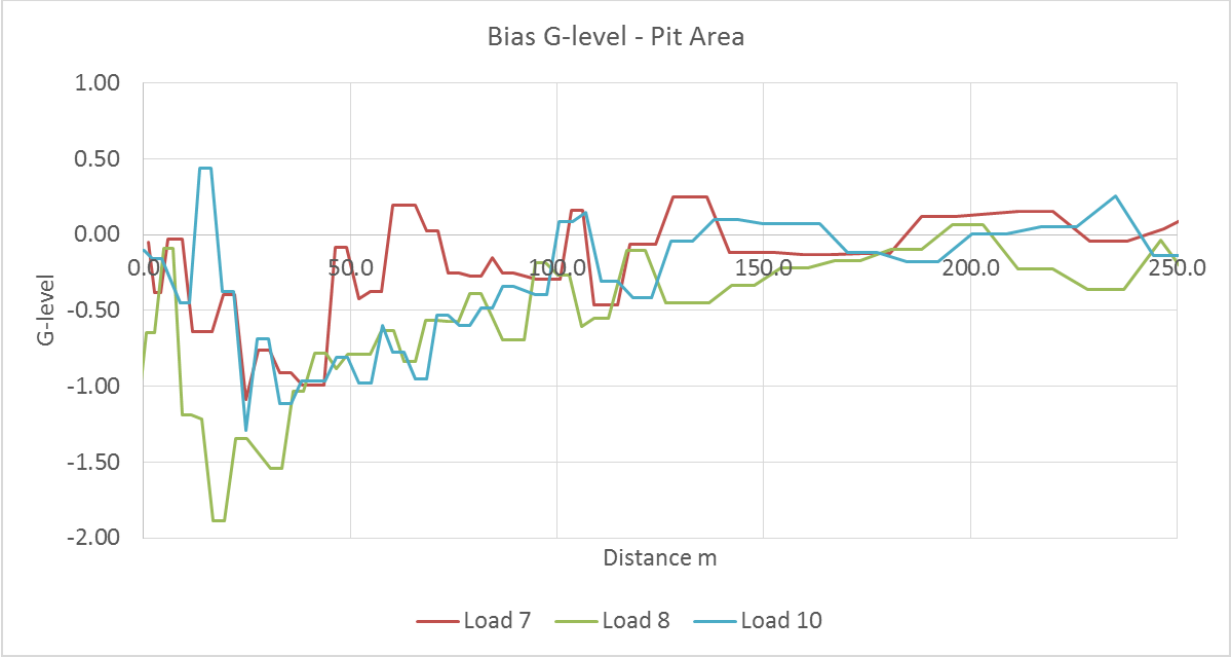
Bias G-level - Pit Area
1.00
0.50
0.00
-0.50
-1.00
-1.50
-2.00
G-level
0.0
50.0
100.0
150.0
200.0
250.0
Distance m
Load 7
Load 8
Load 10

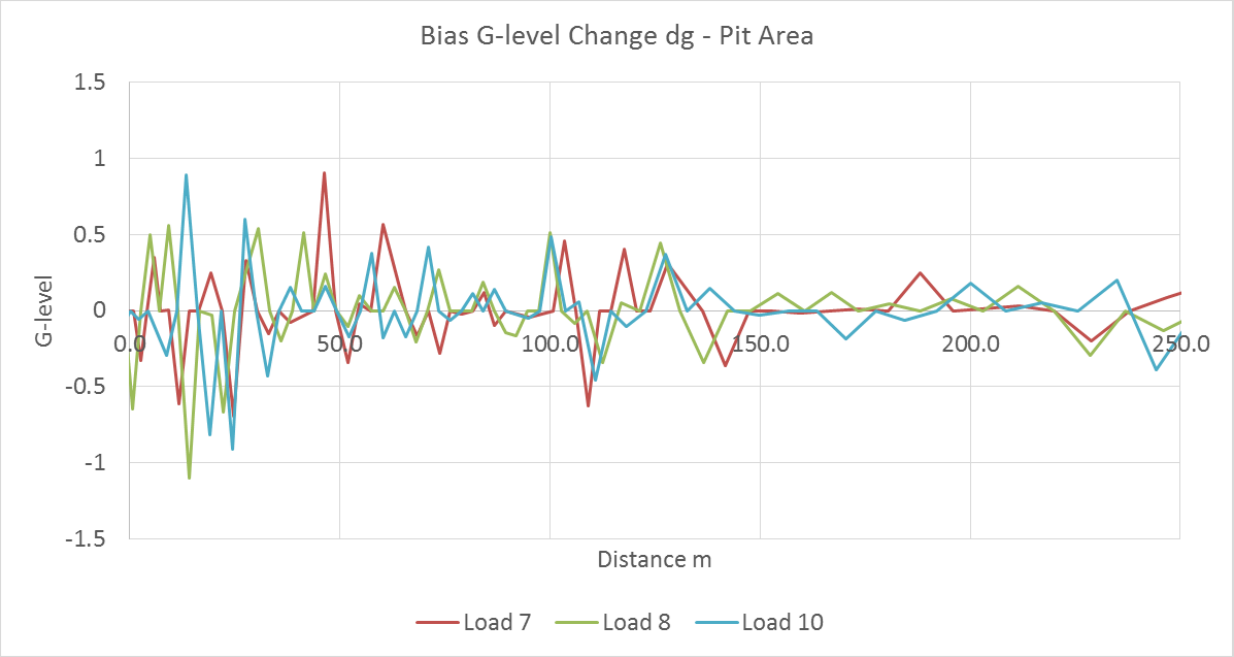
Bias G-level Change dg - Pit Area
1.5
1
0.5
0
-0.5
-1
-1.5
G-level
0.0
50.0
100.0
150.0
200.0
250.0
Distance m
Load 7
Load 8
Load 10

8.3 Appendix C - Haul Road Mapping by G-level Parameters

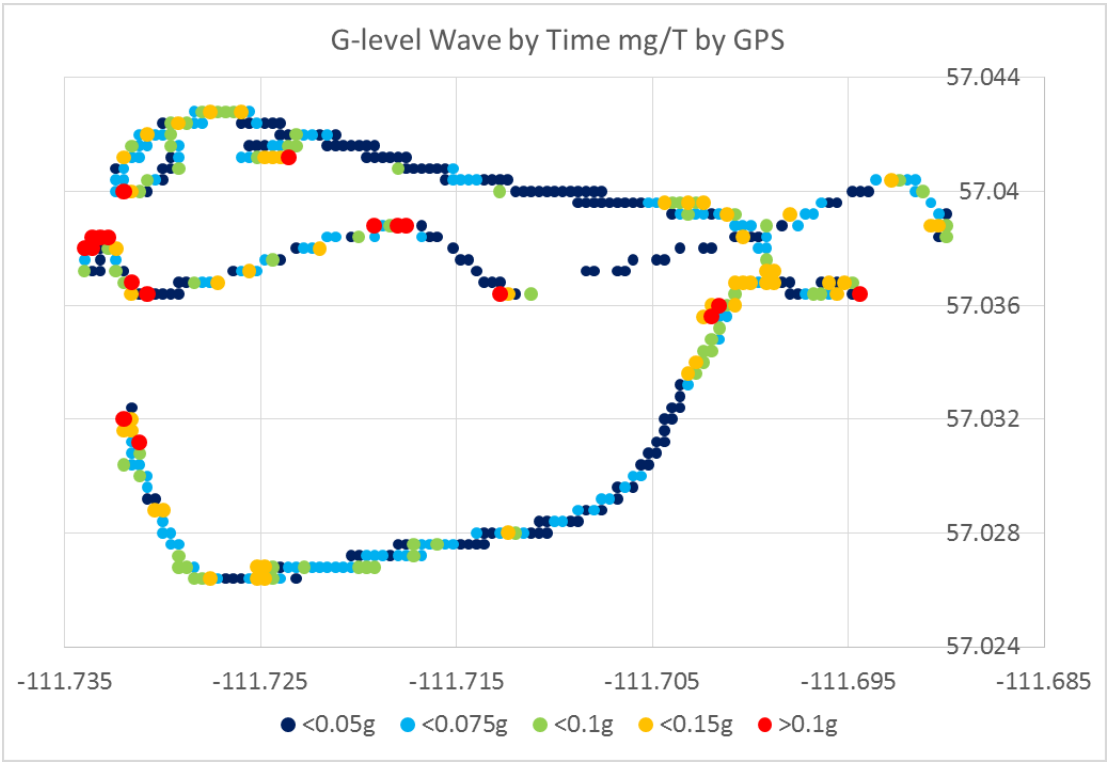

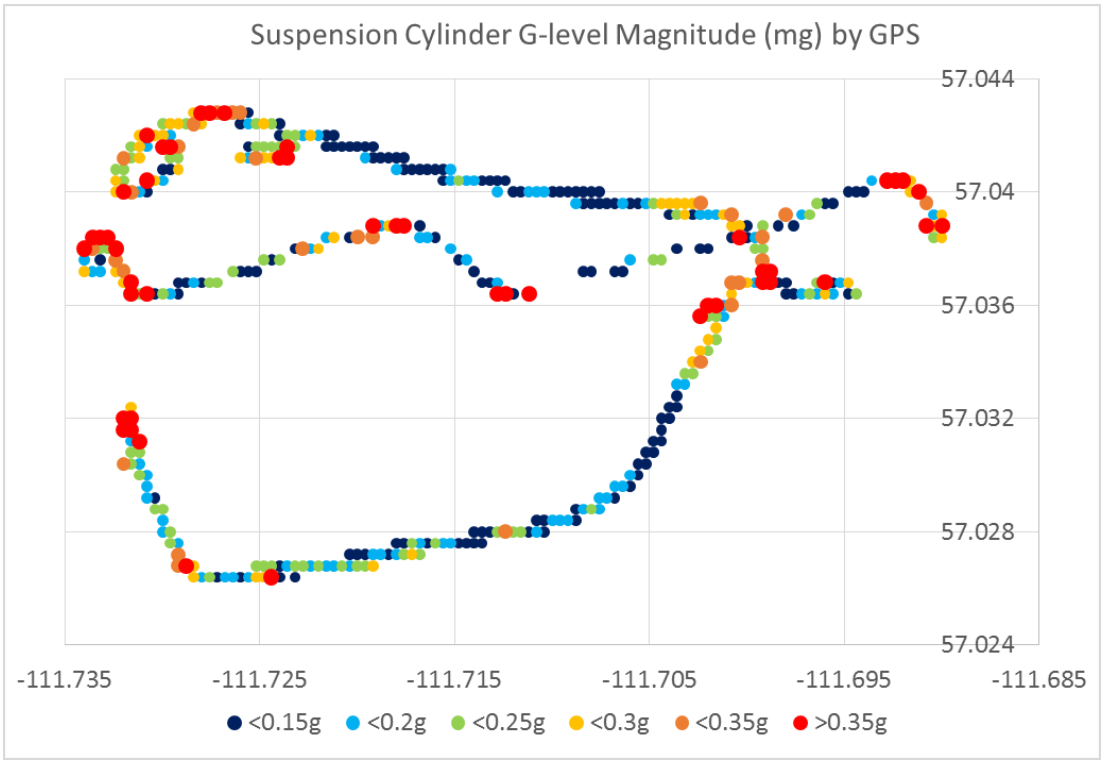

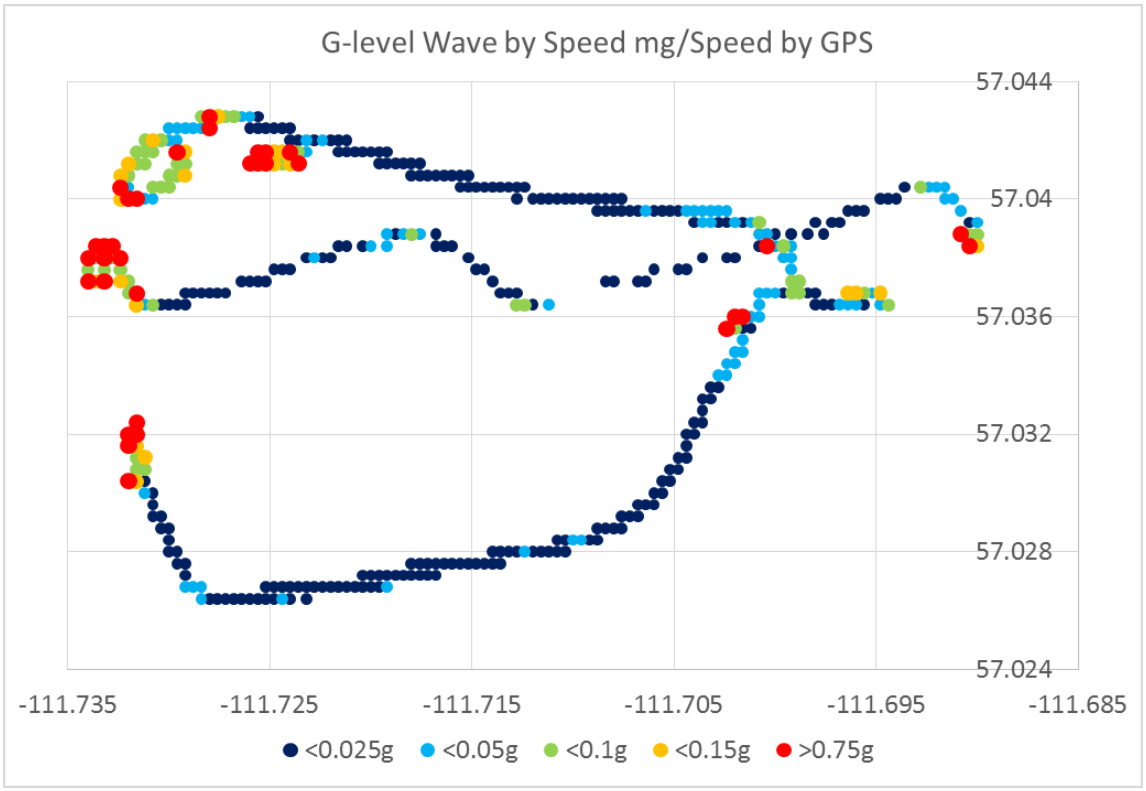
G-level Wave by Speed mg/Speed by GPS
57.044
57.04
57.036
57.032
57.028
57.024
-111.735
-111.725
-111.715
-111.705
-111.695
-111.685
<0.025g
<0.05g
<0.1g
<0.15g
>0.75g

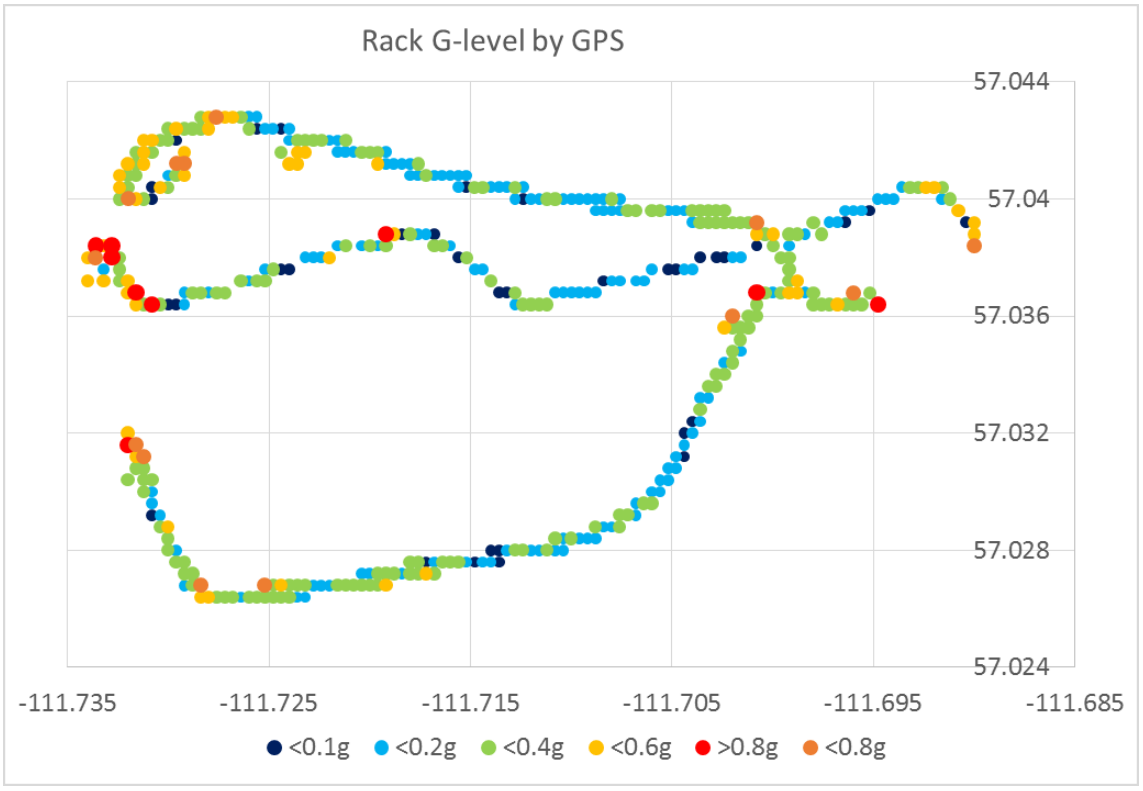
Rack G-level by GPS
57.044
57.04
57.036
57.032
57.028
57.024
-111.735
-111.725
-111.715
-111.705
-111.695
-111.685
<0.1g
<0.2g
<0.4g
<0.6g
>0.8g
<0.8g

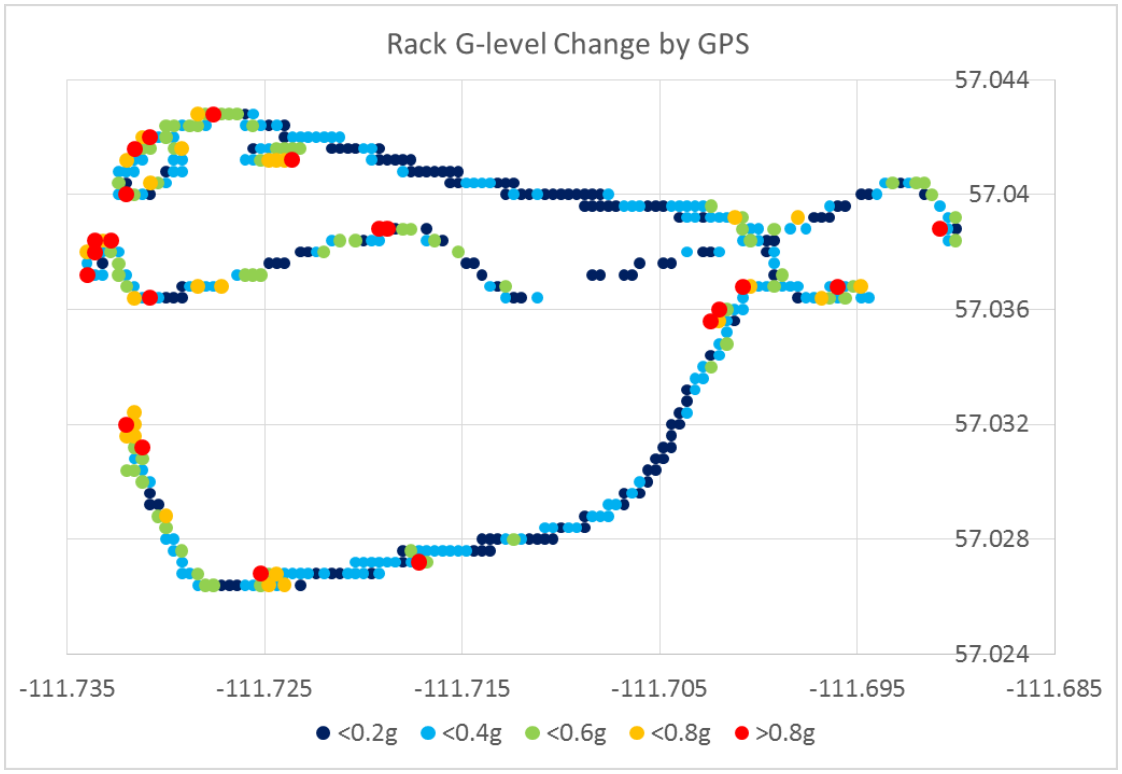
Rack G-level Change by GPS
57.044
57.04
57.036
57.032
57.028
57.024
-111.735
-111.725
-111.715
-111.705
-111.695
-111.685
<0.2g
<0.4g
<0.6g
<0.8g
>0.8g